TARGETED MUTAGENESIS OF THE HOX D LOCUS: A GENETIC ANALYSIS OF LIMB DEVELOPMENT IN THE MOUSE

by

Allan Peter Davis

A dissertation submitted to the faculty of
The University of Utah
in partial fulfillment of the requirements for the degree of

Doctor of Philosophy

Department of Human Genetics

The University of Utah

December 1995

THE UNIVERSITY OF UTAH GRADUATE SCHOOL

SUPERVISORY COMMITTEE APPROVAL

of a dissertation submitted by

Allan Peter Davis

This dissertation has been read by each member of the following supervisory committee and by majority vote has been found to be satisfactory.

Glenn Herrick

Shigeru Sakonju

Carl S. Thummel

THE UNIVERSITY OF UTAH GRADUATE SCHOOL

FINAL READING APPROVAL

To the Graduate Council of the University of Utah:

I have read the dissertation of [redacted] in its final form and have found that (1) its format, citations, and bibliographic style are consistent and acceptable; (2) its illustrative materials including figures, tables, and charts are in place; and (3) the final manuscript is satisfactory to the supervisory committee and is ready for submission to The Graduate School.

Nov 12 1995
Date

[redacted]o R. Capecchi
Ch[redacted], Supervisory Commi[redacted]e

Approved for the Ma[redacted]or Department

[redacted]

Approved for the Graduate Council

[redacted]

Ann W. Hart
Dean of The Graduate School

ABSTRACT

The *Hox Complex* is a matrix of 38 transcription factor genes that play a role in the proper development of the vertebrate body plan by specifying regional information along the embryonic axes. The 5' *Hox D* genes are a subset of this complex that are strongly expressed in the limb buds during embryogenesis, suggesting that they influence the appendicular skeleton. A specific molecular combinatorial *Hox* code has been proposed as a model for the 5' *Hox D* genes in patterning the vertebrate limb. To test this model and resolve the role of these genes in development, a genetic analysis is performed by a mutational approach in the mouse. Specifically, the technique of gene targeting is employed to generate mice individually mutant for *hoxd-11*, *hoxd-12*, and *hoxd-13*. These strains have urogenital tract defects (often resulting in sterility), axial homeosis at the lumbar-sacral region, and malformations in the limb skeleton. The limb phenotypes, however, do not resemble any apparent homeotic transformations as predicted by the combinatorial codes but rather are the result of regional malformations in the shapes, length, and segmentation of bones. To extend these findings, the strains are crossed to each other and to other *Hox*-deficient mice to produce animals with various combinations of mutant alleles. The phenotypes in these animals are more dramatic demonstrating functional redundancy and genetic interaction, especially in the limb. The data allow for a new interpretation where the *Hox D* genes regulate cell proliferation in a proximodistal direction during growth of the limb bud. As such, these genes may not code for distinct positional information, per se, but rather contribute to the number of cells required for proper limb construction. The results are discussed in the context of three models for generating a limb pattern in vertebrates.

...And a mouse is miracle enough to stagger sextillions of infidels.

-Walt Whitman, *Leaves of Grass*

TABLE OF CONTENTS

LIST OF FIGURES

LIST OF TABLES

ACKNOWLEDGMENTS

I thank the members of my committee, Glenn Herrick, Dick Mullen, Shige Sakonju, and Carl Thummel, for their comments on this project. I am especially indebted to Mario R. Capecchi for allowing me the opportunity to be part of his research team. The molecular biology protocols used in this study were taught to me by the numerous postdoctoral fellows in Mario's lab, and the expert assistance of the tissue culture and animal technicians allowed this project to be accomplished.

My training over the last five years was supported by a National Science Foundation Graduate Research Fellowship (1990-1993) and a National Institutes of Health Genetics Training Grant (1993-1995).

The experiments of Chapter 3 would not have been possible without the collaborative efforts of S. Steven Potter, Hsiu M. Hsieh-Li, and David P. Witte of the University of Cincinnati College of Medicine. Chapter 3 originally appeared as an article in *Development* (Volume 120, pages 2187-2198; August 1994), and is reprinted with the permission of The Company of Biologists, Inc. Likewise, Chapter 4 originally appeared as a letter to *Nature* (Volume 375, pages 791-795; 29 June, 1995) and is reprinted with the permission of Macmillan Magazines, Limited.

I appreciate the feedback on my work over the years from the developmental biology research laboratories in the Department of Human Genetics at their weekly group meetings. I have also greatly valued the encouragement of Derry C. Roopenian of The Jackson Laboratory who introduced me to the discipline of mouse genetics and showed me how much fun research can actually be.

Finally, I thank my parents and family for continual support and for at least *trying* to understand why I still do not have a "real" job.

My sanity in Utah has only been maintained by the collaborative efforts of Steiner pool and bottles of Jack Daniel's (though not, however, simultaneously).

Ad Majorem Dei Gloriam.

CHAPTER 1

INTRODUCTION

The mouse *Mus musculus* has been used as an experimental organism by investigators since the turn of the century. This animal is a valued scientific tool for several reasons. It is a small, prolific breeder requiring relatively little care, enabling large colonies to be established and monitored in a cost-effective manner. The embryogenesis and physiology of the mouse are virtually identical to humans. Additionally, the mouse genome is similar to the human genome in several respects: they both share the same complexity (3×10^6 kilobase pairs of DNA containing approximately 100,000 genes distributed over a modest number of chromosomes), large stretches of these genomes show a comparable similarity in structure and genetic information (called synteny), and homologous genes cloned from both organism often show a 95% identity at the nucleotide level (Chapman and Nadeau, 1992). Thus, information obtained about the molecular genetics, development, and physiology of the mouse can often be applied to humans, advancing knowledge about ourselves. Many of these facts were not lost upon the early pioneers in the field of mouse genetics and propelled them to produce, maintain, and analyze hundreds of unique strains (Russell, 1985). Because of their effort and perseverance, we today have a vast knowledge base of the mouse as a laboratory tool (Green, 1966). Currently, there exists approximately 100 inbred strains of the laboratory mouse, over 700 spontaneous and induced mutants, and numerous congenic and recombinant-inbred strains (Lyon and Searle, 1989).

For all of its advantages, however, the mouse does have one particular drawback. The isolation of novel mutations can be a slow process. Historically, there have been three approaches to collecting mutations in the mouse: (1) the consequential spontaneous mutations that show up inherently in large breeding colonies (accounting for the majority of classical mouse mutants), (2) those induced by chemical mutagenesis, and (3) mutations arising from irradiation. All three of these approaches have been extremely successful yet are techniques limited by time and the availability of large breeding facilities. This explains why the induction and collection of mouse

mutants has been limited primarily to only three institutions in the world: The Jackson Laboratory (Bar Harbor, Maine), Oak Ridge National Laboratory (Oak Ridge, Tennessee), and MRC Radiobiology Unit (Harwell, England). It is interesting to note that these last two mouse laboratories were created by national governments during World War II in an interest to resolve the effects of radiation on humans.

Mouse genetics, however, underwent a revolution in the 1980s with the advent of new molecular biology techniques that allowed for the rapid isolation of mutations by direct injection of foreign DNA into mouse embryos (Gordon et al., 1980). The production of these transgenic mice allowed investigators to add to the genomic complement of the mouse. This strategy was primarily used in two designs. The first allowed an exogenous piece of DNA to integrate into the host genome and become active. This technique has been used to express specific genes of interest in the mouse (e.g., Wagner et al., 1981). The second approach was designed as a mutagenesis tool whereby the injected DNA would integrate into an endogenous mouse gene rendering it mutant (e.g., Soriano et al., 1987). This mutation could then be cloned out of the genome by using the injected piece of DNA as a molecular tag (e.g., Gridley et al., 1990; Woychik et al., 1990). Both of these strategies have been successful yet, again, showed certain limitations. Injected DNA often concatamerizes and then randomly integrates into the genome. This can result in a dramatically high copy number of the foreign DNA (sometimes greater than 100 copies) that confuses the interpretation of the resulting phenotype. Second, when foreign DNA randomly integrates it sometimes rearranges the genome by large-scale deletions, inversions, or translocations. This too confounds the interpretations because the phenotype may now be attributed not only to the foreign DNA mutating an endogenous gene but by the chromosomal lesions produced during integration. Finally, the cloning of these lesions by using the molecular tag of the injected DNA has proved to be much more difficult that originally envisioned.

For all of these hindrances, however, the production of transgenic mice has proved fruitful by providing insight into the function of specific genes, the cloning of classical mouse mutations by random integration, and by initiating the procedures and techniques of manipulating the mouse embryo. These advances in molecular biology would be combined with progress in the tissue culture of mouse pluriopotent embryonic stem (ES) cells (Evans and Kaufman, 1981; Martin, 1981) eventually to allow a radically new technique to emerge.

Gene targeting is the process by which genetically modified ES cells are used to produce a mutant mouse (Capecchi, 1989a,b; 1994). This technique differs from standard transgenesis in that the genetic manipulation is controlled entirely by the investigator. A cloned gene is first specifically mutated by recombinant DNA technology *in vitro* and then electroporated into ES cells, which are then enriched for a gene targeting event in tissue culture (Mansour et al., 1988). The homologous recombination of this introduced DNA with the endogenous DNA sequence results in a mutation being targeted to a specific locus, thus circumventing the randomness and gross chromosomal lesions commonly associated with standard transgenesis. This strategy has altered the direction of mutagenesis in the mouse by now advancing the approach of "reverse genetics," whereby the phenotype of a mutant gene is specifically assessed, as opposed to isolating random mutations in an undirected manner. Gene targeting has revolutionized the field of mouse genetics and molecular biology as it has become one of the fastest, easiest, and most used mutagenesis protocols in an astonishingly short period of time.

One particular area of study where gene targeting has been heavily employed is developmental biology. This report is a compilation of experiments which uses the technique of gene targeting to ask what role a defined set of developmental *Hox* genes plays in the embryogenesis of a mammal, specifically with regard to the growth of the vertebrate tetrapod limb.

Hox genes are defined by the presence of a highly conserved 183 nucleotide base pair sequence called the homeobox which translates into a 61 amino acid motif known as the homeodomain. This class of genes was originally discovered in the fruit fly *Drosophila melanogaster* by independent laboratories in the early 1980s (Gehring, 1994). Mutations in these fly *Hox* genes resulted in extraordinary phenotypes whereby specific developmental segments were transformed from one unit to another. The term "homeosis" was borrowed from Bateson (who coined the word nearly a century earlier) to describe these genes (McGinnis, 1994). When several of the *Hox* genes were cloned for the first time from *Drosophila*, the conserved homeobox sequence was interpreted as being similar to the helix-turn-helix DNA binding motif commonly seen in both prokaryotic repressor and yeast mating-type proteins (Laughon and Scott, 1984). In both cases, these proteins function by binding to DNA and acting as regulators, and it was suggested that the same may be true for *Hox* genes. This hypothesis was confirmed by DNA binding studies and the resolution of the three-dimensional structure of the homeodomain (Qian et al., 1989; Kissinger et al., 1990). Thus, these homeotic mutations suggested that the genes responsible were involved in regulating the genetic control of the body plan and opened up a search for homologous genes in other organisms, including the mouse (McGinnis et al., 1984).

To date, 38 *Hox* genes have been identified in the mouse that are arranged together in what is referred to as the *Hox Complex*. This cluster is divided into four loci called Hox A, B, C, and D located on four separate chromosomes with each locus containing between nine to eleven individual *Hox* genes (Fig. 1.1). These genes are delineated into the *Hox* cognate groups numbered 1 through 13 (Scott, 1992). The quartenary matrix is believed to have arisen during evolution by a process of chromosomal duplications since *Hox* genes in the respective cognate families show a higher degree of similarity to each other than they do to neighboring cognate groups

Figure 1.1

The mouse *Hox Complex* compared with the *Drosophila* homeotic genes. The 38 mouse genes are divided onto four loci (Hox A, B, C, and D) located on four separate chromosomes and are grouped into 13 cognate gene families ("paralogues"). These *Hox* genes are aligned with their *Drosophila* homeotic homologues (stippled boxes) The map is drawn in the 3' --> 5' direction, such that the anteriorly expressed genes are located on the left side. The genes studied in this report are marked by black boxes.

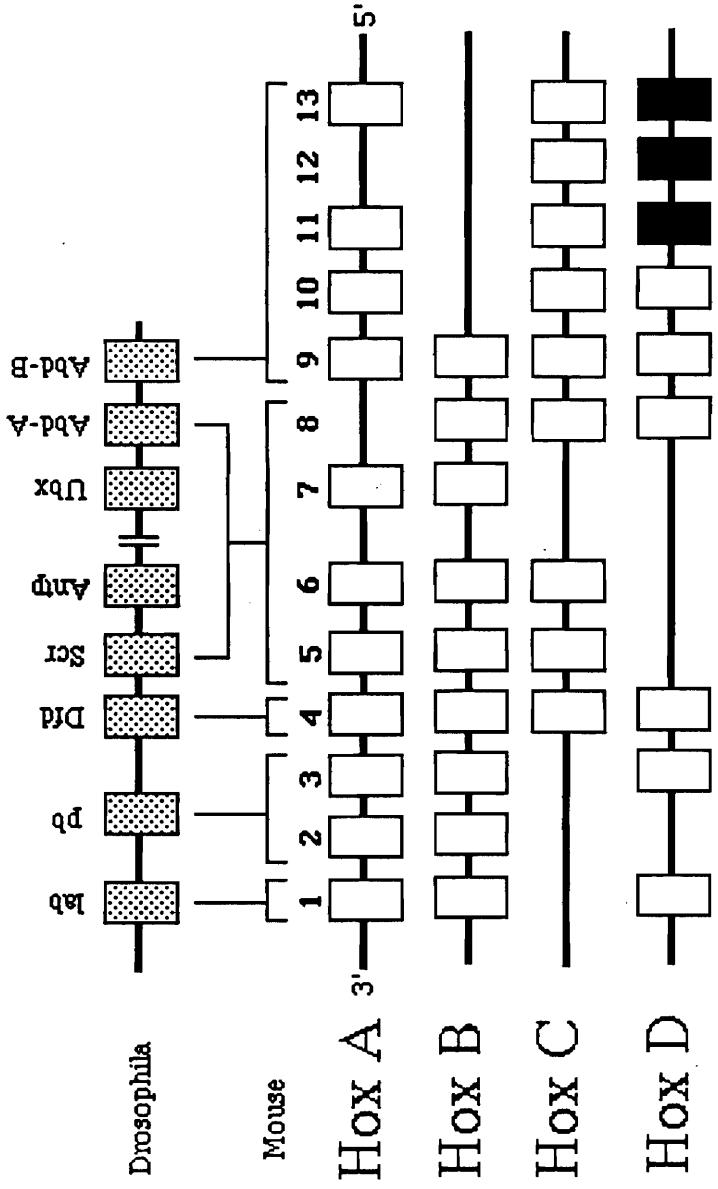
Drosophila
lab
pb
Dfd
Scr
Antp
Ubx
Abd-A
Abd-B
Mouse
1
2
3
4
5
6
7
8
9
10
11
12
13
3'
5'
Hox A
Hox B
Hox C
Hox D

(Ruddle et al., 1994). Members of the same parallel cognate groups are called paralogues.

The mouse *Hox* genes are similar to those in *Drosophila* in three regards. First, sequence similarities in the homeoboxes allow for the alignment of the vertebrate *Hox* genes with their corresponding invertebrate homologues (Fig. 1.1; McGinnis and Krumlauf, 1992). Second, several mammalian *Hox* genes have been shown to function and phenocopy their *Drosophila* equivalents *in vivo* when expressed in transgenic flies (e.g., McGinnis et al., 1990). Third, the physical arrangement of the *Hox* genes on the chromosome reflect their expression domains along the developing anterioposterior (A-P) axis. Thus, genes located at the 3' end of the chromosome have a rostral expression border at the anterior end of the developing embryo whereas genes at the 5' end of the loci are restricted to the most posterior region (Duboule and Dolle, 1989; Graham et al., 1989). This has been termed spatial colinearity in the mouse.

Unique to the mouse, however, is the additional phenomenon of temporal colinearity where the position of the *Hox* gene in the locus also reflects the time at which the gene becomes activated, such that 3' genes are expressed first followed by the progressive activation of each more sequential 5' gene (Izpisua-Belmonte et al. 1991a). This timed cascade of gene activation reflects the process in vertebrate development where the metameric pattern of somite formation follows an A-P polarized direction of growth. Together, these concepts of spatial and temporal colinearity suggested that the *Hox* genes may be determining regional identity along the A-P axis of the developing vertebrate embryo (Duboule, 1992; Izpisua-Belmonte and Duboule, 1992).

This idea has been formalized into the "*Hox* code hypothesis" whereby the metameric pattern of the somites along the A-P axis acquires molecular positional information due to the summation of the *Hox* gene products present in that particular segment (Kessel and Gruss, 1991), a model based upon the original proposal for the homeotic genes in *Drosophila* (Lewis, 1978). This metameric pattern is the

segmentation found in the mammalian axis which later manifests itself in the adult as the vertebral column: a repeated series of similar bones spanning the A-P pole. In the wild-type mouse, these bones include seven cervical (C1-7), thirteen thoracic (T1-13), six lumbar (L1-6), four sacral (S1-4), and a variable number of caudal vertebrae. The "*Hox* code hypothesis" suggests that the anterior region of the developing embryo would be specified by the most 3' *Hox* genes. As development proceeds towards the more caudal end, the sequential activation of the 5' genes would then alter the code to change the molecular identity of the newly added somites. *Hox* paralogues show similar expression domains and activation times, though exact resolution at the cell level has not yet been achieved and leaves open the possibility that subtle differences in the position of all 38 of the combined *Hox* gene products could produce an intricate molecular code along the A-P axis.

The cognate genes *Hox 9-13* represent the most 5' members of the developmental matrix. As such, they are the very last genes to be activated during embryogenesis, and their expression domains become progressively more posterior. Interestingly, however, these genes become reactivated when the limb buds start growing (Dolle et al., 1989, 1991a,b; Nohno et al., 1991; Izpisua-Belmonte et al., 1991a,b; Yokouchi et al., 1991; Haack and Gruss, 1993).

Limb morphogenesis proceeds by the budding of mesenchymal cells from the lateral plate mesoderm (reviewed in Tickle and Eichele, 1994). This outgrowth occurs in the proximodistal (P-D) direction and appears to be controlled by two regions in the limb field. The most distal tip of the limb contains a thickened layer of ectoderm called the apical ectodermal ridge (AER). Immediately beneath this lies a highly proliferating group of undifferentiated mesenchymal cells known as the progress zone (PZ). The AER and PZ communicate by secreting molecules back and forth such that the AER keeps the PZ actively mitotic while the underlying mesoderm maintains the AER. The surgical removal of the AER results in the deterioration of the PZ and the consequential

halting of any further limb development. There is current excitement in the scientific field that fibroblast growth factors are the AER molecules responsible for maintaining the PZ and that sonic hedgehog is a secreted molecule signalling back to the AER (Niswander et al., 1993; Riddle et al., 1993; Fallon et al., 1994; Laufer et al., 1994; Cohn et al., 1995).

At the posterior border of the PZ, a third region called the zone of polarizing activity (ZPA) affects the A-P axis by influencing digit identity. This was first discovered by ectopically transplanting this posterior field to the anterior region of a limb bud and subsequently inducing mirror-image digit duplications (Tickle et al., 1975; 1976). This was interpreted to be the result of the ZPA establishing positional information along the A-P axis by producing a morphogen that diffuses across the limb to create a graded field. Limb cells could interpret this gradient and appropriately respond with a developmental program specific to a particular digit identity. Hence, cells closest to the ZPA constructed digit V whereas those furthest away resulted in digit I. A molecular basis for this graded zonal theory of digit identity was purposed when investigators examined the pattern of *Hox* gene expression in the developing limb buds.

Early analysis of *Hox* genes in the limb demonstrated that the 5' *Hox D* genes are activated in the spatial and temporal colinear order of *hoxd-9*, *-10*, *-11*, *-12*, and then *-13*, such that these genes form an overlapping nested set of transcript domains that become progressively more posterior at the distal tip of the limb (Fig. 1.2). This pattern was suggested to represent a form of molecular positional information (Dolle et al., 1989). Thus, the most posterior region of the limb bud would be identified by the presence of all five *Hox* transcripts. The next most anterior region would contain only four of these *Hox* gene products, and the next rostral domain only three, etc. This model has the effect of dividing the vertebrate limb bud into five distinct molecular zones along the A-P axis. It was implied that these five zones accounted for the fact that most vertebrates only have five digits per limb, with each molecular zone specifying the

Figure 1.2

The *Hox* code model for patterning the limb. The *Hox A* genes (*hoxa-10*, *hoxa-11*, and *hoxa-13*) are expressed in zones along the proximodistal (P-D) axis of the limb bud during embryogenesis (areas indicated by arrows). The three distinct molecular zones created by these domains were suggested to specify the three major zones of the vertebrate tetrapod limb: the stylopod, zeugopod, and autopod. Likewise, the *Hox D* genes were originally described as creating a nested set of overlapping transcript domains delineating five distinct molecular zones along the anteroposterior (A-P) axis of the limb field. These five regions were suggested to specify the five distinct digits (I-V) found in most vertebrates. (All expression domains are drawn schematically.)

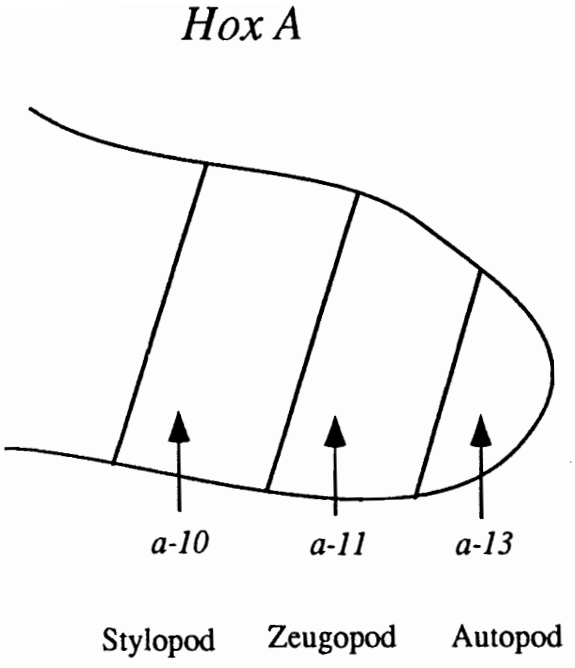

P-D zonal domains

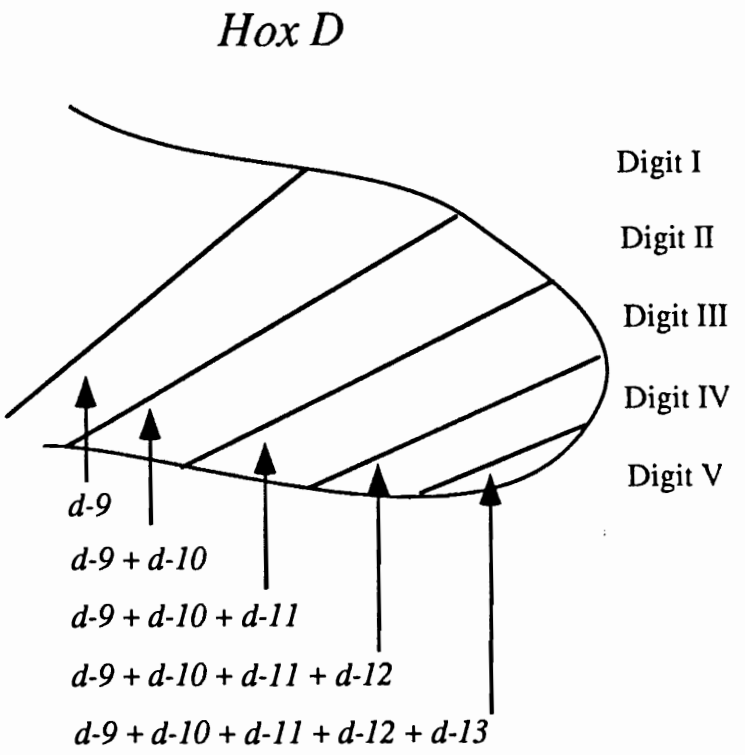

A-P nested sets

growth of a single digit (Tabin, 1992; Morgan and Tabin, 1993). This model provided a molecular explanation for the mirror-image digit duplications seen in ZPA transplantation experiments since mirror-image ectopic *Hox D* gene expression patterns were detected in such treated limb buds prior to ectopic digit growth (Izpisua-Belmonte et al., 1991b; Nohno et al., 1991).

The *Hox A* paralogues were reported to show a different pattern of transcripts where instead of overlapping in the A-P axis of the limb they were interpreted to form distinct zones along the P-D axis (Fig. 1.2). These *Hox A* domains were suggested to code for the three zones that arise during the primary pattern of vertebrate limb development: the stylopod (the humerus in the forelimb), the zeugopod (radius and ulna), and the autopod (a collection of carpals, metacarpals, and phalanges). This pattern is laid down during development by a process of cell condensations in the P-D direction as the limb bud emerges from the main body of the embryo.

The limb grows by the proliferating group of cells that leave the PZ to form the body of the limb. These mesenchymal cells then start to condense. The prechondrogenic condensations start at the proximal end of the limb and progressively grow in the P-D direction continually recruiting more cells. At a particular point in the limb field, this elongated condensation (the presumptive humerus) bifurcates to now yield two branching foci (the radius and ulna) which continue in the P-D direction. Further along, the most posterior condensation (the presumptive ulna) segments to form small clusters which continue to grow, bifurcate, and segment in an anterior direction generating numerous small condensation foci (the presumptive carpals). From this digital arch a further series of five condensation events segment in the P-D direction. These will ossify into the five digits characteristic of most vertebrates. Interestingly, however, these five condensations do not all form at the same time. Instead, they segment in a defined order: digit IV is the first to initiate, then followed by digits III, II, V, and I.

These prechondrogenic condensations represent the primary pattern of limb design (Shubin and Alberch, 1986) which then undergoes secondary modifications that ultimately sculpt the forelimb specific to the animal. These subsequent modifications include the fusion of condensations, the failure of some elements to ossify, and heterochronic growth (Muller, 1991).

The correlation of the 5' *Hox A* gene expression domains with limb regions representing the three zones of limb structure was interpreted as the *Hox* genes establishing a molecular code of positional information that influences the bifurcation points of chondrogenesis (Yokouchi et al., 1991). Together, therefore, simple molecular codes of the *Hox A* and *Hox D* 5' genes were suggested as providing discrete positional information zones used to pattern both the A-P and P-D axis during limb development (Fig. 1.2).

While RNA *in situ* expression experiments are valuable, they do not necessarily dictate true gene expression (i.e., a functioning protein). Thus, it became important to experimentally test this model of *Hox* genes patterning the limb by simple combinatorial codes. The first experiment to test directly this model was done by expressing the mouse *hoxd-11* gene in a developing chick limb (Morgan et al., 1992). By ectopically expressing a *Hox D* gene throughout the entire limb bud, the molecular code along the A-P axis would now be altered to a more posterior fate. Thus, an anterior digit would transform to look like a more posterior one. This indeed was the original conclusion of such experiments, though the data indicated that this homeosis was a rare event (Morgan et al., 1992).

Gene targeting allows the opposite experiment to be performed. By targeted mutagenesis, a specific *Hox D* gene can be removed from the entire limb bud. This will alter the molecular code along the A-P axis, but now in a more anterior direction: predicting a posterior digit will transform into a more anterior one.

In this report, the technique of gene targeting is used to examine the role of the 5' *Hox D* genes *hoxd-11*, *hoxd-12*, and *hoxd-13* in mammalian development by creating specific, targeted disruptions in the mouse in a systematic mutational analysis to then record the skeletal defects. Chapter 2 presents the phenotypes of mice lacking *hoxd-11*. This gene is expressed in three regions of the developing mouse embryo. The first site is in the major body axis where *hoxd-11* transcripts are first detected in the posterior lateral plate mesoderm at embryonic (E) day 8.75. At E12.5 the expression reaches a rostral border of prevertebra 25, representing the lumbar-sacral junction (Izpisua-Belmonte et al., 1991a); additionally, expression is detected in the developing urogenital tracts (Dolle et al., 1991b). In the forelimb, *hoxd-11* becomes activated at E9.0 and contributes to the nested set of transcripts composed of the other 5' *Hox D* genes. Mice mutant for *hoxd-11* shows phenotypes at all three sites of gene expression. These animals have a perturbed axial pattern that includes an extra lumbar vertebra, the forelimb shows minor defects in both the zeugopod and autopod, and males are sterile. These results were later confirmed by an independent laboratory (Favier et al., 1995)

The mild limb defects in *hoxd-11* mutant mice, however, came as a surprise (especially to the proponents of a molecular code specifying digit identity) due to the strong expression patterns seen in the limb by RNA *in situ* experiments. The notion that a paralogue for *hoxd-11* may be compensating in these mice maintained the hopes of the molecular code proponents (as anticipated by Morgan and Tabin, 1993). In a collaborative project, Chapter 3 examines the potential redundancy of *hoxd-11* with one of its paralogues, *hoxa-11*. Mice individually mutant for each of these genes were crossed together to create a double mutant mouse. These results are dramatic with unanticipated phenotypes including perinatal death due to severe kidney deformities, extensive homeotic transformations in the axial column, and the almost total elimination of the zeugopod.

Finally, Chapter 4 presents the mutant limb phenotypes for mice individually lacking *hoxd-12* and *hoxd-13*. These findings are extended by breeding the individual *Hox D* mutant animals to each other to create *trans*-heterozygotes. The results demonstrate that in addition to paralogous interactions, *Hox* genes within the same linkage group co-function during limb formation.

This dissertation summarizes a five year project encompassing a mutational analysis of the 5' *Hox D* genes in the laboratory mouse. The focus of the work centers on the role of these genes in the growth and patterning of the vertebrate tetrapod limb and proposes a new interpretation as to the function of *Hox* genes in limb development.

References

Capecchi, M.R. (1989a). Altering the genome by homologous recombination. *Science* **244**, 1288-1292.

Capecchi, M.R. (1989b). The new mouse genetics: altering the genome by gene targeting. *Trends Genet.* **5**, 70-76.

Capecchi, M.R. (1994). Targeted gene replacement. *Sci. Am.* **270**, 54-61.

Chapman, V.M. and Nadeau, J.H. (1992). The mouse genome: an overview. *Curr. Opin. Genet. Dev.* **2**, 406-411.

Cohn, M.J., Izpisua-Belmonte, J.C., Abud, H., Heath, J.K. and Tickle, C. (1995). Fibroblast growth factors induce additional limb development from the flank of chick embryos. *Cell* **80**, 739-746.

Dolle, P., Izpisua-Belmonte, J.C., Boncinelli, E. and Duboule, D. (1991a). The *Hox-4.8* gene is localized at the 5' extremity of the *Hox-4* complex and is expressed in the most posterior parts of the body during development. *Mech. Dev.* **36**, 3-13.

Dolle, P., Izpisua-Belmonte, J.C., Brown, J.M., Tickle, C. and Duboule, D. (1991b). *Hox-4* genes and the morphogenesis of mammalian genitalia. *Genes Dev.* **5**, 1767-1776.

Dolle, P., Izpisua-Belmonte, J.C., Falkenstein, H., Renucci, A. and Duboule, D. (1989). Coordinate expression of the murine *Hox-5* complex homeobox-containing genes during limb pattern formation. *Nature* **342**, 767-772.

Duboule, D. (1992). The vertebrate limb: a model system to study the Hox/HOM gene network during development and evolution. *BioEssays* **14**, 375-384.

Duboule, D. and Dolle, P. (1989). The structural and functional organization of the murine *Hox* gene family resembles that of *Drosophila* homeotic genes. *EMBO J.* **8**, 1497-1505.

Evans, M.J. and Kaufman, M.H. (1981). Establishment in culture of pluripotential cells from mouse embryos. *Nature* **292**, 154-156.

Fallon, J.F., Lopez, A., Ros, M.A., Savage, M.P., Olwin, B.B. and Simandl, B.K. (1994). FGF-2: apical ectodermal ridge growth signal for chick limb development. *Science* **264**, 104-107.

Favier, B., Le Meur, M., Chambon, P. and Dolle, P. (1995). Axial skeleton homeosis and forelimb malformations in *Hoxd-11* mutant mice. *Proc. Natl. Acad. Sci. USA* **92**, 310-314.

Gehring, W.J. (1994). A history of the homeobox. In *Guidebook to the Homeobox Genes* (Ed., D. Duboule), pp. 3-10. New York: Oxford University Press, Inc.

Gordon, J.W., Scangos, G.A., Plotkin, D.J., Barbosa, J.A. and Ruddle, F.H. (1980). Genetic transformation of mouse embryos by microinjection of purified DNA. *Proc. Natl. Acad. Sci. USA* **77**, 7380-7384.

Graham, A., Papalopulu, N. and Krumlauf, R. (1989). The murine and *Drosophila* homeobox gene complexes have common features of organization and expression. *Cell* **57**, 367-378.

Green, E.L. (1966). *The Biology of the Laboratory Mouse*, 2nd edition. New York: Dover.

Gridley, T., Gray, D.A., Orr-Weaver, T., Soriano, P., Barton, D.E., Francke, U. and Jaenisch, R. (1990). Molecular analysis of the *Mov* 34 mutation: transcript disrupted by proviral integration in mice is conserved in *Drosophila*. *Development* **109**, 235-242.

Haack, H. and Gruss, P. (1993). The establishment of murine *Hox-1* expression domains during patterning of the limb. *Dev. Biol.* **157**, 410-422.

Izpisua-Belmonte, J.C., Falkenstein, H., Dolle, P., Renucci, A. and Duboule, D. (1991a). Murine genes related to the *Drosophila AbdB* homeotic gene are sequentially expressed during development of the posterior part of the body. *EMBO J.* **10**, 2279-2289.

Izpisua-Belmonte, J.C., Tickle, C., Dolle, P., Wolpert, L. and Duboule, D. (1991b). Expression of the homeobox *Hox-4* genes and the specification of position in chick wing development. *Nature* **350**, 585-589.

Izpisua-Belmonte, J.C. and Duboule, D. (1992). Homeobox genes and pattern formation in the vertebrate limb. *Dev. Biol.* **152**, 26-36.

Kessel, M. and Gruss, P. (1991). Homeotic transformations of murine vertebrae and concomitant alteration of *Hox* codes induced by retinoic acid. *Cell* **67**, 89-104.

Kissenger, C.R., Liu, B., Martin-Blanco, C., Kornberg, T.B. and Pabo, C.O. (1990). Crystal structure of an engrailed homeodomain-DNA complex at 2.8 Å resolution: a framework for understanding homeodomain-DNA interactions. *Cell* **63**, 579-590.

Laufer, E., Nelson, C.E., Johnson, R.L., Morgan, B.A. and Tabin, C. (1994). *Sonic hedgehog* and *fgf-4* act through a signaling cascade and feedback loop to integrate growth and patterning of the developing limb bud. *Cell* **79**, 993-1003.

Laughon A. and Scott, M.P. (1984). Sequence of a *Drosophila* segmentation gene: protein structure homology with DNA-binding proteins. *Nature* **310**, 25-31.

Lewis, E.B. (1978). A gene complex controlling segmentation in *Drosophila. Nature* **276**, 565-570.

Lyon, M.F. and Searle, A.G. (1989). *Genetic Variants and Strains of the Laboratory Mouse*. New York: Oxford University Press.

Mansour S.L., Thomas, K.R. and Capecchi, M.R. (1988). Disruption of the proto-oncogene *int-2* in mouse embryo-derived stem cells: a general strategy for targeting mutations to nonselectable genes. *Nature* **336**, 348-352.

Martin, G.R. (1981). Isolation of a pluripotent cell line from early mouse embryos cultured in medium conditioned by teratocarcinoma stem cells. *Proc. Natl. Acad. Sci. USA* **78**, 7634-7636.

McGinnis, N., Kuziora, M.A. and McGinnis, W. (1990). Human *Hox-4.2* and *Drosophila Deformed* encode similar regulatory specificities in *Drosophila* embryos and larvae. *Cell* **63**, 969-976.

McGinnis, W., Garger, R.L., Wirz, J., Kuroiwa, A. and Gehring, W.J. (1984). A homologous protein-coding sequence in *Drosophila* homeotic genes and its conservation in other metazoans. *Cell* **37**, 403-408.

McGinnis, W. and Krumlauf, R. (1992). Homeobox genes and axial patterning. *Cell* **68**, 283-302.

McGinnis, W. (1994). A century of homeosis, a decade of homeoboxes. *Genetics* **137**, 607-611.

Morgan, B.A., Izpisua-Belmonte, J.C., Duboule, D. and Tabin, C.J. (1992). Targeted misexpression of *Hox-4.6* in the avian limb bud causes apparent homeotic transformations. *Nature* **358**, 236-239.

Morgan, B.A. and Tabin, C.J. (1993). The role of homeobox genes in limb development. *Curr. Opin. Genet. Dev.* **3**, 668-674.

Muller, G.B. (1991). Evolutionary transformation of limb pattern: heterochrony and secondary fusion. In *Developmental Patterning of the Vertebrate Limb* (J.R. Hinchliffe, J.M. Hurle, and D. Summerbell, eds.), pp. 395-406. New York: Plenum Press.

Niswander, L., Tickle, C., Voge, A., Booth, I. and Martin, G.R. (1993). FGF-4 replaces the apical ectodermal ridge and directs outgrowth and patterning of the limb. *Cell* **75**, 579-587.

Nohno, T., Noji, S., Koyama, E., Ohyama, K., Myokai, F., Kuroiwa, A., Saito, T. and Taniguchi, S. (1991). Involvement of the *Chox-4* chicken homeobox genes in

determination of anteroposterior axial polarity during limb development. *Cell* **64**, 1197-1205.

Qian,Y.Q., Billeter, M., Otting. G., Muller, M., Gehring, W.J. and Wuthrich, K. (1989). The structure of the *Antennapedia* homeodomain determined by NMR spectroscopy in solution: comparison with prokaryotic repressors. *Cell* **59**, 573-580.

Riddle, R. Johnson, R.L., Laufer, E. and Tabin, C.J. (1993). *Sonic hedgehog* mediates the polarizing activity of the ZPA. *Cell* **75**, 1401-1416.

Ruddle, F.H., Bartels, J.L., Bentley, K.L., Kappen, C., Murtha, M.T. and Pendleton, J.W. (1994). Evolution of *Hox* genes. *Annu. Rev. Genet.* **28**, 423-442.

Russell, E.S. (1985). A history of mouse genetics. *Annu. Rev. Genet.* **19**, 1-28.

Scott, M.P. (1992). Vertebrate homeobox gene nomenclature. *Cell* **71**, 551-553.

Shubin, N.H. and Alberch, P. (1986). A morphogenetic approach to the origin and basic organization of the tetrapod limb. *Evol. Biol.* **20**, 319-387.

Soriano, P., Gridley, T. and Jaenisch, R. (1987). Retroviruses and insertional mutagenesis in mice: proviral integration at the *Mov-34* locus leads to early embryonic death. *Genes Dev.* **1**, 366-375.

Tabin, C.J. (1992). Why we have (only) five fingers per hand: *Hox* genes and the evolution of paired limbs. *Development* **116**, 289-296.

Tickle, C., Shellswell, G., Crawley, A. and Wolpert, L. (1976). Positional signalling by mouse limb polarizing region in the chick wing-bud. *Nature* **259**, 396-397.

Tickle, C., Summerbell, D. and Wolpert, L. (1975). Positional signalling and specification of digits in chick limb morphogenesis. *Nature* **254**, 199-202.

Tickle, C. and Eichele, G. (1994). Vertebrate limb development. *Annu. Rev. Genet.* **10**, 121-152.

Wagner, T.E., Hoppe, P.C., Jollick, J.D., Scholl, D.R., Hodinka, R.L. and Gault, J.B. (1981). Microinjection of a rabbin beta-globin gene into zygotes and its subsequent expression in adult mice and their offspring. *Proc. Natl. Acad. Sci. USA* **78**, 6376-6380.

Weiher, H., Noda, T., Gray, D.A., Sharpe, A.H. and Jaenisch, R. (1990). Transgenic mouse model of kidney disease: insertional inactivation of ubiquitously expressed gene leads to nephrotic syndrome. *Cell* **62**, 425-434.

Woychik, R.P., Maas, R.L., Zeller, R., Vogt, T.P. and Leder, P. (1990). "Formins": proteins deduced from the alternative transcripts of the *limb deformity* gene. *Nature* **346**, 850-853.

Yokouchi, Y., Sasaki, H. and Kuroiwa, A. (1991). Homeobox gene expression correlated with the bifurcation process of limb cartilage development. *Nature* **353**, 443-445.

CHAPTER 2

AXIAL HOMEOSIS AND APPENDICULAR SKELETON DEFECTS IN MICE WITH A TARGETED DISRUPTION OF *hoxd-11*

The following chapter is a reprint of an article coauthored by Mario R. Capecchi and me. This article was originally published in *Development*, Volume 120, pages 2187-2198, August, 1994 (Copyright 1994 by The Company of Biologists, Limited). It is reprinted here with the permission of the coauthor and The Company of Biologists, Limited.

Development 120, 2187-2198 (1994)
Printed in Great Britain © The Company of Biologists Limited 1994

Axial homeosis and appendicular skeleton defects in mice with a targeted disruption of *hoxd-11*

Allan Peter Davis and Mario R. Capecchi*

Howard Hughes Medical Institute, Department of Human Genetics, University of Utah School of Medicine, Salt Lake City, Utah 84112, USA

*Author for correspondence

SUMMARY

Using gene targeting, we have created mice with a disruption in the homeobox-containing gene *hoxd-11*. Homozygous mutants are viable and the only outwardly apparent abnormality is male infertility. Skeletons of mutant mice show a homeotic transformation that repatterns the sacrum such that each vertebra adopts the structure of the next most anterior vertebra. Defects are also seen in the bones of the limb, including regional malformations at the distal end of the forelimb affecting the length and structure of phalanges and metacarpals, inappropriate fusions between wrist bones, and defects at the most distal end in the long bones of the radius and ulna. The phenotypes show both incomplete penetrance and variable expressivity. In contrast to the defects observed in the vertebral column, the phenotypes in the appendicular skeleton do not resemble homeotic transformations, but rather regional malformations in the shapes, length and segmentation of bones. Our results are discussed in the context of two other recent gene targeting studies involving the paralogous gene *hoxa-11* and another member of the *Hox D* locus, *hoxd-13*. The position of these limb deformities reflects the temporal and structural colinearity of the *Hox* genes, such that inactivation of 3′ genes has a more proximal phenotypic boundary (affecting both the zeugopod and autopod of the limb) than that of the more 5′ genes (affecting only the autopod). Taken together, these observations suggest an important role for *Hox* genes in controlling localized growth of those cells that contribute to forming the appendicular skeleton.

Key words: gene targeting, *Hox* genes, homeotic transformation, limb development, limb defects

INTRODUCTION

In vertebrates there is a matrix of 38 genes that collectively make up the *Hox complex*. These genes are distributed in four linkage groups, Hox A, Hox B, Hox C and Hox D, which are located on four separate chromosomes. This organization is believed to have arisen during prevertebrate phylogeny by quadruplication of an ancestral complex to create the current linkage groups, making genes in one locus homologous to their corresponding parallel genes in the other linkage groups (Pendleton et al., 1993). Such homologous genes are called paralogues.

A *Hox* gene product is defined by the presence of a highly conserved 61 amino acid motif called the homeodomain that has DNA-binding properties (Kissinger et al., 1990; Otting et al., 1990). In *Drosophila*, the homeodomain-encoding genes of the *Bithorax* and *Antennapedia* homeotic complexes (HOM-C) are used to pattern the developing embryo (Lewis, 1978; Akam, 1987). The vertebrate *Hox* genes are similar to those in the HOM-C in three regards. First, sequence similarities in the homeodomains allow for the alignment of mammalian *Hox* genes with their counterpart *Drosophila* genes (detailed in McGinnis and Krumlauf, 1992). Second, several mammalian *Hox* genes have been shown to function and phenocopy their *Drosophila* HOM-C homologues in vivo when expressed ectopically in transgenic flies (McGinnis et al., 1990). Third, the chromosomal position of the *Hox* genes reflects the order of the anterior boundaries of expression for each gene along the anteroposterior (A-P) axis. The 3′ genes extend more anteriorly while those on the 5′ end of the complex are limited to more posterior regions (Duboule and Dollé, 1989; Graham et al., 1989). This latter property has been termed structural colinearity.

Metamere formation along the primary axis of the vertebrate embryo is intrinsically coordinated with time since the somites that generate this pattern condense and mature in an anterior-to-posterior direction. Consequently, the order of *Hox* genes on the chromosome also correlates with their time of activation, with 3′ members being activated before their 5′ neighbors (Izpisúa-Belmonte et al., 1991a). This temporal progression of *Hox* gene activation may play as important a role as the spatial distribution of *Hox* gene expression in executing the developmental program for patterning the mammalian embryo.

The structural and temporal colinearity of *Hox* gene expression suggested that the encoded proteins may determine regional identity along the body axis of the embryo. This hypothesis has been amply confirmed by the analysis of mice with targeted disruptions in *Hox* genes. These mutant mice

show either regional loss of tissues and structures, or apparent localized homeotic transformations along the A-P axis (Chisaka and Capecchi, 1991; Lufkin et al., 1991; Chisaka et al., 1992; LeMouellic et al., 1992; Ramirez-Solis et al., 1993; Carpenter et al., 1993; Mark et al., 1993; Condie and Capecchi, 1993; Jeannotte et al., 1993; Dollé et al., 1993; Small and Potter, 1993; Gendron-Maguire et al., 1993; Rijli et al., 1993; Kostic and Capecchi, 1994).

In addition to patterning the embryo along the A-P axis, a subset of 15 or more *Hox* genes located at the 5′ end of the Hox A, Hox C and Hox D linkage groups are also likely to be involved in patterning the limb. Interestingly, during the early phases of limb bud growth, the spatial and temporal expression patterns of these *Hox* genes within the limb also reflect the order of the genes on the chromosome (Dollé et al., 1989, 1991a; Nohno et al., 1991; Izpisúa-Belmonte et al., 1991a,b; Yokouchi et al., 1991; Haack and Gruss, 1993). These 5′ *Hox* genes express within the developing limb a nested set of transcripts which have been suggested to establish polarity and patterning, as well as influencing the number of digits (Duboule, 1992; Izpisúa-Belmonte and Duboule, 1992; Tabin, 1992).

The vertebrate limb initially appears as a bud of mesenchyme that originates from the lateral plate mesoderm. The outgrowth of the limb bud is controlled by the apical ectodermal ridge (AER), which maintains the underlying mesoderm (the progress zone) in a highly proliferative state. As the limb grows, cells leave the progress zone and participate in forming the prechondrogenic condensations that generate the limb bones (Hinchliffe, 1991). As a result, patterning of the limb is polarized such that the proximal bones (the stylopod and zeugopod) are laid down prior to the distal element (the autopod). An important component of patterning the limb along the A-P axis is a signal emanating from the zone of polarizing activity (ZPA) located at the posterior proximal margin of the limb bud (Tickle et al., 1975; Saunders, 1977). Although the nature of this signal and how it is distributed along the A-P axis of the limb has not been defined, there is current excitement that *sonic hedgehog* might be the long sought signaling molecule (Echelard et al., 1993; Riddle et al., 1993). Because the anterior expression boundaries of the 5′-*Hox D* genes vary along the A-P axis of the developing limb bud, it has been postulated that these genes may be involved in interpreting the ZPA signal. Consistent with this hypothesis, ZPA transplantations to the anterior side of the chick limb bud generate mirror-image duplications of the 5′-*Hox D* expression patterns that precede and resemble the characteristic mirror-image limb duplications that are induced by the ectopic ZPA (Izpisúa-Belmonte et al., 1991b; Nohno et al., 1991).

Hoxd-11 (formerly *hox-4.6*) is situated in the center of the 5′-set of *Hox D* genes. It is expressed both along the primary body axis and in the developing limb. The earliest expression is noted at day E8.75 in lateral plate mesoderm of the most posterior region of the embryo. At E12.5 the expression of *hoxd-11* reaches an anterior border along the A-P axis in the sclerotome condensations of prevertebra 25, near the junction between the lumbar and sacral vertebrae (Izpisúa-Belmonte et al., 1991a). *Hoxd-11* expression is also seen in the developing urogenital tracts (Dollé et al., 1991b). In the limb, expression of *hoxd-11* is first noted at E9.0. With the outgrowth of the limb, *hoxd-11* transcripts contribute to the nested set of *Hox D* transcripts that vary along both the proximodistal (Pr-D) and A-P axes (Dollé et al., 1989, 1991a).

While RNA in situ studies suggest possible sites of gene function, a more direct approach to defining the developmental roles for Hox proteins is to employ the technique of gene targeting to create specific mutations in the mouse (Capecchi, 1989, 1994). Towards this end, we have created mice homozygous for a mutation in the *hoxd-11* gene. These mice have a homeotic transformation encompassing the entire sacral region of the axial column as well as regional malformations at the distal end of the forelimb. Our results are compared with the recent targeted analysis of two other *Hox* genes that also affect patterning of the sacrum and the limb: *hoxa-11*, a paralogue of *hoxd-11* (Small and Potter, 1993); and *hoxd-13*, another member of the 5′ *Hox D* locus (Dollé et al., 1993).

MATERIALS AND METHODS

Construction of a *hoxd-11* targeting vector

A DNA fragment containing the *hoxd-11* gene was isolated from a genomic lambda library made from mouse CC1.2 embryo-derived stem (ES) cell DNA, using a probe 5′ to the *hoxd-10* locus. The *hoxd-11* gene was identified by hybridization to a 45-mer oligonucleotide from the human homologue, HOX4F (Acampora et al., 1989), and the homeobox was sequenced to confirm its identity (Izpisúa-Belmonte et al., 1991a). A replacement type targeting vector (Thomas and Capecchi, 1987; Thomas et al., 1992; Deng et al., 1993) carrying 9.5 kilobases (kb) of genomic DNA containing *hoxd-11* and flanked by two herpes simplex virus thymidine kinase genes was constructed in a Bluescript-based plasmid. KT3NP4, a 3.1 kb neomycin (*neo*) resistance cassette driven by the RNA polymerase II promoter, was inserted into a *Bst*1107I site in the *hoxd-11* homeobox (Fig. 1A). This site corresponds to amino acid 23 of the homeodomain so that the insertion disrupts the coding sequence at the end of the first helix of the DNA-binding motif. Since the KT3NP4 *neo* cassette contains a very efficient poly(A) addition signal cloned from the *hprt* gene (Deng et al., 1993), *hoxd-11* transcripts 3′ of the *neo* insertion should not be synthesized. In the numerous other cases in which we have used RT-PCR to detect the presence of such transcripts, none were found. Therefore, this targeting vector should generate a loss-of-function mutation with respect to DNA binding. The potential exists for an NH_2-terminal fragment of *hoxd-11* to be synthesized and to retain some biological activity aside from DNA binding (Zappavigna et al., 1994). However, such a polypeptide fragment, if synthesized, is likely to be rapidly degraded relative to the intact, normal *hoxd-11* protein (Capecchi et al., 1974; Rechsteiner, 1987). Thus, whether the concentration of such a polypeptide fragment within the cells of the embryo could reach the critical concentration necessary to elicit a biological response is questionable.

Electroporation and ES cell line analysis

The targeting vector was linearized and electroporated into CC1.2 ES cells (Deng and Capecchi, 1992). The cells were grown in media containing the drugs G418 and FIAU to enrich for cells that had undergone a homologous recombination event (Mansour et al., 1988). Cell colonies that survived selection were picked and their DNA extracted as described (Condie and Capecchi, 1993). A primary screen of the cell lines was performed by Southern blot analysis of *Sac*I-digested genomic DNA, using the 1.0 kb *Sal*I-*Xho*I 5′ flanking probe D immediately adjacent to the targeting vector DNA (Fig. 1A). The expected shift in band size is from 13.9 kb (wild-type band) to 6.2 kb (mutant band). Targeted cell lines were confirmed by Southern blot analysis using the 3′-flanking probe I (a 1.3 kb *Xho*I-*Eco*RV fragment; see Fig. 1A,B) and a *neo*-specific probe. Six out of 90 cell lines (7%)

tested positive for a gene targeting event. The targeted ES cell line 3f-15 was injected into C57BL/6J (B6) blastocysts to produce a chimeric male that, when mated to B6 females, transmitted the mutation through the germline. Sib matings and backcrosses to B6 mice produced animals with largely B6 genetic background. All progeny were genotyped by Southern blot analysis of tail or skin DNA using a *Sac*I digest and probe D, as described above.

Skeleton preparations and whole-mount in situ hybridization

Newborn pups were collected within 48 hours of birth and killed by CO_2 asphyxiation. Skin was removed from the carcasses and used for genotyping. Skeleton preparations were made as described (Mansour et al., 1993). Bone lengths were measured under a microscope using a Digital Filar Eyepiece and M/XM processor (LASICO). For Table 2, the bones of three sex- and age-matched *hoxd-11*$^{-}$/*hoxd-11*$^{-}$ and *hoxd-11*$^{+}$/*hoxd-11*$^{+}$ animals were measured individually, averaged and the data expressed as the per cent ratio of the length of the mutant limb to that of the wild-type limb.

For whole-mount in situ hybridization, E10.5-E12.5 mouse embryos were fixed and processed as described (Carpenter et al., 1993). The digoxigenin RNA probe was transcribed from a 300 bp fragment containing the *hoxd-11* homeobox and 3′ untranslated region (Izpisúa-Belmonte et al., 1991a).

RESULTS

Creating a *hoxd-11* mutant mouse

A replacement-type gene targeting vector was constructed from mouse genomic DNA containing the *hoxd-11* gene which was disrupted by insertion of a *neo*-resistance cassette into the homeodomain encoding exon (Fig. 1A and Materials and Methods for details). The vector was introduced into CC1.2 ES cells which were then cultured under conditions chosen to enrich for a homologous recombination event. DNA isolated from individual ES cell colonies was analyzed by Southern blot hybridization for a gene targeting event using three probes (the 5′ flanking probe D, the 3′ flanking probe I and a *neo*-specific probe) and three different restriction enzyme digests (Fig. 1A). 7% of the ES cell clones analyzed had the anticipated DNA structure as a result of a *hoxd-11* gene targeting event; a representative analysis is shown in Fig. 1B. This targeted ES cell line was injected into B6-derived blastocysts to produce a chimeric male that passed the mutation through the germline. All subsequent progeny were genotyped by analysis of tail or skin DNA.

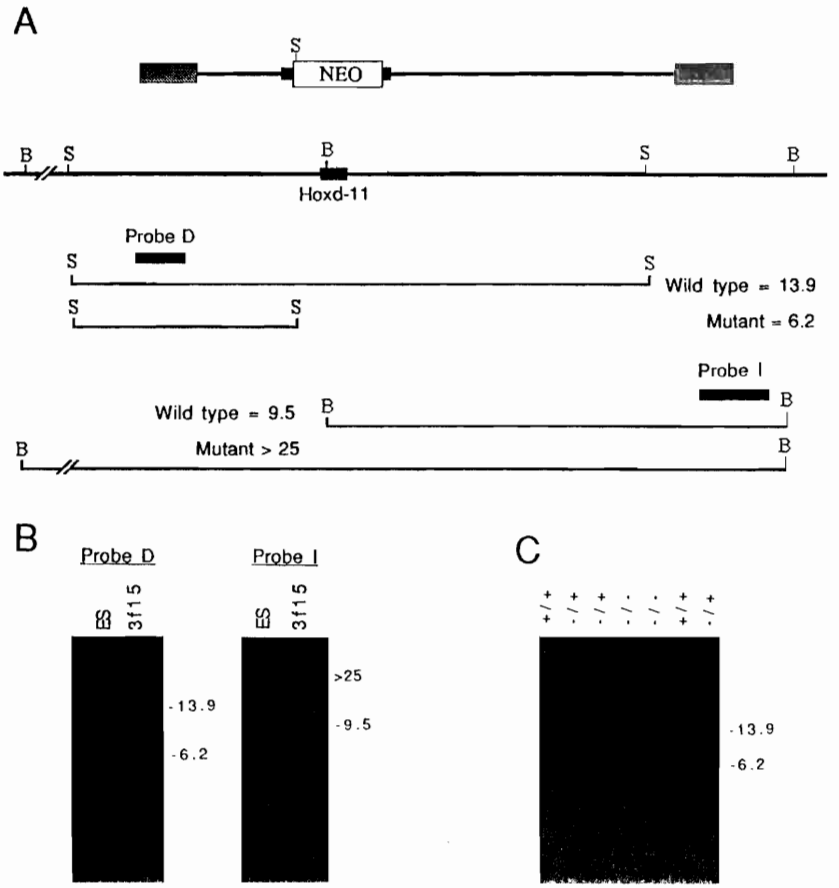

Fig. 1. Gene targeting of *hoxd-11* and genotype analysis of cell lines and mice. (A) Diagram of the targeting vector and anticipated restriction fragment lengths resulting from gene targeting. The upper line is the targeting vector. The black box indicates the homeobox of *hoxd-11*, the white box is the disrupting *neo* cassette and the grey boxes on the ends are the thymidine kinase genes. The thick line underneath is the genomic locus with restriction enzyme sites marked. Ligation of the *neo* cassette into the homeobox of *hoxd-11* destroys an endogenous *Bst* 1107 site in the gene. The expected restriction fragment lengths (in kb) for the wild-type and the targeted alleles are shown beneath for the two flanking probes D (5′ probe) and I (3′ probe). (B) Southern blot analysis of parental CC1.2 ES cells and the isolated cell line 3f-15. DNA from each cell line was digested with *Sac*I and hybridized with probe D or digested with *Bst*1107 I and hybridized with probe I to demonstrate a gene targeting event. (C) Southern blot analysis of progeny mice resulting from *hoxd-11* heterozygote intercrosses. Tail DNA from each pup was digested with *Sac*I and hybridized with probe D to allow genotyping of the animals (indicated above each lane). B=*Bst*1107 I, S=*Sac* I.

Disruption of *hoxd-11* is not lethal

Mice heterozygous for the *hoxd-11* mutation were intercrossed to produce homozygous mutant animals. Homozygosity for this mutation caused neither embryonic nor postnatal lethality as the predicted Mendelian ratio of alleles was observed among the newborn and adult mice. All pups were examined visually for general health and all appeared outwardly normal. However, *hoxd-11*$^{-}$/*hoxd-11*$^{-}$ male animals produced no offspring, suggesting that they are infertile (5/5 mice tested). Male mutants were killed and their reproductive tract was examined. Their reproductive organs and penian bone appeared anatomically normal. Sperm collected from the vas deferens appeared normal, were present in normal amounts and were motile. However, no vaginal plugs have been observed in wild-type females mated with males homozygous for the *hoxd-11* mutation. The reason for the apparent male infertility has not yet been determined.

Homeosis in the sacral vertebrae

Skeleton preparations of newborn pups were prepared to examine the structure of the vertebral column. A summary of the vertebrae patterns for the *hoxd-11*$^{-}$/*hoxd-11*$^{-}$ animals and their wild-type littermates is provided in Table 1. The lower vertebral column of a normal mouse is characterized by six lumbar and four sacral vertebrae (L6:S4 pattern), with the latter fusing together at their transverse processes to form the sacral bone (Figs 2A, 3A). Approximately 10% of wild-type mice show five lumbar vertebrae instead of six (L5:S4 pattern) in the axial skeleton (Green, 1954). While most of our wild-type mice have the L6:S4 pattern, 13% (2/16 mice) display the variant pattern L4:A1:S4, which is similar to L5:S4 except that the most posterior lumbar vertebra is asymmetric (Green, 1954). All *hoxd-11*$^{-}$ heterozygotes (30/30 mice) examined showed only the wild-type L6:S4 pattern. *Hoxd-11*$^{-}$ homozygous mice, however, were abnormal in the patterning of these posterior vertebrae. This phenotype showed incomplete penetrance (86%) and variable expressivity.

Table 1. Distribution of the vertebral phenotypes for *hoxd-11* mice

	No. of animals with the designated genotype		
Vertebrae Pattern	(+/+)	(−/+)	(−/−)
L4 : A1 : S4*	2	0	0
L6 : S4†	14	30	4
L6 : S5	0	0	7
L6 : A2 : S4*	0	0	2
L7 : S4	0	0	15

*A1 and A2 designate the asymmetric vertebra that follows four or six lumbar vertebrae, respectively.
†Wild-type pattern.

The most abundant phenotypic class of the homozygous mutants (15/28 mice) had one additional lumbar vertebra. Instead of the normal six, a seventh lumbar vertebra is present followed by four sacral vertebrae, creating an L7:S4 pattern (Figs 2B, 3B). There are two possible interpretations to account for this anomaly: (1) the *hoxd-11* mutation causes formation of a supernumerary lumbar vertebra, or (2) the mutation causes an anterior homeotic transformation of the entire sacral region in which the first sacral vertebra is transformed into lumbar 7 (S1→L7) and each subsequent sacral vertebra adopts the structure of the next most anterior vertebra.

The second possibility suggests that a deficiency of one vertebra should occur somewhere posterior to the transformation event. Unfortunately, in the remaining caudal region of the mouse the axial skeleton shows a natural variation in the number of vertebra, making such a determination impossible. However, the *hoxd-11* mutation shows variable expressivity and this variation in phenotype lends support for the second hypothesis. The next most abundant phenotypic class (7/28 mice) displayed the correct number of six lumbar vertebrae, but an additional sacral vertebra was seen (L6:S5 pattern). The additional sacral vertebra always resembled S1, such that the pattern was S1-S1-S2-S3-S4 (Fig. 3C). In addition, two *hoxd-11*$^{-}$ homozygous animals clearly showed six normal lumbar vertebrae followed by the intermediate, asymmetric vertebra

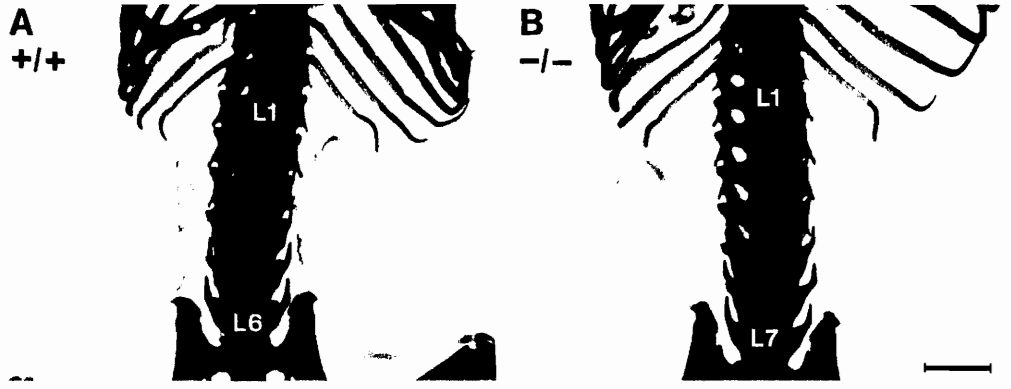

Fig. 2. *Hoxd-11* mutant mice show an additional lumbar vertebra. Ventral views of the posterior axial columns of newborn skeleton preparations from wild-type (A; genotype +/+) and *hoxd-11* mutant mice (B; −/−). The first lumbar vertebra is denoted as L1 and the last lumbar vertebra as either L6 (in A) or as the additional vertebra L7 (in B). Skeletons were stained for bone (with alizarin red) and cartilage (with alcian blue). Scale bar, 1 mm.

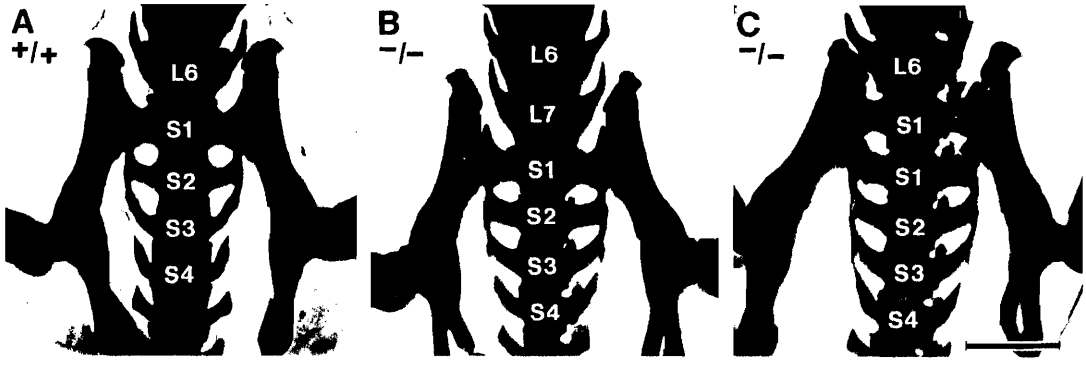

Fig. 3. Homeosis of the sacrum in *hoxd-11* mutant mice. (A) Wild-type mouse (+/+) with four sacral vertebrae (S1 through S4) following the sixth lumbar vertebra (L6) creating the L6:S4 pattern. (B) *Hoxd-11* mutant (−/−) mouse with four sacral vertebrae following the seventh lumbar vertebra (L7) creating the L7:S4 pattern. (C) *Hoxd-11* mutant (−/−) mouse demonstrating variable expressivity of the mutation. Here, five sacral vertebrae (S1-S1-S2-S3-S4) are present following the sixth lumbar segment, creating the intermediate L6:S5 pattern. Scale bar, 1 mm.

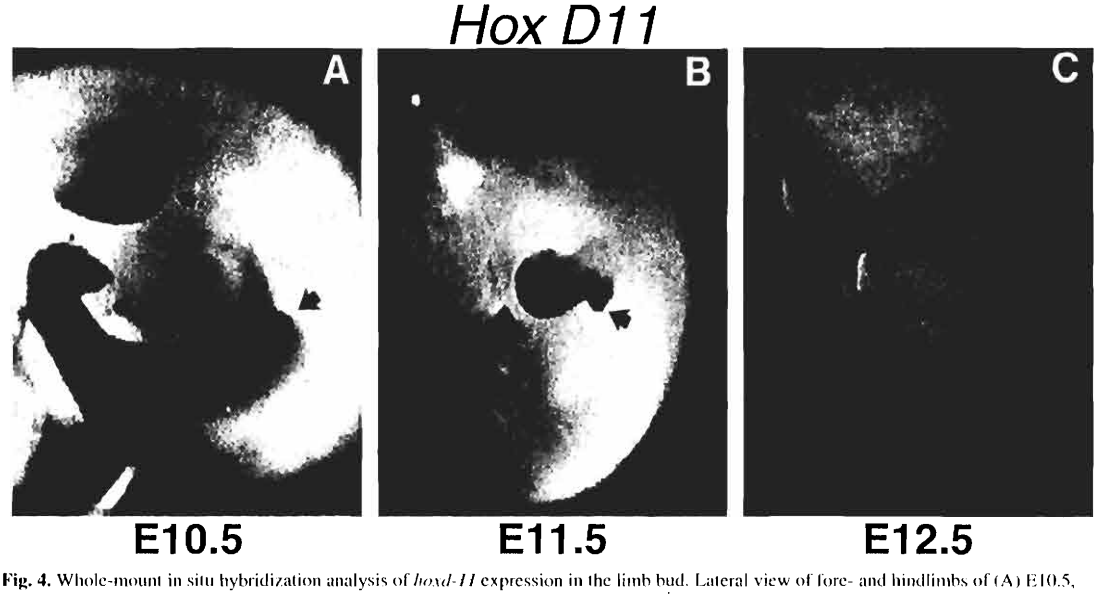

Fig. 4. Whole-mount in situ hybridization analysis of *hoxd-11* expression in the limb bud. Lateral view of fore- and hindlimbs of (A) E10.5, (B) E11.5 and (C) E12.5 embryos. *Hoxd-11* expression is initially restricted to the proximal/posterior region of the limb buds (arrows in A) and then increases in complexity, first forming two stripes (arrows in B) and then becoming more restricted to the perichondrium (C).

A2, in which the right half resembled a lumbar vertebra with an unfused transverse process, while the left half was reminiscent of S1 with its process fused to the sacral bone (Green, 1954). In this mutant, A2 was then followed by four sacral vertebrae (L6:A2:S4 pattern). Both of these examples may represent trapped intermediates in which S1 has failed to fully transform into L7 but all of the other sacral vertebrae (and at least one caudal vertebra) have undergone homeosis. To account for these intermediate phenotypes, the first explanation would have to be modified to suggest that this *hoxd-11* mutation at times causes an additional lumbar vertebra, or causes an additional sacral vertebra but not both at the same time since we never see an L7:S5 pattern. Instead, we prefer the second hypothesis, i.e., that the mutation causes an anterior homeotic transformation event that affects the entire sacrum and that variable expressivity can account for the range of phenotypes observed.

Abnormal forelimbs in *hoxd-11*$^{-}$/*hoxd-11*$^{-}$ mice

Hoxd-11 transcripts have been reported in the mouse limb bud starting at E9.0 (Dollé et al., 1989). From E9.0 to E10.5, *hoxd-11* transcripts are restricted to the proximal/posterior region of

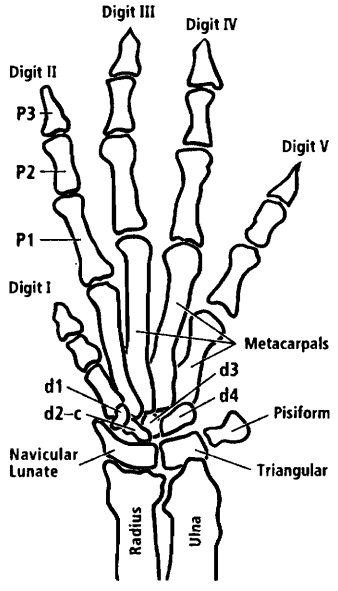

Fig. 5. Diagram of a dorsal view of the wild-type mouse forelimb skeleton. Digit I has only two phalanges (P2 and P1); all other digits have three. The distal carpal bones are labelled d1 through d4; d2-c represents the fusion between d2 and the central carpal bone c. Distal is up, proximal down, anterior to the left and posterior to the right.

Table 2. Lengths of *hoxd-11*$^{-}$/*hoxd-11*$^{-}$ forelimb bones as percent of average wild-type length

	Digit				
	I	II	III	IV	V
Phalange 3	–*	99	106	105	86
Phalange 2	110	**63**	86	88	**66**
Phalange 1	87	79	86	81	82
Metacarpal	98	**63**	**74**	**78**	89

Ulna = 99
Radius = 95

*Digit I does not have a third phalange.
Numbers in bold type represent strongest reduction in size.
Collectively, the measurements have an average standard deviation of ±7% bone length.

Proximal to the distal carpals are the navicular lunate, the triangular and the pisiform bones.

There are two readily apparent forelimb phenotypes observed in *hoxd-11*$^{-}$ homozygous animals. The length of the metacarpals (especially on digit II) is reduced, making the paw smaller, and a large gap exists between the radius and ulna (Fig. 6). There is, however, no evidence of a homeotic transformation event in which any digit adopts the structure of another. Closer examination of the forelimb revealed that phalange (P) 2 of digits II and V was also noticeably reduced in length (Fig. 7). The lengths of the metacarpals and phalanges were measured, and the results are given in Table 2. Articulations between the phalanges are sometimes malformed, especially those involving P1 and P2 of digit II which are fused in over 40% of the mutant animals (Fig. 7B).

the developing limb bud (Dollé et al., 1989; and Fig. 4A). However, by E11.5 the pattern of *hoxd-11* expression is observed to increase in complexity showing two stripes of expression, a distal and a more proximal one, which extend from the posterior to the anterior margin of the limb bud (Fig. 4B). By E12.5, *hoxd-11* expression appears to be restricted to the perichondrium (Fig. 4C). Both in terms of position and intensity, the patterns of *hoxd-11* expression are similar in the forelimbs and hindlimbs.

Since *hoxd-11* transcripts are detected in the mouse limb buds during development, skeleton preparations were examined for defects in both the forelimbs and hindlimbs. A diagram of a wild-type mouse forelimb is shown in Fig. 5. Beneath the metacarpals of each digit, there are four distal carpal bones called d1, d2, d3 and d4. In some strains of mice, d2 is split to produce an additional central carpal bone (called c). Our parental mouse strain B6, which is the predominant genetic background in the *hoxd-11* colony, does not show this division of d2 into d2 plus c. Instead, d2 remains as one larger carpal bone (referred to here as d2-c); occasionally, however, d2 has a line demarcating c, but the two bones are never fully separated.

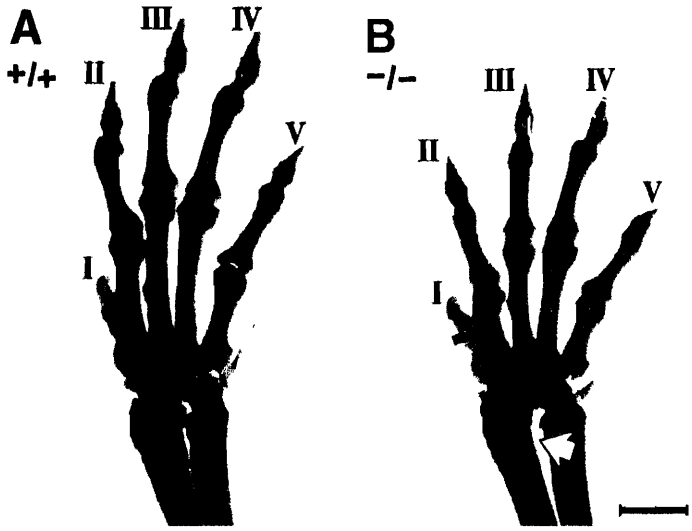

Fig. 6. Comparison of *hoxd-11*$^{-}$/*hoxd-11*$^{-}$ and wild-type forelimbs. Dorsal view of the forelimbs of a wild-type (A; +/+) and *hoxd-11* mutant littermate (B; –/–). The mutant has a large gap between the radius and ulna (open arrow in B), and the overall size of the paw is smaller due to the reduction in lengths of the metacarpals (especially digit II, closed arrow in B). Digits are labelled I through V. Notice that none of the digits has undergone any type of a homeotic transformation. Scale bar, 1 mm.

Table 3. Carpal bone phenotypes for adult *hoxd-11* mice

	No. of animals with the designated genotype		
	(+/+)	(−/+)	(−/−)
d2-c fusion*; all other carpals normal	5	1	1
d2, c separate; all other carpals normal	0	7	0
d2, c separate; NL-T fusion; P misshapen	0	0	3
d2, c separate; NL separate; T-P fusion	0	0	4
d2, c separate; NL-T-P fusion	0	0	9

*Sometimes a line demarcating d2 from c is present, but the bones are not separated.

NL (navicular lunate), T (triangular), P (pisiform).

In the distal carpals of *hoxd-11*$^-$ homozygous mice, d2 was always split into d2 plus the central bone c (Fig. 8A,B) The proximal carpal bones of these animals were also malformed. The navicular lunate, triangular and pisiform were fused together to form one large bone with the pisiform portion misshapen (Fig. 8). As with the axial skeleton, the limb phenotype showed incomplete penetrance (94%) and variable expressivity. 25% of the mutant animals had a detached navicular lunate but the triangular bone was fused to the malformed pisiform. The remaining mutants showed a fusion between the navicular lunate and the triangular while the pisiform remained separated yet malformed (Table 3). *Hoxd-11*$^-$heterozygotes also displayed a mild phenotype in the wrist. These animals had d2 separated into d2 plus c but no other defects in any of the carpal bones (Table 3).

In addition, both the radius and ulna showed minor abnormalities in *hoxd-11*$^-$/*hoxd-11*$^-$ animals. At the distal head of the ulna, the styloid process was smaller and more rounded than normal, and the radial epiphysis had a minor excrescence on its dorsal ridge and a thinning on the ventral medial side (Fig. 8A,B). Over half of the mutants (9/17 mice) also had a small sesamoid bone located on the ventral side between the radius and ulna at the distal end just below the carpals that was never seen in heterozygotes or wild-type sibs (data not shown). We believe it is a combination of these bone defects together with the fusion of the proximal carpal bones, that lead to the formation of the noticeable gap between the radius and ulna of the mutant limbs (Fig. 6B).

A summary of the forelimb defects observed in *hoxd-11*$^-$ homozygous mice is provided in Fig. 9. Interestingly, the set of defects is distributed over the autopod and extends into the zeugopod. This mutation appears to affect limb patterning along both the Pr-D and A-P axes since the lengths of the phalanges and metacarpals as well as the shapes of the wrist bones, radius and ulna are all affected.

Hindlimb phenotypes

The hindlimbs of *hoxd-11*$^-$ homozygous mice did not have any major abnormalities. However, a sesamoid bone lateral to the tibiale mediale was either absent or greatly reduced in the

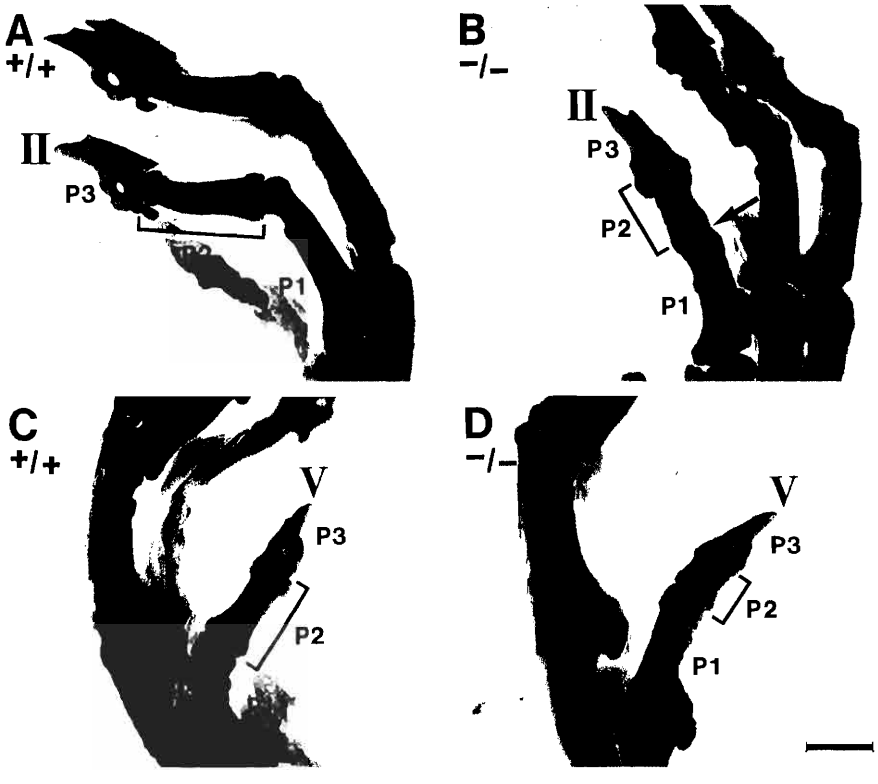

Fig. 7. Reduction in length of phalanges in *hoxd-11* mutants. Digit II of wild-type mouse (A; +/+) and *hoxd-11* mutant mouse (B; −/−). In the mutant, phalange 2 (P2) is greatly reduced (brackets) and shows partial fusion to P1 (arrow in B). Digit V of wild-type mouse (C; +/+) and *hoxd-11* mutant mouse (D; −/−). Again, P2 in the mutant is severely reduced in length (brackets). Scale bar, 0.5 mm.

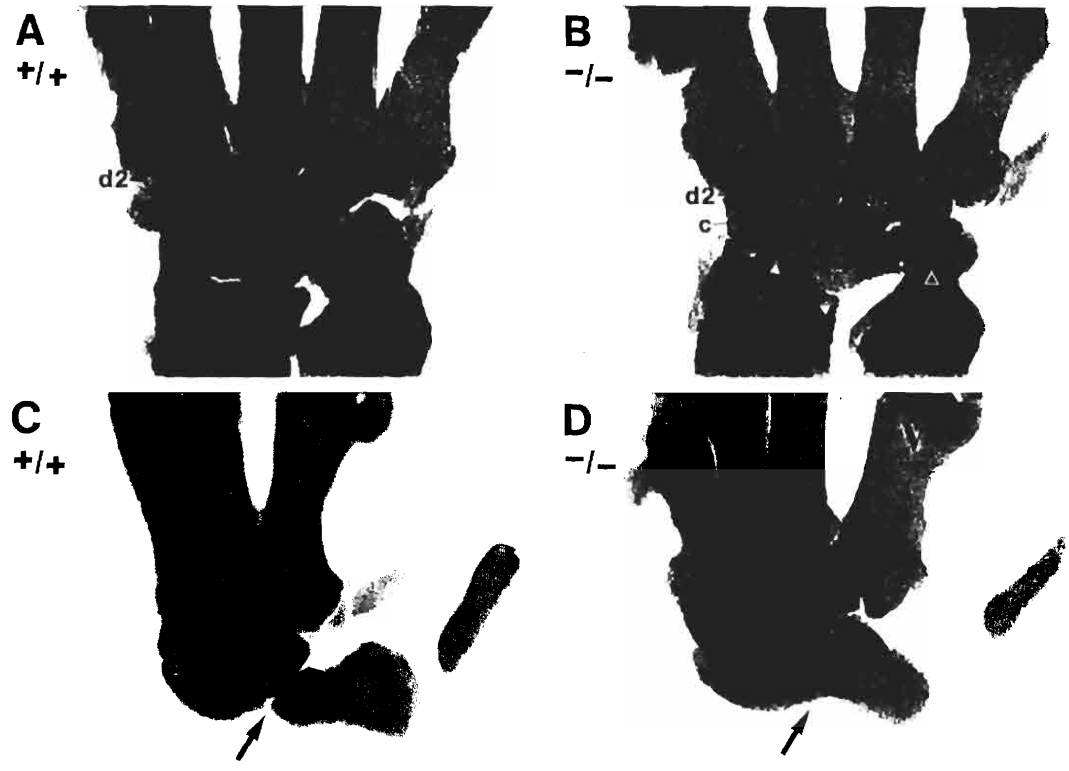

Fig. 8. Wrist bone and zeugopod phenotype in *hoxd-11* mutant mice. Dorsal view of the carpal region of a wild-type mouse (A; +/+) and *hoxd-11* mutant (B; −/−). In the mutant (B), the single carpal bone d2-c is split into two distinct bones called d2 and c; in addition, the navicular lunate and triangular bones which remain separate in the wild-type sib are fused together in the mutant (compare arrows in A and B). In the zeugopod, the distal tip of the radius (r) has a minor excrescence on its dorsal ridge and a thinning on the medial side (open arrowheads, B) while the ulna (u) has a smaller and more rounded styloid process (closed arrowhead, B). Note the large gap between the radius and the ulna in the mutant (B) as compared to the wild-type sib (A). Side view of the wrist in a wild-type mouse (C; +/+) and *hoxd-11* mutant (D; −/−) shows the fusion of a misshapen pisiform (p) to the triangular bone beneath Digit V in the mutant (compare arrows in C, D).

hoxd-11$^-$ heterozygous and homozygous animals (Fig. 10A, B). In addition, as with the distal carpal bones of the forelimb, there often existed a fusion between the tarsal navicular and cuneiforme 3 in wild-type mice while, in most of the heterozygous (6/8 mice) and homozygous mutants (16/17 mice), these two bones were completely separate (Fig. 10C-F). The absence of a severe phenotype in the hindlimbs may be due to compensation by two paralogues of *hoxd-11*. We might anticipate a greater degree of redundancy of function among the three paralogous genes in forming the hindlimb since *hoxc-11* is expressed in the hindlimb but not in the forelimb (S. L. Hostikka and Capecchi, unpublished results).

DISCUSSION

Hoxd-11$^-$ homozygotes are viable and appear outwardly normal. The only apparent abnormality is male infertility. However, the cause of male infertility has not yet been determined. The male reproductive organs and penian bone appear anatomically normal and normal amounts of motile sperm are produced. Examination of the mutant skeletons shows defects in the formation of the vertebral column and the limbs. Thus, structure of the skeleton along the major body axis as well as along the appendicular axis is affected, emphasizing that *Hox* genes function as a multiaxial patterning system in mammals.

Anterior homeotic transformation of the sacrum

Hoxd-11$^-$/*hoxd-11*$^-$ animals have a deviant vertebral pattern in the lumbar/sacral region. Instead of the wild-type pattern of six lumbar and four sacral vertebrae (L6:S4), the homozygous mutants generally have seven lumbar and four sacral vertebrae (L7:S4). This mutant pattern may be the result of an anterior homeotic transformation of the entire sacral region initiating with S1. This conclusion is supported by the intermediate phenotypes produced by variable expressivity of the mutation (see Results). There exists ample precedence that loss-of-function mutations in *Hox* genes cause apparent homeotic transforma-

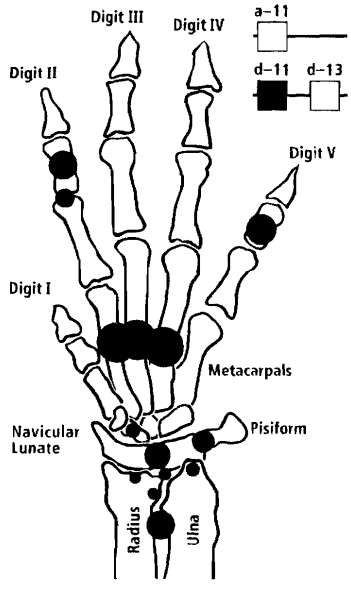

Fig. 9. Summary of the major forelimb phenotypes seen in *hoxd-11* mutant mice. Red dots represent the site of limb defects. From proximal to distal, these include: a large gap between the radius and ulna, malformations of both the radial and ulnar epiphysis, an aberrant sesamoid bone between the radius and ulna, two fusions between the three proximal carpal bones, a split of the carpal bone d2-c, the reduction in metacarpal lengths (digits II, III, IV), a fusion between P1 and P2 (digit II) and a strong reduction in the length of P2 (digits II and V).

tions of components of the vertebral column (LeMouellic et al., 1992; Ramirez-Solis et al., 1993; Jeannotte et al., 1993; Kostic and Capecchi, 1994; Condie and Capecchi, 1994). Disruption of *hoxd-13*, another member of the 5′-*Hox D* locus, also produces an apparent homeotic transformation in the sacral region (Dollé et al., 1993). This phenotype, however, is restricted to the most posterior portion of the sacrum (i.e., a transformation of S4 to S3). The site of homeosis for *hoxd-11* mutants is consistent with its anterior limit of expression in the prevertebrae, thus supporting the posterior prevalence model (Duboule, 1991). However, since the transformation in the *hoxd-11* mutant mouse requires each vertebra to adopt the structure of the next most anterior vertebra, as opposed to transformation of the entire region to one vertebral fate, a more complex scenario involving a fine-tuning mechanism must be envisioned.

Interestingly, disruption of *hoxa-11*, a paralogue of *hoxd-11*, appears to result in the same homeotic transformation of the sacral vertebrae observed in *hoxd-11* mutant mice (Small and Potter, 1993). In this case, however, the anterior limit of expression for *hoxa-11* is reported to be at prevertebra 20 rather than at prevertebra 25, the site where homeosis of the sacrum is initiated. Perhaps, the disruption of *hoxa-11* alters the expression pattern of *hoxd-11*, thereby accounting for the identical transformation of the sacrum. Alternatively, *hoxa-11* and *hoxd-11* may function together to specify the morphology of the sacrum. In this context, it will be of interest to analyze mice defective for both *hoxa-11* and *hoxd-11*.

Forelimb defects in *hoxd-11* mutant mice

Hoxd-11^{-}/*hoxd-11*$^{-}$ animals show several malformations in the appendicular skeleton of the forelimb. From proximal to distal, these defects include: a large gap between the radius and ulna, malformations of both the radial and ulnar epiphysis, the presence of an aberrant sesamoid bone between the radius and ulna, a fusion between the three proximal carpal bones (navicular lunate, triangular and a misshapen pisiform), a split of the distal carpal bone d2-c into d2 plus a central bone (called c), reduction in metacarpal length (digit II, III, IV), fusion between phalanges 1 and 2 (digit II), and a strong reduction in length of phalange 2 (digit II, V).

Surprisingly, the hindlimbs of these mutant animals appear fairly normal, except for the failure of a fusion between two tarsal bones and a reduction in the size of a sesamoid bone located next to the tibiale mediale. The absence of more severe hindlimb defects may reflect overlapping functions supplied by a paralogous member of the *Hox C* linkage group which is expressed in hindlimbs but not in forelimbs. It should be noted that, with respect to the *hoxa-11* and *hoxd-13* mutant phenotypes, the forelimbs and hindlimbs are equally affected. As might be expected, the degree of overlapping function between paralogous *Hox* genes varies from gene to gene.

The set of digit defects observed in *hoxd-11* mutant mice is difficult to interpret in terms of a model where digit identity is specified solely by a gradient of a diffusible morphogen emanating from the zone of polarizing activity (Tabin, 1991). Thus, the set of defects of the digits does not appear to be polarized with respect to the ZPA. The length of phalange 2 of digits II and V is strongly affected with much less effect on the lengths of the same phalanges in digits III and IV. In contrast, the lengths of the metacarpals of digits II, III and IV are reduced without alteration in the metacarpal lengths of digits I and V. Based on the nested set of *Hox D* gene expression patterns in the limb and the observation that ectopic expression of mouse *hoxd-11* in the chick limb sometimes resulted in a homeotic transformation of digit identity, a *Hox D* code was proposed for specifying digit identity (Morgan et al., 1992). The limb phenotype associated with disruption of *hoxd-11* does not support this model. From a comparison of the phenotypes resulting from disruption of *hoxa-11*, *hoxd-11* and *hoxd-13*, it also appears unlikely that even combining mutations in paralogous 'limb' *Hox* genes will reveal homeosis of the digits (see below).

Overlap of phenotypes among *hoxd-11*, *hoxa-11* and *hoxd-13* mutant mice

The recent description of mice with targeted disruptions in *hoxa-11*, a paralogue of *hoxd-11* (Small and Potter, 1993), and another member of the *Hox D* linkage group, *hoxd-13* (Dollé et al., 1993), allows us to compare the limb phenotypes of these mutant mice with those of *hoxd-11* mutants. Fig. 11 summarizes the forelimb phenotypes for mice carrying disruptions in *hoxa-11*, *hoxd-11* and *hoxd-13*. Four points are evident. First, there are overlapping defects for *hoxd-11* with both *hoxa-11* (ulnar epiphysis, sesamoid bone, carpal bone fusions, misshapen pisiform) and *hoxd-13* (metacarpal and phalanges) mutants. Secondly, each mutant shows unique phenotypes not

present in the other two (for details see Dollé et al., 1993; Small and Potter, 1993). Thirdly, targeted disruption of these *Hox* genes does not cause homeosis of the digits. Lastly, the position of the most proximal phenotype for all three mice parallels both the chromosome position (structural colinearity) and the activation order of these genes (temporal colinearity). *Hoxa-11* and *hoxd-11* deformities are initiated in the zeugopod (the radius and ulna long bones) while *hoxd-13* mutant animals are limited to defects in the later forming distal autopod.

The overlapping phenotypes seen in *hoxa-11* and *hoxd-11* mutant mice might have been anticipated, since defects in mice with mutations in paralogous genes appear to be restricted to the same regions of the embryo (Chisaka and Capecchi, 1992; Condie and Capecchi, 1993). We would like to suggest that in the regions of overlap the two paralogous gene products may function synergistically to regulate the growth of localized groups of cells. This suggestion is influenced by our recent analysis of mice doubly mutant for the two paralogous genes, *hoxa-3* and *hoxd-3* (unpublished data). Even though mice with mutations in one or the other of these genes show no overlap in phenotype, the double mutants demonstrate that these two genes strongly interact. The *hoxa-3* mutant phenotype is exacerbated in mice homozygous for both targeted disruptions. Likewise, the *hoxd-3* phenotype is exacerbated in the double mutant. The interactions appear to be quantitative since the degree of exacerbation of the *hoxd-3* phenotype in (*hoxd-3*$^-$/*hoxd-3*$^-$; *hoxa-3*$^-$/*hoxa-3*$^+$) mice is intermediate to that observed in (*hoxd-3*$^-$/*hoxd-3*$^-$; *hoxa-3*$^+$/*hoxa-3*$^+$) or (*hoxd-3*$^-$/*hoxd-3*$^-$; *hoxa-3*$^-$/*hoxa-3*$^-$) mutant mice. The interactions between these genes and the resultant phenotypes are readily interpretable in terms of models in which these genes synergistically control the rates of proliferation of localized groups of cells. In light of the above discussion, it will be of interest to examine the limbs (and the sacrum) of mice mutant for both *hoxa-11* and *hoxd-11*. Since these genes are on separate chromosomes, double mutants can be generated by intercrosses.

The overlap of forelimb phenotypes observed in *hoxd-11* and *hoxd-13* mutant mice is also intriguing. Again we can postulate that, in the regions of overlap, the two gene products

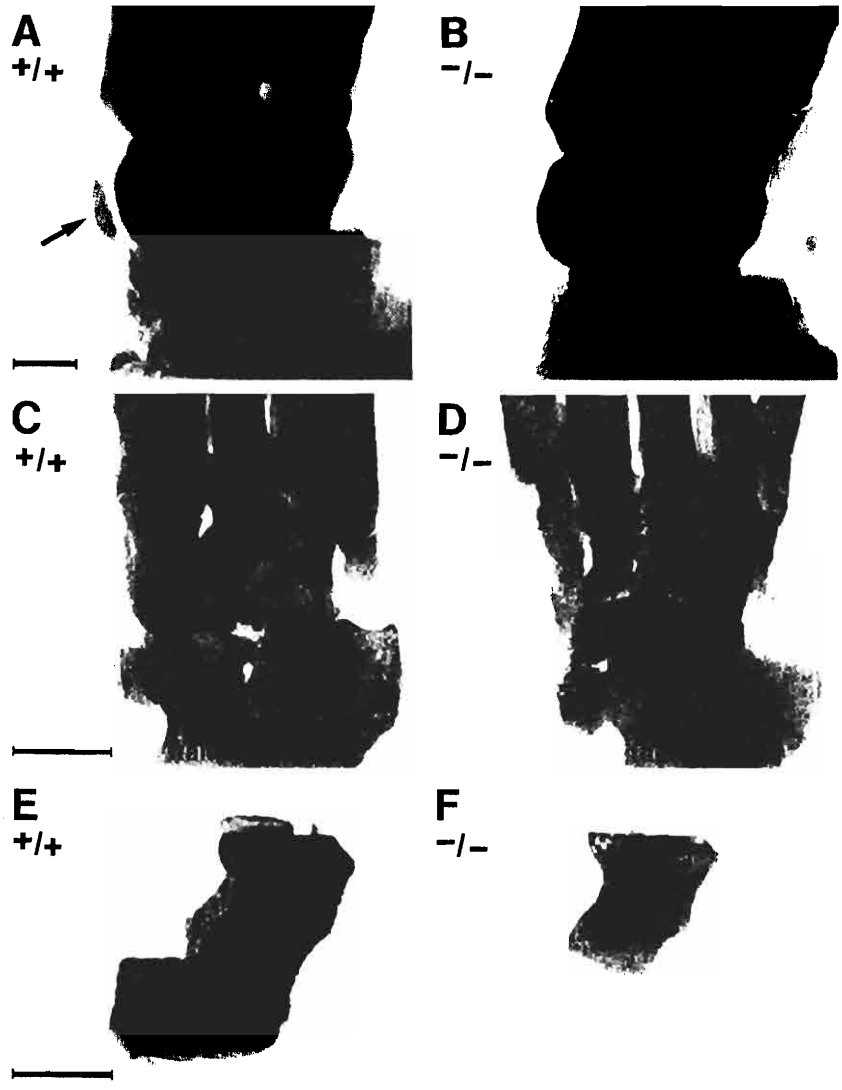

Fig. 10. Hindlimb defects in *hoxd-11* mutant mice. A sesamoid bone next to the tibiale mediale (tm) in the wild-type mouse (arrow in A; +/+) is absent in the mutant (B; −/−). The normal fusion between the tarsal bones navicular (n) and cuneiforme 3 (c3) in the wild-type mouse (arrow in C; +/+) does not appear in the mutant (arrow in D; −/−). Dissection of the tarsal bones shows how the navicular and cuneiforme 3 remain fused in the wild-type mouse (E) but separate in the mutant (F). Scale bars, (A, B) 0.25 mm; (C, D) 0.5 mm; (E, F) 0.4 mm. The talus is the most proximal tarsal bone and is labelled for orientation.

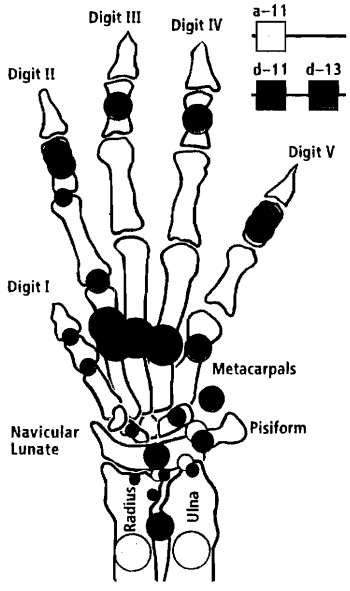

Fig. 11. A composite diagram of the mouse forelimb phenotypes from individual gene targeting experiments of *hoxd-11* (this report), *hoxa-11* (Small and Potter, 1993) and *hoxd-13* (Dollé et al., 1993). The colored dots represent the physical position of a mutant phenotype when compared to wild-type sibs. *Hoxa-11* is a paralogue of *hoxd-11* and *hoxd-13* is another member of the *Hox D* locus. The diagram illustrates several points: (1) the overlapping phenotypes that *hoxd-11* mutant mice share with both *hoxa-11* and *hoxd-13* animals, (2) the unique phenotypes each mutant displays, (3) that *hoxd-11* mutants show more proximal phenotypes than *hoxd-13* mutants reflecting both structural and temporal colinearity, and (4) that the loss-of-function mutations of *Hox* genes in the limb do not cause homeosis, but instead result in localized malformation of several bones that do not appear to be polarized with respect to the ZPA.

are cooperating in regulating the formation of bones. Alternatively, some of the defects observed in *hoxd-11* mutant mice could be caused by disruption of the temporal sequence of activation of other *Hox D* genes. For example, phalange 2 of digits II and V in *hoxd-11* mice is severely reduced in length; in *hoxd-13* mutant animals, however, these elements are entirely missing. Disruption of *hoxd-11* may influence *hoxd-13* by retarding its activation, and thereby mimicking its phenotype, though with a reduced severity. Mice doubly mutant for *hoxd-11* and *hoxd-13* might resolve the issue of whether these two gene products interact synergistically to control the proliferation rates of common precursor cells or whether a mutation in *hoxd-11* disrupts the temporal progression of the *Hox D* gene activation during patterning of the limb.

In summary, limb bones are formed from prechondrogenic condensations as the limb bud grows. The pattern of these condensations may be inherently dependent upon the overall limb geometry (Oster et al., 1988). A sequence of segmentations and bifurcations of these condensations occurs in a Pr-D direction to create the long bones (humerus, then radius and ulna). This is followed by condensations progressing in an A-P manner to generate the carpals, metacarpals and digits (Shubin and Alberch, 1986). Disruption of *hoxd-11*, as described here, affects the morphology of bones arising from both the Pr-D and A-P condensations. In addition, malformations of the same bones are independently affected by disruptions in *hoxa-11* and *hoxd-13* (see Fig. 11). These observations taken together suggest that these *Hox* genes do not code for distinct positional information, per se, dictated solely by an A-P morphogenic gradient. Rather, what is emerging is a more complex set of interactions among these *Hox* genes, in which each is responsible for localized regions of cell growth. Perturbations in the pattern of localized growth rates of the cells contributing to the prechondrogenic condensations could then lead to the loss of structures, fusion between bones and even additional elements. All three phenotypes are seen in mice mutant for *hoxa-11, hoxd-11 and hoxd-13.*

We want to acknowledge and thank S. L. Hostikka for doing the whole-mount in situ hybridizations. We also want to thank M. Allen, S. Barnett, C. Lenz, E. Nakashima and S. Tamowski for excellent technical assistance. K. Thomas, D. Spyropoulos and T. Tsuzuki provided certain DNA probes and vector cassettes, D. Rancourt provided the phage library of CC1.2 genomic DNA, and B. Condie and T. Musci provided help with histology. We thank C. S. Thummel for the use of the Digital Filar Eyepiece and M/XM processor. L. Oswald helped with the preparation of the manuscript. A. P. D. is the recipient of an NSF predoctoral fellowship and an NIH genetics training grant.

REFERENCES

Acampora, D., D'Esposito, M., Faiella, A., Pannese, M., Migliaccio, E., Morelli, F., Stornauiolo, A., Nigro, V., Simeone, A. and Boncinelli, E. (1989). The human hox gene family. *Nucleic Acids Res.* **17**, 10385-10402.

Akam, M. E. (1987). The molecular basis for metameric pattern in the *Drosophila* embryo. *Development* **101**, 1-22.

Capecchi, M. R., Capecchi, N. E., Hughes, S. H. and Wahl, G. M. (1974). Selective degradation of abnormal proteins in mammalian tissue culture cells. *Proc. Natl. Acad. Sci. USA* **71**, 4732-4736.

Capecchi, M. R. (1989). Altering the genome by homologous recombination. *Science* **244**, 1288-1292.

Capecchi, M. R. (1994). Targeted gene replacement. *Sci. Am.* **270**, 54-61.

Carpenter, E. M., Goddard, J. M., Chisaka, O., Manley, N. R. and Capecchi, M. R. (1993). Loss of *Hoxa-1 (Hox-1.6)* function results in the reorganization of the murine hindbrain. *Development* **118**, 1063-1075.

Chisaka, O. and Capecchi, M. R. (1991). Regionally restricted developmental defects resulting from targeted disruption of the mouse homeobox gene *hox-1.5*. *Nature* **350**, 473-479.

Chisaka, O., Musci, T. S. and Capecchi, M. R. (1992). Developmental defects of the ear, cranial nerves and hindbrain resulting from targeted disruption of the mouse homeobox gene *Hox-1.6*. *Nature* **355**, 516-520.

Condie, B. G. and Capecchi, M. R. (1993). Mice homozygous for a targeted disruption of *Hoxd-3 (Hox-4.1)* exhibit anterior transformations of the first and second cervical vertebrae, the atlas and the axis. *Development* **119**, 579-595.

Deng, C. and Capecchi, M. R. (1992). Reexamination of gene targeting frequency as a function of the extent of homology between the targeting vector and the target locus. *Mol. Cell. Biol.* **12**, 3365-3371.

Deng, C., Thomas, K. R. and Capecchi, M. R. (1993). Location of crossovers during gene targeting with insertion and replacement vectors. *Mol. Cell. Biol.* **13**, 2134-2140.

Dollé, P., Dierich, A., LeMeur, M., Schimmang, T., Schuhbaur, B., Chambon, P. and Duboule, D. (1993). Disruption of the *Hoxd-13* gene induces localized heterochrony leading to mice with neotenic limbs. *Cell* **75**, 431-441.

Dollé, P., Izpisúa-Belmonte, J. C., Boncinelli, E. and Duboule, D. (1991a). The *Hox-4.8* gene is localized at the 5′ extremity of the *Hox-4* complex and is expressed in the most posterior parts of the body during development. *Mech. Dev.* **36**, 3-13.

Dollé, P., Izpisúa-Belmonte, J. C., Brown, J. M., Tickle, C. and Duboule, D.

(1991b). *Hox-4* genes and the morphogenesis of mammalian genitalia. *Genes Dev.* 5, 1767-1776.

Dollé, P., Izpisúa-Belmonte, J. C., Falkenstein, H., Renucci, A. and Duboule, D. (1989). Coordinate expression of the murine *Hox-5* complex homeobox-containing genes during limb pattern formation. *Nature* **342**, 767-772.

Duboule, D. (1991). Patterning in the vertebral limb. *Curr. Opin. Genet. Dev.* **1**, 211-216.

Duboule, D. (1992). The vertebrate limb: a model system to study the Hox/HOM gene network during development and evolution. *BioEssays* **14**, 375-384.

Duboule, D. and Dollé, P. (1989). The structural and functional organization of the murine *Hox* gene family resembles that of *Drosophila* homeotic genes. *EMBO J* **8**, 1497-1505.

Echelard, Y.,Epstein, D. J., St-Jacques, B., Shen, L., Mohler, J., McMahon, J. A. and McMahon, A. P. C. (1993). *Sonic hedgehog*, a member of a family of putative signaling molecules, is implicated in the regulation of CNS polarity. *Cell* **75**, 1417-1430.

Gendron-Maguire, M., Mallo, M., Zhang, M. and Gridley, T. (1993). *Hoxa-2* mutant mice exhibit homeotic transformation of skeletal elements derived from cranial neural crest. *Cell* **75**, 1317-1331.

Graham, A., Papalopulu, N. and Krumlauf, R. (1989). The murine and *Drosophila* homeobox gene complexes have common features of organization and expression. *Cell* **57**, 367-378.

Green, E. L. (1954). Quantitative genetics of skeletal variations in the mouse. I. Crosses between three short-ear strains (P, NB, SEC/2). *J. Natl. Cancer Inst.* **15**, 609-627.

Haack, H. and Gruss, P. (1993). The establishment of murine Hox-1 expression domains during patterning of the limb. *Dev. Biol.* **157**, 410-422.

Hinchliffe, R. (1991). Developmental approaches to the problem of transformation of limb structure in evolution. In *Developmental Patterning of the Vertebrate Limb* (Eds. J. R. Hinchliffe, J. M. Hurle and D. Summerbell). New York: Plenum Publishing Corp.

Izpisúa-Belmonte, J.-C., Falkenstein, H., Dollé, P., Renucci, A. and Duboule, D. (1991a). Murine genes related to the *Drosophila AbdB* homeotic gene are sequentially expressed during development of the posterior part of the body. *EMBO J.* **10**, 2279-2289.

Izpisúa-Belmonte, J.-C., Tickle, C., Dollé, P., Wolpert, L. and Duboule, D. (1991b). Expression of the homeobox *Hox-4* genes and the specification of position in chick wing development. *Nature* **350**, 585-589.

Izpisúa-Belmonte, J.-C. and Duboule, D. (1992). Homeobox genes and pattern formation in the vertebrate limb. *Dev. Biol.* **152**, 26-36.

Jeannotte, L., Lemieux, M., Charron, J., Poirier, F. and Robertson, E. J. (1993). Specification of axial identity in the mouse: role of the *Hoxa-5* (*Hox-1.3*) gene. *Genes Dev.* **7**, 2085-2096.

Kissinger, C. R., Liu, B., Martin-Blanco, E., Kornberg, T. B. and Pabo, C. O. (1990). Crystal structure of an engrailed homeodomain-DNA complex at 2.8 Å resolution: a framework for understanding homeodomain-DNA interactions. *Cell* **63**, 579-590.

Kostic, D. and Capecchi, M. R. (1994). Targeted disruptions of the murine *hoxa-4* and *hoxa-6* genes result in homeotic transformations of components of the vertebral column. *Mech. Dev.* In press.

LeMouellic, H., Lallemand, Y. and Brûlet, P. (1992). Homeosis in the mouse induced by a null mutation in the *Hox-3.1* gene. *Cell* **69**, 251-264.

Lewis, E. B. (1978). A gene complex controlling segmentation in *Drosophila*. *Nature* **276**, 565-570.

Lufkin, T., Dierich, A., LeMeur, M., Mark, M. and Chambon, P. (1991). Disruption of the *Hox-1.6* homeobox gene results in defects in a region corresponding to its rostral domain of expression. *Cell* **66**, 1105-1119.

Mansour, S. L., Thomas, K. R. and Capecchi, M. R. (1988). Disruption of the proto-oncogene *int-2* in mouse embryo-derived stem cells: A general strategy for targeting mutations to nonselectable genes. *Nature* **336**, 348-352.

Mansour, S. L., Goddard, J. M. and Capecchi, M. R. (1993). Mice homozygous for a targeted disruption of the proto-oncogene *int-2* have developmental defects in the tail and inner ear. *Development* **117**, 13-28.

Mark, M., Lufkin, T., Vonesch, J. L., Ruberte, E., Olivo, J.-C., Dollé, P., Gorry, P., Lumsden, A. and Chambon P. (1993). Two rhombomeres are altered in *Hoxa-1* mutant mice. *Development* **119**, 319-338.

McGinnis, N., Kuziora, M. A. and McGinnis, W. (1990). Human *Hox-4.2* and Drosophila *Deformed* encode similar regulatory specificities in Drosophila embryos and larvae. *Cell* **63**, 969-976.

McGinnis, W. and Krumlauf, R. (1992). Homeobox genes and axial patterning. *Cell* **68**, 283-302.

Morgan, B. A., Izpisúa-Belmonte, J.-C., Duboule, D. and Tabin, C. J. (1992). Targeted misexpression of *Hox-4.6* in the avian limb bud causes apparent homeotic transformations. *Nature* **358**, 236-239.

Nohno, T., Noji, S., Koyama, E., Ohyama, K., Myokai, F., Kuroiwa, A., Saito, T. and Taniguchi, S. (1991). Involvement of the *Chox-4* chicken homeobox genes in determination of anteroposterior axial polarity during limb development. *Cell* **64**, 1197-1205.

Oster, G. F., Shubin, N., Murray, J. D. and Alberch, P. (1988). Evolution and morphogenetic rules: the shape of the vertebrate limb in ontogeny and phylogeny. *Evolution* **42**, 862-884.

Otting, G., Qian, Y. Q., Billeter, M., Muller, M., Affolter, M., Gehring, W. J. and Wuthrich, K. (1990). Protein--DNA contacts in the structure of a homeodomain--DNA complex determined by nuclear magnetic resonance spectroscopy in solution. *EMBO J.* **9**, 3085-3092.

Pendleton, J. W., Nagai, B. K., Murtha, M. T. and Ruddle, F. H. (1993). Expansion of the *Hox* gene family and the evolution of chordates. *Proc. Natl. Acad. Sci. USA* **90**, 6300-6304.

Ramirez-Solis, R., Zheng, H., Whiting, J., Krumlauf, R. and Bradley, A. (1993). *Hoxb-4* (*Hox-2.6*) mutant mice show homeotic transformation of a cervical vertebra and defects in the closure of the sternal rudiments. *Cell* **73**, 279-294.

Rechsteiner, M. (1987). Ubiquitin-mediated pathways for intracellular proteolysis. *A. Rev. Cell. Biol.* **3**, 1-30.

Riddle, R., Johnson, R. L., Laufer, E. and Tabin, C. (1993). *Sonic hedgehog* mediates the polarizing activity of the ZPA. *Cell* **75**, 1401-1416.

Rijli, F. M., Mark, M., Lakkaraju, S., Dierich, A., Dollé, P. and Chambon, P. (1993). A homeotic transformation is generated in the rostral branchial region of the head by disruption of *Hoxa-2*, which acts as a selector gene. *Cell* **75**, 1333-1349.

Saunders, J. W. (1977). The experimental analysis of chick limb bud development. In *Vertebrate Limb and Somite Morphogenesis*. (Eds. D. A. Ede, J. R. Hinchliffe and M. Balls). Cambridge: Cambridge University Press, pp. 289-314.

Shubin, N. H. and Alberch, P. (1986). A morphogenetic approach to the origin and basic organization of the tetrapod limb. *Evol. Biol.* **20**, 319-387.

Small, K. M. and Potter, S. S. (1993). Homeotic transformations and limb defects in *Hoxa-11* mutant mice. *Genes Dev.* **7**, 2318-2328.

Tabin, C. J. (1991). Retinoids, homeoboxes and growth factors: toward molecular models for limb development. *Cell* **66**, 199-217.

Tabin, C. J. (1992). Why we have (only) five fingers per hand: Hox genes and the evolution of paired limbs. *Development* **116**, 289-296.

Thomas, K. R. and Capecchi, M. R. (1987). Site-directed mutagenesis by gene targeting in mouse embryo-derived stem cells. *Cell* **51**, 503-512.

Thomas, K. R., Deng, C. and Capecchi, M. R. (1992). High-fidelity gene targeting in embryonic stem cells by using sequence replacement vectors. *Mol. Cell. Biol.* **12**, 2919-2923.

Tickle, C., Summerbell, D. and Wolpert, L. (1975). Positional signalling and specification of digits in chick limb morphogenesis. *Nature* **254**, 199-202.

Yokouchi, Y., Sasaki, H. and Kuroiwa, A. (1991). Homeobox gene expression correlated with the bifurcation process of limb cartilage development. *Nature* **353**, 443-445.

Zappavigna, V., Sartori, D. and Mavilio, F. (1994). Specificity of HOX protein function depends on DNA-protein and protein-protein interactions, both mediated by the homeo domain. *Genes Dev.* **8**, 732-744.

(Accepted 2 May 1994)

CHAPTER 3

ABSENCE OF RADIUS AND ULNA IN MICE LACKING *hoxa-11* AND *hoxd-11*

The following chapter is a reprint of an article coauthored by David P. Witte, Hsiu M. Hsieh-Li, S. Steven Potter, Mario R. Capecchi, and me. This article was originally published in *Nature*, Volume 375, pages 791-795, 29 June, 1995 It is reprinted here with the permission of the coauthors and Macmillan Magazines, Limited.

Absence of radius and ulna in mice lacking *hoxa-11* and *hoxd-11*

Allan Peter Davis*, David P. Witte†, Hsiu M. Hsieh-Li†, S. Steven Potter† & Mario R. Capecchi*‡

* Howard Hughes Medical Institute, Department of Human Genetics, University of Utah School of Medicine, Salt Lake City, Utah 84112, USA
† Division of Basic Science Research and Pathology, Children's Hospital Research Foundation and Department of Pediatrics, University of Cincinnati College of Medicine, Cincinnati, Ohio 45229, USA
‡ To whom correspondence should be addressed

MICE with targeted disruptions[1] in *Hox* genes have been generated to evaluate the role of the *Hox* complex in determining the mammalian body plan. This complex of 38 genes encodes transcription factors that specify regional information along the embryonic axes. Early in vertebrate evolution an ancestral complex shared with invertebrates was duplicated twice to give rise to the four linkage groups (Hox A, B, C and D)[2,3]. As a consequence, corresponding genes on the separate linkage groups, called paralogues, are most closely related to each other. Based on sequence similarities, the *Hox* genes have been subdivided into 13 paralogous groups. The five most 5′ groups (*Hox* 9–13) pattern the posterior region of the vertebrate embryo and the appendicular skeleton[4–18]. Mice with individual mutations in the paralogous genes *hoxa-11* and *hoxd-11* have been described[15–18]. By breeding these two strains together we have generated double mutants which have dramatic phenotypes not apparent in mice homozygous for the individual mutations. The radius and the ulna of the forelimb are almost entirely eliminated, the axial skeleton shows homeotic transformations, and there are severe kidney defects not present in either single mutant. The limb and axial phenotypes are quantitative: as more mutant alleles are added to the genotype, the phenotype becomes progressively more severe. The appendicular skeleton defects suggest that paralogous *Hox* genes function together to specify limb outgrowth and patterning along the proximodistal axis.

For simplicity, we use 'A' (wild-type allele) and 'a' (mutant allele) to designate the *hoxa-11* genotype, and similarly 'D' and 'd' for *hoxd-11*. Compound heterozygotes (Aa; Dd) were crossed to each other to generate all nine genetic states. Four (aa; dd) adults were weaned from a total of 313 progeny. This is fewer than the 20 expected; most double mutants suffer perinatal death as a consequence of kidney dysfunction (see below). All other genotypes occurred in the expected Mendelian ratios.

The vertebrate forelimb is divided into three zones: the stylopod (humerus), zeugopod (radius and ulna), and autopod (carpals, metacarpals and phalanges) (Fig. 1*a*). The hindlimb is similarly arranged. All four limbs of the double mutants are severely affected. Synergistic effects of *hoxa-11* and *hoxd-11* are dramatic in the forelimb zeugopod wherein individual mutant homozygotes (aa; DD) and (AA; dd) show subtle malformations of the zeugopod (Fig. 1*b*, *c*), but, remarkably, the radius and ulna are almost entirely absent from double-mutant limbs (Fig. 1*d*). These extraordinary malformations result in a paw that is rotated 90° off its normal axis.

There are similar effects in the autopod. The wrist contains seven bones: three proximal carpals (pisiform, triangular and navicular lunate) and four distal carpals (d1–d4). In (aa; DD) and (AA; dd) forelimbs the proximal carpal bones are fused together[15–17]. Although individual heterozygotes never show this defect, compound heterozygotes (Aa; Dd) do (Table 1). This suggests that any two mutant alleles (either both from *hoxa-11* or *hoxd-11*, or one from each locus) will cause carpal fusions. Genotypes (Aa; dd) and (aa; Dd), with three mutant alleles, have more severe defects of the proximal carpal bones in which the triangular and pisiform bones are grossly malformed, and the navicular lunate is slightly deformed (results not shown).

TABLE 1 Axial and carpal bone phenotypes of (*hoxa-11*; *hoxd-11*) mice

	Axial column phenotypes			Carpal bone phenotypes				
						Carpal bone fusions¶		
Genotype*	Phenotype†	Frequency (%)‡	Comments§	Genotype	Wild-type (%)	NL-T	T-P	NL-T-P
(AA; DD)	T13:L6	100	wild-type	(AA; DD)	100			
(Aa; DD)	T13:L6	50	wild-type	(Aa; DD)	100			
	T12:L7	50	PHT					
(aa; DD)	T12:L8	50	PHT and AHT	(aa; DD)	33	17%	50%	
	T12:L7:AL/s	50	PHT and AHT					
(AA; Dd)	T13:L6	100	wild-type	(AA; Dd)	100			
(AA; dd)	T13:L7	50	AHT	(AA; dd)		17%	17%	67%
	T13:L6:AL/s	50	AHT					
(Aa; Dd)	T12:L7	33	PHT	(Aa; Dd)	17	17%	33%	33%
	T13:L7	33	AHT					
	T12:AT/L:L6	17	PHT					
	T12:AT/L:L7	17	PHT and AHT					
(Aa; dd) and (aa; Dd)‖	T12:L8	67	PHT and AHT					
	T13:L7	33	AHT					
(aa; dd)	T12:L9	75	PHT and AHT					
	T12:L8:AL/s	25	PHT and AHT					

* A, *hoxa-11* wild-type allele; a, mutant allele; D, *hoxd-11* wild-type allele; d, mutant allele.
† T13:L6, wild-type pattern with 13 thoracics (T) followed by 6 lumbars (L). AL/s is an asymmetric vertebra: half is lumbar-like, half is sacral-like. AT/L is an asymmetric vertebra: half is thoracic-like, half is lumbar-like.
‡ Examined six animals for each genotype, except for (aa; dd) where only four were available.
§ PHT (posterior homeotic transformation); AHT (anterior homeotic transformation).
‖ (Aa; dd) and (aa; Dd) data combined.
¶ Percentage of animals either showing a wild-type pattern of carpals (none fused) or a fusion between the navicular lunate (NL), triangular (T), and pisiform (P) carpal bones.

The distal carpals in these animals appear normal. With the addition of a fourth mutant allele, the autopod of the mouse is even more dramatically altered. All of the proximal carpal bones are affected: the pisiform is missing, the triangular is also either absent or is fused to the distal carpals, and the navicular lunate is deformed (Fig. 2*a*, *b*). The metacarpals are reduced in length, especially in digits II, III and V. In addition, digits I, II and III curve preaxially and are 'fused' together by the overlaying skin, perhaps owing to a failure of normally occurring cell death between the digits. The phalangeal bones P2 and P1 of digit III are often fused, and P2 is missing from digits II and V (Fig. 2*a*–*d*).

The zeugopodal phenotype is evident at E13.5 when the radius and ulna branch off from the humerus (Fig. 2*e*, *f*). At this stage the (aa; dd) zeugopod is already shorter than the wild type. In addition, the autopod condensations are altered. The wild-type autopod has initiated a full complement of digits, but condensa-

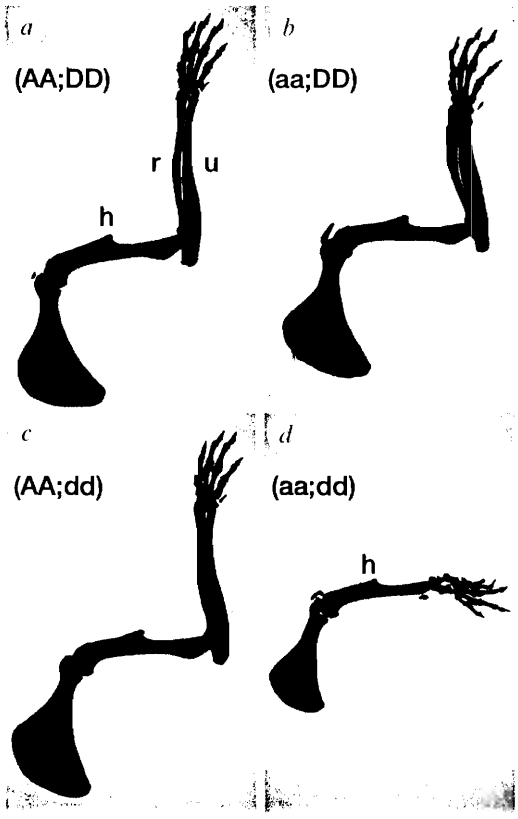

FIG. 1 Loss of the radius and ulna in the double-mutant mouse. Dorsal view of the right forelimbs from adult mouse skeleton preparations. *a*, Wild-type mouse (AA; DD) with a normal humerus (h), radius (r), and ulna (u). *b*, *Hoxa-11* mutant (aa; DD) with a slightly thicker and shorter zeugopod. *c*, *Hoxd-11* mutant (AA; dd) with subtle limb defects in the zeugopod and autopod[16]. *d*, The double mutant (aa; dd) showing an unexpected and dramatic reduction of the radius and ulna. The forepaw is also malformed and rotated 90° compared with wild type. Four (aa; dd) mice survived to adulthood and were examined. All four showed complete penetrance and expressivity of the limb phenotype.
METHODS. All animals were genotyped by Southern blot analysis of tail DNA, and adult skeleton preparations were stained with Alizarin red as described[15,16].

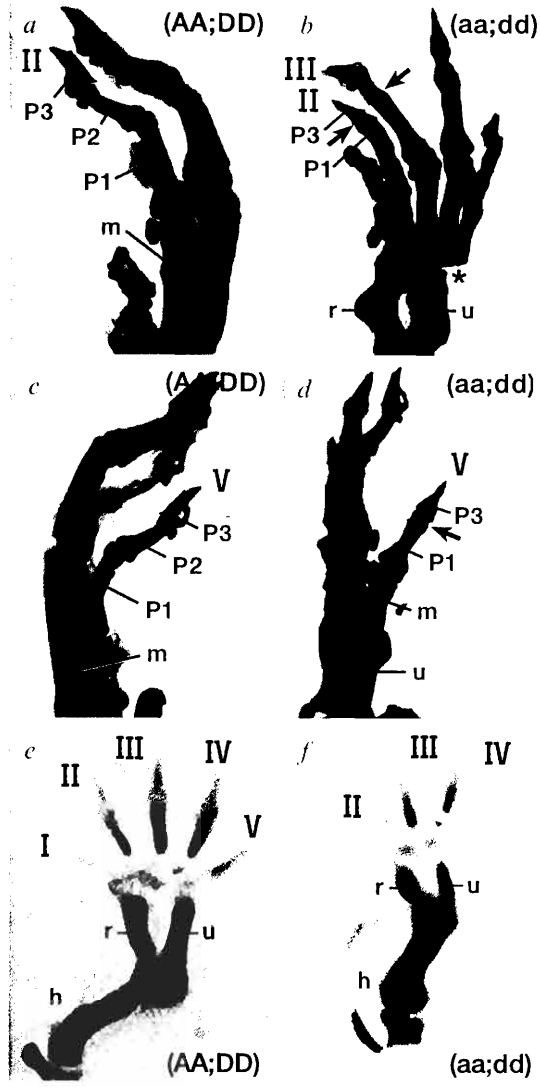

FIG. 2 Autopod defects in the double-mutant mouse. *a*, Wild-type (AA; DD) digit II with normal phalanges (P3, P2, P1) and metacarpal (m). *b*, The double mutant (aa; dd) shows several defects in the autopod. P2 is missing from digit II and is fused to P1 in digit III (arrows). The pisiform and triangular carpal bones are missing (star) and the navicular lunate is deformed. A small vestige of the radius (r) and ulna (u) remains. Digits I, II and III curve preaxially. Digit IV appears relatively normal. *c*, Wild-type (AA; DD) digit V with normal phalanges and metacarpal. *d*, The double mutant (aa; dd) digit V lacks P2 (arrow). *e*, Cartilage condensations in the developing right forelimb of wild-type mouse (AA; DD) at embryonic stage E13.5, showing the humerus (h), radius (r) and ulna (u) with digits I–V all initiated. *f*, Zeugopod defect is already evident in the double mutant (aa; dd) with a reduced radius and ulna. Only digits IV, III and part of II have started to condense. The scapula became detached from the mutant limb and is not shown.
METHODS. Embryos were collected, genotyped and stained with Alcian blue as described[19].

tions in the double mutant (aa; dd) paw are delayed with only digits IV, III and part of II formed.

Intermediate genotypes with three mutant alleles produce intermediate phenotypes in the radius and ulna. These animals have a reduction in the length of the zeugopod as well as a substantial bowing of the radius (Fig. 3*a*–*c*). As predicted from a quantitative phenotype, (Aa; dd) and (aa; Dd) limbs cannot be distinguished from each other by inspection. The hindlimbs of the double mutant are also affected (Fig. 3*d*, *e*). In double-mutant mice, the fibula is thickened and flared at its distal end and is never fused with the tibia, all in contrast to wild-type mice. Most noticeable, however, is the absence of the proximal tarsal bones (the talus and calcaneus/processus trochlearis) from double-mutant mice. This forces the tibia and fibula to join the foot at the mid-tarsals. Interestingly, the hindlimb phenotype is not quantitative with respect to the number of mutant alleles because intermediate genotypes (aa; Dd) and (Aa; dd) do not have intermediate phenotypes.

The normal mouse axial skeleton is characterized by 7 cervical (C1–7), 13 thoracic (T1–13), 6 lumbar (L1–6), 4 sacral (S1–4), and a variable number of caudal vertebrae. The transverse processes on S1–3 fuse to form the sacrum. Table 1 shows a summary of the vertebral phenotypes for mice generated from intercrosses of compound heterozygotes. Both the (aa; DD) and the (AA; dd) mutant mice show an apparent homeotic transformation of the first sacral vertebra towards a lumbar vertebra (S1→L)[15–17]. Half of the compound heterozygotes (Aa; Dd) show this same transformation, a phenotype never observed in either of the individual heterozygotes (Aa; DD) and (AA; Dd). Again, this quantitative phenotype suggests that only two mutant alleles (either of *hoxa-11*, or *hoxd-11*, or one from each locus) are necessary to induce this homeosis. The double mutant (aa; dd) has nine lumber vertebrae (Table 1). These can be accounted for by both a posterior homeotic transformation (T13→L1) and a double anterior homeotic transformation (S1, S2→L8, L9). In addition, the sacral vertebrae do not fuse to form a sacrum, and in some cases the second sacral vertebra and one caudal vertebra are deleted.

hoxa-11 and *hoxd-11* are expressed in the primitive blastemal cells that populate the nephrogenic zone of the developing kidney (ref. 18, and S.S.P., unpublished results). Whereas mice mutant for either *hoxa-11* or *hoxd-11* have normal kidneys[15,16], double mutants (aa; dd) suffer renal malformations that generally result in perinatal death (Fig. 4*a*, *b*). Some double-mutant mice are born lacking one or both kidneys. Newborn (aa; dd) mice with kidneys show severe renal hypoplasia (Fig. 4*b*), with poorly developed cortex and medulla and little or no nephrogenic activity in the subcapsular region (Fig. 4*c*, *d*). The rare adult (aa; dd) kidney has a thick wall of cortical tissue and poorly developed renal papillae. The renal tubules present are well developed and the glomerulae, although severely reduced in number, show only mild compensatory hypertrophy (results not shown). There were no abnormalities in the lower renal tract to suggest urinary obstruction. With rare exceptions, one wild-type allele of either *hoxa-11* or *hoxd-11* was sufficient for normal kidney development. Urogenital malformations also include homeotic transformation of the vas deferens towards an epididymis. This is apparent at the gross level, with the vas deferens of (aa; dd) mice being smaller in diameter and more coiled than normal (Fig. 4*e*, *f*), and also evident at the histological level, with the mutant vas deferens showing reduction of the muscle layer, lack of convolution of the epithelial layer, and an epididymis-like epithelial cell morphology with nuclei positioned peripherally instead of centrally (Fig. 4*g*, *i*).

We expect that quantitative interactions between *Hox* genes will be the rule rather than the exception. Previously we demon-

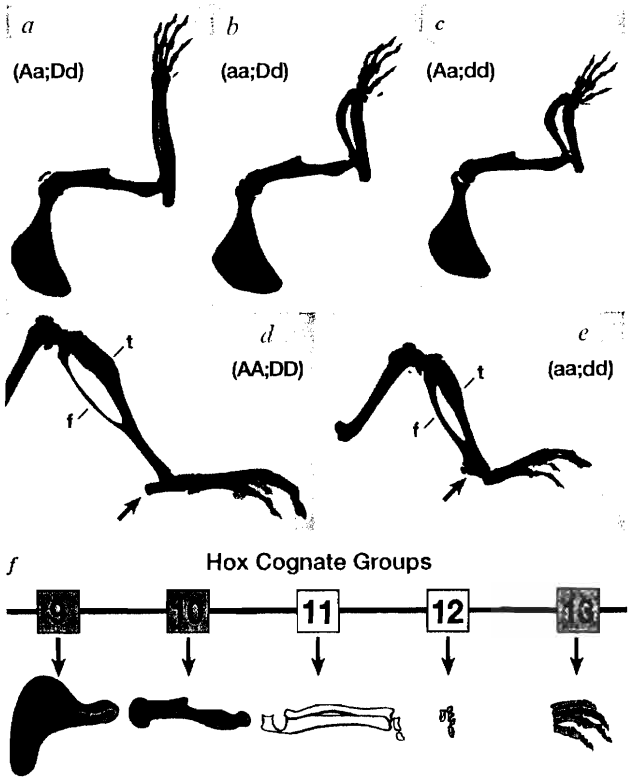

FIG. 3 Genetic quantification and synergy in the limb phenotypes. *a*, Compound heterozygote (Aa; Dd) forelimb. *b*, *c*, Mice with three mutant alleles (*b*, (aa; Dd) and *c*, (Aa; dd)) show intermediate phenotypes with a shortening and thickening of the zeugopod and with a substantial bowing of the radius. *d*, Wild-type (AA; DD) right hindlimb with normal tibia (t) and fibula (f) and proximal tarsal bones present (arrow). *e*, Double mutant (aa; dd) has malformed tibia and fibula that are slightly thicker and never fuse together, the proximal tarsal bones are also missing (arrow). *f*, A model for the role of *Hox* genes in limb development. The Hox cognate groups 9–13 represent the combined paralogous genes of the *Hox* loci and are drawn in the 3′ to 5′ direction. We propose that the cognate genes work in union to specify limb bone formation in the proximal to distal direction (left to right). In the double-mutant mouse (aa; dd), both *hoxa-11* and *hoxd-11* are mutated; this results in the loss of the radius, ulna and proximal carpals (yellow coded bones). In addition to these paralogous interactions, *Hox* genes in the same linkage group or across groups may also interact during limb development.

strated that the two paralogues *hoxa-3* and *hoxd-3* interact quantitatively to specify the craniocervical joint[19] and that *hoxb-5* and *hoxb-6* function together to specify cervical and thoracic vertebrae[20]. Here we describe quantitative, synergistic genetic interactions between *hoxa-11* and *hoxd-11*. In the vertebral column and carpal bones, compound heterozygotes have phenotypes similar to mice homozygous for mutations in either *hoxa-11* or *hoxd-11*. The quantitative effect is further revealed in animals with three mutant alleles: forelimbs in (aa; Dd) and (Aa; dd) mice show more severe defects in the zeugopod and autopod than are found in animals with only two mutant alleles. Synergy is seen in the axial column, limbs, kidneys and vas deferens, where phenotypes of the double mutant (aa; dd) are more pronounced than the sum of the phenotypes seen in the individual mutant homozygotes.

Limb bones are formed from prechondrogenic condensations that segment and bifurcate along the proximodistal axis to create the long bones (humerus, then radius and ulna). This is followed by proximodistal and anteroposterior condensations to generate the carpals, metacarpals and digits[21,22]. Mice with targeted disruptions of either *hoxa-11* or *hoxd-11* show regional malformations in the shape, length and segmentations of bones in the zeugopod and autopod[15–17]. These defects do not resemble homeotic transformations, but rather perturbations in the growth of the cells contributing to the prechondrogenic condensations. Further, the defects are not polarized with respect to the anteroposterior axis. It is therefore surprising that in double mutants the radius and ulna are almost entirely eliminated. In addition, the phenotype of the (aa; dd) autopod is strongly polarized. The more posterior proximal carpals are severely affected, whereas the distal carpals seem normal. The digits are also malformed. Digit IV seems to be normal, but the severity in phenotypes increases through digit III (a fusion between P2 and P1) to a maximum in digits II and V (both lacking P2). This phenotypic progression parallels the developmental 'limb plan' that proposes a basic axis of development that proceeds through the humerus, the ulna, and then anteriorly through the wrist such that the anterior distal carpals are the last to be made[21,23]. These wrist cartilages then branch to form the digits in a specific temporal sequence: digits IV and III are the first to be made, followed by digits I, II and V[21].

The limb phenotype of the double mutants (aa; dd) suggests that these two genes function together to specify the radius and the ulna. *Hox* genes are activated in the limb bud in a temporal sequence with the 3′ genes expressed first and the 5′ genes last, creating a transcriptional cascade of *Hox-9, -10, -11, -12* and then *-13* (ref. 11). We propose that it is the activation order and the interaction of the paralogues that specify patterns of prechondrogenic condensations along the proximodistal axis (Fig. 3*f*). Their role may be achieved by regulating cell proliferation and/or survival as well as specifying cell identity (that is, the number of chondrocytes). Thus the *Hox* group 11 genes would specify the zeugopod. In the double mutant mouse, *hoxa-11* and *hoxd-11* gene products are both absent, and this region is made as a rudiment at best. But once this crisis period is over, the *Hox* group 12 genes would be activated and limb develop-

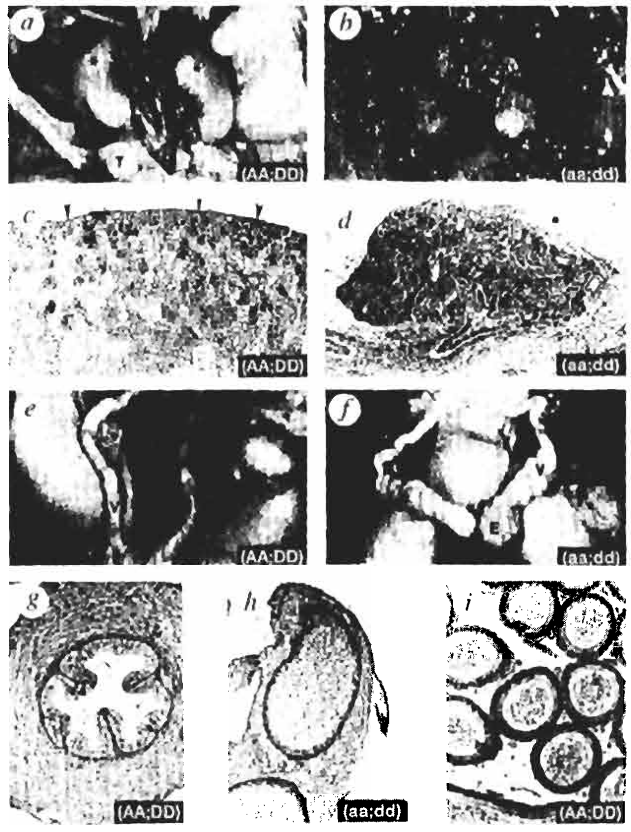

FIG. 4 Urogenital defects in the double-mutant mouse. *a*, Urinary tract of a wild-type newborn. The kidneys are indicated by the asterisk just above the testes (T). *b*, Urinary tract in the (aa; dd) mutant. The kidneys are extremely hypoplastic but the testes (T) are normal in size. *c*, Histology of wild-type kidney. Note the uniform zone of active nephrogenesis just beneath the renal capsule (arrowheads). The immature tubules and primitive glomeruli just beneath the capsule are separated by nests of undifferentiated blastemal cells. *d*, Histology of the (aa; dd) mutant kidney. In contrast with the wild-type kidney, the entire mutant kidney is easily seen at the same magnification. Although the tubules and glomeruli present are well developed, there is a decrease in total number of nephrons, with little nephrogenesis in the subcapsular zone. *e*, Dissected male reproductive tract from a wild-type mouse. There is a sharp transition from the epididymis (E) to the vas deferens (V). The vas deferens is a thick cord with a relatively straight configuration. *f*, Reproductive tract from the (aa; dd) mutant. The transition from the epididymis (E) to the vas deferens (V) is more obscure. The proximal vas deferens has a highly coiled configuration. *g*, Histology of the wild-type vas deferens. The epithelial layer has prominent folds and the lining cells have a large amount of cytoplasm with their nuclei in the middle or apical aspect of the cells. There is also a well developed smooth muscle layer in the wall of the vas deferens. *h*, Histology of the (aa; dd) mutant vas deferens. The epithelial lining is simple with no folds, and the cells are columnar and have nuclei with a uniform distribution in the basal aspects of the cells. The layer of smooth muscle cells in the wall is greatly reduced. *i*, Histology of a normal epididymis. The tubules are lined by a simple layer of columnar cells with nuclei that are uniformly arranged in the basal aspects of the epithelial cells. Note the close resemblance of this epithelial lining to that of the vas deferens from the double-mutant mice in *h*.
METHODS. Tissue samples were fixed in Bouin's solution and processed as described[18]. Sections were stained with haematoxylin and eosin.

ment resumed. In this sense, it is important to note that after the zeugopodal defect, limb development does proceed in the double-mutant mouse, albeit with some dysmorphology. But clearly the autopod is less affected than the zeugopod. The autopodal phenotypes distal to the major zeugopodal defects are likely to be the result of a coupling between proximodistal and anteroposterior patterning[24–28]. This coupling may be genetic, with group 11 genes directly influencing the timing of activation of group 12 and group 13 genes. Alternatively, morphological coupling may account for these defects. The elimination of both *hoxa-11* and *hoxd-11* gene products may reduce the overall mesenchymal cell population available to form the zeugopod and posterior carpals. A deficiency of cells may also alter the timing ('heterochrony') of formation of the rest of the limb. The second crisis would therefore be revealed at the end of autopod formation, when cartilaginous elements are competing to recruit the few remaining cells. This heterochrony would explain the delay in digit condensation seen during embryogenesis of the double mutant and account for the more severe phalangeal defects seen in digits II and V, which are the last elements formed in the last digits specified.

It is interesting that in the double mutants the forelimbs are more affected than the hindlimbs. Also, whereas (aa; Dd) and (Aa; dd) mice show an intermediate forelimb phenotype, the presence of a third mutant allele does not alter the hindlimb phenotype beyond what is seen in (aa; DD) or (AA; dd) mice. These differences may be a consequence of a third paralogue, *hoxc-11*, which is expressed more strongly in the hindlimbs[29] and could provide a compensatory function. This hypothesis would predict that in (*hoxa-11*, *hoxc-11*, *hoxd-11*) triple mutants, the tibia and fibula would be completely eliminated and show quantitative dependence on the dosage of mutant alleles. Also, the last vestige of the forelimb radius and ulna observed in the double mutant would be predicted to be absent.

Our model is supported by the *hoxd-13* mutant mouse in which the mutant limb phenotype is restricted to the autopod[13], and predicts that in a (*hoxa-13*, *hoxd-13*) double mutant the forepaw should be absent. *hoxd-12* has no paralogue in the *Hox A* family and may therefore act on its own (or in conjunction with *hoxc-12*) to influence formation of the carpals and tarsals. Alternatively, *hoxd-12* may recruit its closest *Hox A* paralogue (*hoxa-11* or *hoxa-13*) to help specify this region. Single-mutant mice for *hoxa-10*, *hoxc-10* and *hoxd-10* should show subtle defects in the humerus and femur, but double and triple mutants should affect strongly the entire stylopod and initiate a cascade of less severe phenotypes downstream through the zeugopod and autopod. Consistent with the model, individual *hoxd-10* and *hoxc-10* mutant homozygotes show mild malformations of the humerus and femur (E. M. Carpenter, J. M. Goddard and M.R.C., unpublished results; S. L. Hostikka and M.R.C., unpublished results). From this model, the appendicular ground state would be achieved in an animal lacking all of the *Hox* 10–13 cognate genes. This should be a limbless mouse. □

Received 10 April; accepted 18 May 1995.

1. Capecchi, M. R. *Scient Am.* **270,** 54–61 (1994).
2. Holland, P. W. H., Garcia-Fernandez, J., Williams, N. A. & Sidow, A. *Development* (Suppl.), 125–133 (1994).
3. Ruddle, F. H. *et al. A. Rev. Genet.* **28,** 423–442 (1994).
4. Dollé, P., Izpisúa-Belmonte, J.-C., Falkenstein, H., Renucci, A. & Duboule, D. *Nature* **342,** 767–772 (1989).
5. Dollé, P., Izpisúa-Belmonte, J.-C., Brown, J. M., Tickle, C. & Duboule, D. *Genes Dev.* **5,** 1767–1776 (1991).
6. Duboule, D. *Curr. Opin. Genet. Dev.* **1,** 211–216 (1991).
7. Izpisúa-Belmonte, J.-C., Tickle, C., Dollé, P., Wolpert, L. & Duboule, D. *Nature* **350,** 585–589 (1991).
8. Izpisúa-Belmonte, J. C., Falkenstein, H., Dollé, P., Renucci, A. & Duboule, D. *EMBO J.* **10,** 2279–2289 (1991).
9. Yokouchi, Y., Sasaki, H. & Kuroiwa, A. *Nature* **353,** 443–445 (1991).
10. Duboule, D. *BioEssays* **14,** 375–384 (1992).
11. Izpisúa-Belmonte, J.-C. & Duboule, D. *Devl Biol.* **152,** 26–36 (1992).
12. Morgan, B. A., Izpisúa-Belmonte, J.-C., Duboule, D. & Tabin, C. *Nature* **358,** 236–239 (1992).
13. Dollé, P. *et al. Cell* **75,** 431–441 (1993).
14. Haack, H. & Gruss, P. *Devl Biol.* **157,** 410–422 (1993).
15. Small, K. M. & Potter, S. S. *Genes Dev.* **7,** 2318–2328 (1993).
16. Davis, A. P. & Capecchi, M. R. *Development* **120,** 2187–2198 (1994).
17. Favier, B., Le Meur, M., Chambon, P. & Dollé, P. *Proc. natn. Acad. Sci. U.S.A.* **92,** 310–314 (1994).
18. Li, H. M. H. *et al. Development* **121,** 1373–1385 (1995).
19. Condie, B. G. & Capecchi, M. R. *Nature* **370,** 304–307 (1994).
20. Rancourt, D. E., Tsuzuki, T. & Capecchi, M. R. *Genes Dev.* **9,** 108–122 (1995).
21. Shubin, N. H. & Alberch, P. *Evol. Biol.* **20,** 319–387 (1986).
22. Oster, G. F., Shubin, N., Murray, J. D. & Alberch, P. *Evolution* **42,** 862–884 (1988).
23. Duboule, D. *Science* **266,** 575–576 (1994).
24. Tabin, C. *Cell* **80,** 671–674 (1995).
25. Niswander, L., Tickle, C., Vogel, A., Booth, I. & Martin, G. R. *Cell* **75,** 579–587 (1993).
26. Fallon, J. F. *et al. Science* **264,** 104–107 (1994).
27. Niswander, L., Jeffrey, S., Martin, G. R. & Tickle, C. *Nature* **371,** 609–612 (1994).
28. Cohn, M. J., Izpisúa-Belmonte, J. C., Abud, H., Heath, J. K. & Tickle, C. *Cell* **80,** 739–746 (1995).
29. Peterson, R. L., Papenbrock, T., Davda, M. M. & Awgulewitsch, A. *Mech. Dev.* **47,** 253–260 (1994).

ACKNOWLEDGEMENTS. A.P.D. was supported by an NSF predoctoral fellowship and an NIH genetics training grant. We thank K. Saalfeld, T. Smith and C. Lewis for technical support, and L. Oswald for help with the preparation of the manuscript

CHAPTER 4

A MUTATIONAL ANALYSIS OF THE 5' *HOX D* GENES: DISSECTION OF GENETIC INTERACTIONS DURING LIMB DEVELOPMENT IN THE MOUSE

Summary

Using gene targeting in mice, we have undertaken a systematic mutational analysis of the homeobox-containing 5' *Hox D* genes. In particular, we have characterized the limb defects observed in mice with independent targeted disruptions of *hoxd-12* and *hoxd-13*. Animals defective for *hoxd-12* are viable and fertile and appear outwardly normal yet have minor autopodal defects in the forelimb which include a reduction in the bone length of metacarpals and phalanges and a malformation of the distal carpal bone d4. The limb phenotypes for *hoxd-13* mutant mice, however, are more extensive, with strong reductions, complete absence, or improper segmentations of many metacarpal and phalangeal bones. Additionally, the d4 carpal bone is not properly formed and instead yields a carpal which often produces an extra rudimentary digit. To examine the genetic interactions between the 5' *Hox D* genes, we bred these mutant strains to each other and to our previously characterized *hoxd-11* mouse to produce a series of *trans*-heterozygotes. The skeletal analysis of these mice reveals that these genes interact in the formation of the vertebrate limb since the *trans*-heterozygotes display phenotypes not present in the individual heterozygotes including more severe carpal, metacarpal, and phalangeal defects. Some of these phenotypes appear to be accounted for by a delay in the ossification events in the autopod, which lead to the failure of fusion or elimination of cartilaginous elements. Characteristically, these mutations lead to the overall truncation of digits II and V on the forelimb. Additionally, some *trans*-animals show the growth of an extra postaxial digit VI which is composed of a bony element resembling a phalange. The results demonstrate that in addition to the previously characterized paralogous interactions, the *Hox Complex* uses a multitude of genetic combinations to finely sculpt the forelimb and could therefore act as a major genetic tool for the evolutionary adaptation of the vertebrate limb.

Introduction

The vertebrate tetrapod limb has been a favorite system of study for developmental biologists since the turn of the century due to it being a nonvital structure that is accessible to experimental manipulation (detailed in Hinchliffe and Johnson, 1980). Additionally, the variety in form and function of the limb throughout the extant animal kingdom and fossil record allows for a merging between the disciplines of genetics, development, and evolution (Hinchliffe, 1994). We are interested in understanding what role a set of developmental genes called the *Hox Complex* plays in the proper patterning and formation of the vertebrate tetrapod limb.

Hox genes are defined by the presence of a conserved nucleotide sequence (the homeobox) that codes for an amino acid motif (the homeodomain) capable of binding DNA (reviewed in Duboule, 1994a). There are at least 38 genes in the mammalian *Hox Complex* that are divided into four linkage groups called Hox A, B, C, and D located on four separate chromosomes. Each locus contains between nine to eleven closely linked individual *Hox* genes forming a genetic matrix believed to have arisen by a process of chromosomal duplication (Ruddle et al., 1994). Thus, corresponding genes in separate linkage groups are referred to as paralogues since they are most similar to each other in sequence information and expression patterns. The 5' ends of the Hox loci carry the five paralogous gene families *Hox 9-13*. Mutational analysis of some of these genes has demonstrated that they play an important role in limb development (Dolle et al., 1993; Small and Potter, 1993; Davis and Capecchi, 1994; Davis et al., 1995; Favier et al., 1995).

At the early stages, the limb bud is composed of highly proliferating mesenchymal cells of the progress zone (PZ) at its distal tip that is covered by a layer of cells called the apical ectodermal ridge (AER; Tickle and Eichele, 1994). Together these two components maintain each other to allow the limb to grow out of the body in a proximodistal direction as cells leave the PZ to form the body of the limb tissue (Niswander et al., 1993; Fallon et

al., 1994; Cohn et al., 1995; Tabin, 1995). A zone of polarizing activity (ZPA) influences the anteroposterior patterning of the limb (Tickle and Eichele, 1994). It is during this early stage of limb bud growth that the *Hox 9-13* genes become consecutively activated (Dolle et al., 1989, 1991a,b; Izpisua-Belmonte et at., 1991). The completed appendicular skeleton is divided into three zones called the stylopod, zeugopod, and autopod. In the forelimb, the stylopod is made up of the humerus; the zeugopod contains both the radius and ulna; and the autopod is comprised of carpals, metacarpals, and phalanges. These bones are determined by the prechondrogenic condensations that are laid down during the early stages of limb growth from cells that have vacated the PZ. The bifurcation and segmentation of these condensations ultimately give rise to the ossified bones in the finished limb (Shubin and Alberch, 1986). Chondrogenic growth and patterning occur in the proximodistal direction; thus, the distal limb structures (i.e., the autopod) are inherently dependent upon the growth of the proximal segments (i.e., the stylopod).

Hoxd-12 and *hoxd-13* constitute the last two genes of the Hox D locus on Chromosome 2 of the mouse. These genes are activated in a strict temporal and spatial pattern during development such that the more 3' gene (*hoxd-12*) is expressed earlier and in a more proximal manner than the more 5' gene (*hoxd-13*; Duboule, 1992; Izpisua-Belmonte and Duboule, 1992). This feature of temporal and spatial colinearity of the *Hox* genes may play an important role in the patterning of the limb by determining regional identity along the appendicular axis and controlling the properly timed cellular proliferations required for the building of the limb (Duboule, 1994b; Davis et al., 1995; Duboule, 1995). We have taken a mutational approach to the analysis and understanding of these genes with respect to limb development by creating targeted disruptions in mice (Capecchi, 1989). Inactivation of *hoxd-12* results in subtle phenotypes restricted to the autopod, specifically, the reduction in length of certain metacarpal and phalangeal bones and the malformation of a distal carpal. The *hoxd-13* mutant mouse, however, displays

severe defects of the forepaw including the strong reduction or elimination of certain phalanges and metacarpals, wrist defects, and the growth of a rudimentary postaxial digit.

With only 38 individual genes in the *Hox Complex*, it is believed that these products interact with each other to produce numerous novel combinations that may allow for the vast diversity seen in higher vertebrate body plans. In support of this, it has been demonstrated that *Hox* paralogues function together to specify both the axial and appendicular skeleton of the mouse (Condie and Capecchi, 1994; Davis et al., 1995; Horan et al., 1995). Additionally, it has been shown that *Hox* genes within the same linkage group work together to also control axial patterning (Rancourt et al., 1995). We speculated that genetic interactions within the same linkage group might also control appendicular patterning. To test this, we generated a series of *trans*-heterozygous mice for the *hoxd-11*, *hoxd-12*, and *hoxd-13* mutations. These *trans*-animals show more severe autopodal phenotypes than do the individual heterozygotes, demonstrating a genetic interaction. We believe these phenotypes are best explained in terms of the *Hox* genes influencing the number of cells in the limb, and that these cells manifest a "limb pattern" as the result of inherent local interactions. Thus, modulating the potential combinations of the *Hox 9-13* genes may allow the vertebrate limb to be sculpted in the enormously different arrays observed over the course of evolution.

Materials and Methods

Construction of *hoxd-12* and *hoxd-13* targeting vectors

A DNA fragment containing both *hoxd-12* and *hoxd-13* was isolated from a genomic lambda library made from mouse CC1.2 embryo-derived stem (ES) cell DNA using a probe 5' to the *hoxd-11* locus. The genes were identified and confirmed by sequencing the homeoboxes from each (Izpisua-Belmonte et al., 1991). Replacement-type gene targeting vectors (Thomas and Capecchi, 1987; Thomas et al., 1992; Deng et al., 1993) were constructed individually for *hoxd-12* and *hoxd-13* using the identical 12.3

kilobases (kb) of genomic DNA flanked by two *thymidine kinase* genes in a Bluescript-based plasmid. The previously described *neo* cassette KT3NP4 (Davis and Capecchi, 1994) was inserted into the respective homeodomains for each of the individual genes. For the *hoxd-12* targeting vector, the *Xmn*I site in the homeobox was cut open and replaced by a *Cla*I linker to which KT3NP4 was then inserted in the opposite orientation of *hoxd-12* transcription. This site corresponds to amino acid 18 of the homeodomain. For the *hoxd-13* targeting vector, the *Pvu*II site in the homeobox was cut open and replaced by a *Cla*I linker to which KT3NP4 was inserted in the same orientation as *hoxd-13* transcription. This site corresponds to amino acid 36 of the homeodomain.

Electroporation and ES cell line analysis

In separate experiments, the targeting vectors were individually linearized and electroporated into R1 ES cells. Cell selection and DNA extraction were performed as described (Davis and Capecchi, 1994). A primary screen of the cell lines was analyzed by Southern blots.

For *hoxd-12*, cell line genomic DNA was digested with *Xho*I and hybridized with a 1.0 kb *Sal*I-*Xho*I 3' flanking probe (D) to look for a band shift from 8.6 kb (wild-type) to 5.3 kb (mutant). Targeted cell lines were additionally confirmed by Southern analysis using a *Not*I digest hybridized with a *neo* specific probe to detect a unique 18 kb band in targeted cell lines only, a *Cla*I digest hybridized with a 0.3 kb *Eco*RI-*Xho*I 5' flanking probe (Z) to detect a band shift from 25 kb (wild-type) to 19 kb (mutant), and a *Not*I + *Cla*I double digest hybridized with two independent internal probes: 1.0 kb *Eco*RV-*Xho*I fragment (probe N) to detect a band shift from 14 kb (wild-type) to 8 kb (mutant) and a 3.4 kb *Xba*I-*Sal*I fragment (probe C) to detect a band shift from 14 kb (wild-type) to 6.3 kb (mutant).

For *hoxd-13*, cell line genomic DNA was digested with *Eco*RV in a primary screen and hybridized with the 5' flanking probe Z to detect a band shift from 6.2 kb

(wild-type) to 4.5 kb (mutant). Targeted cell lines were confirmed with a *Eco*RI digest hybridized with a *neo* specific probe to detect a unique 5.5 kb band in targeted cell lines only, a *Not*I digest hybridized with a *neo* specific probe to detect a unique 18 kb band in targeted cell lines only, and a *Cla*I digest hybridized with the 3' flanking probe C to detect a band shift of 25 kb (wild-type) to 6.3 kb (mutant).

Breeding, genotyping, and skeletal analysis

The *hoxd-12* and the *hoxd-13* mice were individually made by injecting the appropriately targeted ES cell lines into C57BL/6J (B6) blastocysts. Germline transmission of the mutant alleles was confirmed by Southern analysis, and individual breeding colonies were established for *hoxd-12* and *hoxd-13*. The *hoxd-11* mouse has been previously described (Davis and Capecchi, 1994). To genotype progeny of crosses, a PCR assay for tail DNA was designed that distinguishes all three *Hox D* mutations. PCR was performed in 12.5 ul reactions amplified for 25 cycles at 94°C (30 seconds), 60°C (20 seconds), and 72°C (60 seconds). The *hoxd-11* primers included one that was specific to the intron 5' of the homeobox (5' primer) and the other specific to the 3' untranslated region downstream from the homeobox (3' primer). The *neo* primer was located at the 5' end of the KT3NP4 cassette. The *hoxd-12* and *hoxd-13* primers were similarly designed with a 5' primer and a 3' primer. The oligonucleotide sequences are provided:

hoxd-11 5' primer: 5'-CCTTTTTCCTATCTCAGTGCCAG-3';

hoxd-11 3' primer: 5'-GGGGTACATCCTGGAGTTCTCA-3';

hoxd-12 5' primer: 5'-AGTTGATCTGAGCGAGCTGACAT-3';

hoxd-12 3' primer: 5'-CTTGGTCCAAAAGGGCAGGCTT-3';

hoxd-13 5' primer: 5'-GCTTAGGTGTTCCAAGTATCCAG-3';

hoxd-13 3' primer: 5'-CCACATCAGGAGACAGTGTCTTT-3'; and

KT3NP4 *neo* primer: 5'-TTCAAGCCCAAGCTTTCGCGAG-3'.

The PCR products were analyzed using Trevi-Gel agarose electrophoresis. For *hoxd-11*, the products are 507 bp (wild-type) and 367 bp (mutant); for *hoxd-12*: 334 bp (wild-type) and 226 bp (mutant); and for *hoxd-13*: 311 bp (wild-type) and 235 bp (mutant).

For adult skeletal analysis, mice were collected at 7-12 weeks of age and stained with Alizarin red. Newborn skeletons were stained with both Alizarin red and Alcian blue. Embryos were timed, collected, and stained with alcian blue only. All staining and bone length measurements were done as previously described (Condie and Capecchi, 1994; Davis and Capecchi, 1994).

Results

Creating *hoxd-12* and *hoxd-13* mice

Replacement-type gene targeting vectors were constructed from mouse genomic DNA containing individual disruptions in *hoxd-12* or *hoxd-13* by insertion of a *neo* resistance cassette into the homeodomain encoding exon (Fig. 4.1; Materials and Methods for details). The vectors were independently electroporated into R1 ES cells in two separate experiments and cultured under conditions to enrich for a homologous recombination event (Mansour et al., 1988). Genomic DNA was isolated from selected cells and characterized by Southern blotting to confirm a gene targeting event for each gene (Materials and Methods for details). A representative targeted ES cell line for each mutation was separately injected into B6-derived blastocysts to produce chimeric males that passed the mutation through the germline. All subsequent progeny were confirmed by Southern blotting or PCR analysis using tail DNA, and independent breeding colonies were established for each mutant strain.

Phenotypes of *hoxd-12* and *hoxd-13* mice

Mice heterozygous for *hoxd-12* were intercrossed to produce homozygous mutant animals. This mutation is not lethal as the proper Mendelian ratio of alleles was observed

Figure 4.1

Targeted mutagenesis of the 5' *Hox D* genes in mice. (A) Schematic representation of the 5' end of the Hox D locus. The genomic array (top line) is drawn in the 3' to 5' direction with the orientation of gene transcription denoted by arrows. Three independent gene targeting vectors were constructed (bottom lines) to specifically mutate each gene by the insertion of a disrupting neomycin resistance cassette (neo) in the homeobox exon. (B) Dorsal view of the forelimb autopods for a wild-type animal and the three mutant mouse strains produced by gene targeting. The *hoxd-11* mouse has already been described by us (Davis and Capecchi, 1994) and confirmed by others (Favier et al., 1995). The *hoxd-12* mouse is described in this paper. The *hoxd-13* mouse is also reported here and shows identical phenotypes to those described by Dolle et al. (1993). (C) Diagram of a mouse appendicular skeleton and a summary of the sites of the major forelimb phenotypes seen in *hoxd-11*, *hoxd-12*, and *hoxd-13* mutant animals.

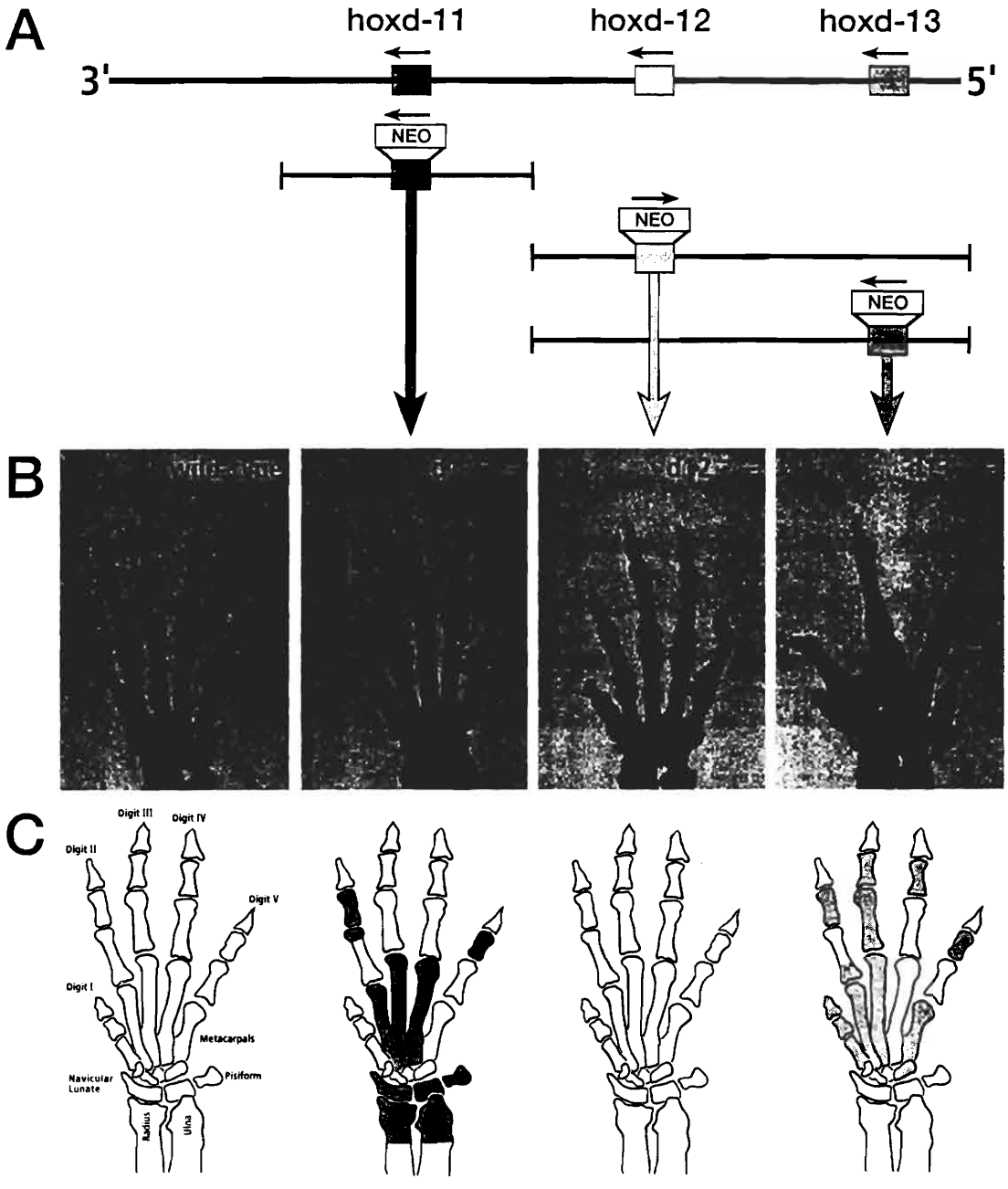
A
hoxd-11
hoxd-12
hoxd-13
3'
5'
NEO
NEO
NEO
B
C
Digit III
Digit IV
Digit II
Digit V
Digit I
Metacarpals
Navicular
Lunate
Pisiform
Radius
Ulna

in weaned adult mice. Both sexes were fertile and showed no outwardly apparent abnormalities. Skeleton preparations were made to look for limb defects. Subtle malformations were seen in the forelimb of mice homozygous mutant for *hoxd-12*. These phenotypes include reductions in the length of a number of autopodal bones. The metacarpals of digits II and V are shortened (Table 4.1 and Fig. 4.2). Phalange 1 (P1) of digit II shows a slight reduction (80% normal bone length) whereas P2 of digit V shows the strongest limb phenotype (55% normal bone length; Table 4.1 and Fig. 4.2). Overall, this results in both digits II and V being significantly shorter when compared with control limbs (Table 4.1). Additionally, in the wrist the carpal bone d4 shows a subtle, characteristic indentation at its distal border that is never seen in control animals (Fig. 4.2) that we believe is due to the improper fusion of the appropriate prechondrogenic condensations (discussed below). This condition is never seen in control animals. The autopods of mice heterozygous for *hoxd-12* appear normal except for the low penetrance (~6%) of a very small bony element that forms postaxially to digit V (not shown).

On the other hand, mutations in *hoxd-13* result in extensive limb defects in homozygotes. Mutant mice for this gene have been previously described (Dolle et al., 1993), and the animals reported here show identical phenotypes. Appendicular skeleton defects include a much smaller paw with strong reduction of the metacarpals and the absence of, or reduction in, P2 on digits II and V (Fig. 4.2). Phalangeal bones on other digits are also greatly reduced or never properly segmented and thus remain fused together. Additionally, a webbed effect is sometimes seen when bony elements fuse the interdigital regions (Fig. 4.2). In the wrist, the prechondrogenic condensations that are supposed to fuse together to form the d4 carpal bone never do, yielding an extra carpal bone from which often grows a rudimentary digit VI (Fig. 4.2). Minor carpal defects in d4 (including the indentation) and the same type of postaxial bone as in *hoxd-12* (-/+) are seen in individual *hoxd-13* (-/+) heterozygotes at a penetrance of 34%. This higher penetrance of limb phenotypes in *hoxd-13* heterozygotes -- as opposed to that seen in

Table 4.1

Lengths of mutant forelimb bones, as percent of control (%)

Hox Genotype	Bone	Digit II	III	IV	V
d-12 (-/-)	Phalange 2	86	85	94	**55**
	Phalange 1	**80**	90	85	86
	Metacarpal	**78**	91	88	**82**
	Total	**81**	89	88	**77**
	control: *hoxd-12* (+/+)				
{*d-11 (-/+), d-13 (+/-)*}	Phalange 2	**0/65***	91	**82**	**33**
	Phalange 1	93	92	90	90
	Metacarpal	**80**	98	97	95
	Total	**75**	95	92	**79**
	*variable expressivity from 0 to 65%				
	control: *hoxd-11 (-/+), hoxd-13 (+/+)*				
{*d-11 (-/+), d-12 (+/-)*}	Phalange 2	85	89	**83**	**60**
	Phalange 1	**79**	88	88	87
	Metacarpal	**79**	**83**	86	86
	Total	**80**	86	86	**81**
	control: *hoxd-12 (-/+), hoxd-13 (+/+)*				
{*d-12 (-/+), d-13 (+/-)*}	Phalange 2	**81**	86	85	**0/55***
	Phalange 1	**84**	94	93	93
	Metacarpal	85	102	98	89
	Total	**84**	96	93	**77**
	*variable expressivity from 0 to 55%				
	control: *hoxd-12 (-/+), hoxd-13 (+/+)*				

Numbers in **bold** represent strongest reduction in size (greater than 3 standard deviations, where s.d. = ± 5% bone length).

Digit I and Phalange 3 were not recorded since they proved to be un-informative.

Figure 4.2

Phenotypes for *hoxd-12* and *hoxd-13* mutant mice. Autopod of a wild-type forelimb is compared to that of *hoxd-12* and *hoxd-13* mutant animals. The metacarpal of digit V is shorter in *hoxd-12* mice (B) when compared to controls (A); also, d4 carpal shows an indentation at its distal border (B, arrow). *Hoxd-13* mice show massive phenotypes including the formation of an extra post-axial digit (C, "VI") and interdigital webbing (C, arrow). Digits II and V in the mutant animals are compromised when compared to controls (D, G). *Hoxd-12* mice show a substantial reduction in the length of P2 in digit II (E) while *hoxd-13* mice completely lack this bone (F, arrow). Likewise, P2 in digit V is severely reduced in *hoxd-12* animals (H) and is gone in *hoxd-13* mice (I, black arrow). Additionally, in the *hoxd-13* strain, d4 is never properly made and instead yields an extra carpal bone from which grows the postaxial digit VI (I, white arrow).

wild-type
d12 −/−
d13 −/−
carpals
digit II
digit V
A
B
C
D
E
F
G
H
mV
p2
"VI"

hoxd-12 (-/+) mice (6%) or *hoxd-11* (-/+) mice (0%) -- is not totally unexpected. The homozygous mutant phenotype for *hoxd-13* is more severe than for *hoxd-11* or *hoxd-12* mutant mice (Fig. 4.1). If *Hox* gene products function quantitatively to control skeleton patterning, than the dosage of gene products will play an important factor in proper limb formation. Thus, due to the extensive phenotypes seen in *hoxd-13* (-/-) mice, it is not surprising to see a partial phenotype for *hoxd-13* heterozygotes.

Trans-heterozygote analysis

The sites of limb defects for *hoxd-11*, *hoxd-12*, and *hoxd-13* individual mutant mice are summarized (Fig. 4.1). The lack of any prominent limb phenotype in *hoxd-12* mutant mice suggested that perhaps another gene of the *Hox Complex* may be compensating for the loss of *hoxd-12*, as has been previously demonstrated for *hoxd-11* (Davis et al., 1995). Since the limb phenotypes for *hoxd-11* and *hoxd-13* mutant mice show an overlap in their sites of defects (Fig. 4.1), it remained a possibility that one or both of these genes provided enough compensation to allow for the fairly normal development of the autopod even in the absence of a functioning *hoxd-12* gene. We could test this possibility by creating mice doubly mutant for (*hoxd-11/hoxd-12*) and (*hoxd-12/hoxd-13*). However, these types of strains cannot be generated by simple breeding strategies since to generate such homozygous double mutant would require a cross-over event between the two genes of interest. Instead, we decided to create mice *trans*-heterozygous for the *hoxd-11*, *hoxd-12*, and *hoxd-13* mutations to look for additional limb phenotypes, not apparent in mice heterozygous for individual *Hox D* mutations, suggesting interaction between these gene products. For all strains described below, *trans*-heterozygotes were generated by breeding a female homozygous mutant for one gene to a male heterozygous for the second gene. The resulting progeny will be an equal distribution of *trans*-heterozygotes and control littermates (single heterozygotes).

(*Hoxd-11/hoxd-13*) *trans*-heterozygotes {*hoxd-11*(-/+), *hoxd-13* (+/-)} display several strong limb defects in the autopod. The base of metacarpal III consistently shows a bony outgrowth. Carpal bones d3 and d4 fuse together at their proximal borders, and d4 shows the same indentation seen in *hoxd-12* (-/-) mice (Fig. 4.3). Digits II and V in (*hoxd-11/ hoxd-13*) *trans*-heterozygotes are shorter due to the absence or strong reduction of P2 (Table 4.1 and Fig. 4.3). The phenotype of P2 on digit II shows variable expressivity from total absence of the bone (Fig. 4.3) to a strong reduction in its length (Table 4.1). Overall, these defects lead to the characteristic shortening of digits II and V of the forelimb.

To examine genetic interactions of *hoxd-12* with either *hoxd-11* or *hoxd-13*, we bred both (*hoxd-11/ hoxd-12*) *trans*-heterozygotes {*hoxd-11* (-/+), *hoxd-12* (+/-)} and (*hoxd-12/ hoxd-13*) *trans*-heterozygotes {*hoxd-12* (-/+), *hoxd-13* (+/-)}. In the wrist of (*hoxd-11/ hoxd-12*) *trans*-animals, a fusion is often seen between the navicular lunate and triangular proximal carpal bones (Fig. 4.4). This is a phenotype characteristic of *hoxd-11* (-/-) mice, but never seen in the *hoxd-11* (-/+) heterozygotes (Davis and Capecchi, 1994; Davis et al., 1995). Again, there is a significant reduction in the lengths of specific phalangeal and metacarpal bones that result in the overall truncation of both digits II and V (Table 4.1) with P2 of digit V showing the strongest phenotype with the greatest reduction (Fig. 4.4).

Lastly, (*hoxd-12/ hoxd-13*) *trans*-heterozygotes {*hoxd-12* (-/+), *hoxd-13* (+/-)} show the strongest interaction of these *Hox D* genes in the limb. The wrists of these animals show similar phenotypes as in (*hoxd-11/ hoxd-13*) *trans*-heterozygotes with a bony outgrowth of metacarpal III, the fusion of d3 and d4 carpal bones at their proximal borders, and the indentation of d4 (Fig. 4.4). However, additional phenotypes are also evident. An extension of d4 is sometimes seen that covers the entire base of metacarpal V (Fig. 4.4). Another animal shows the gross fusion of metacarpals III and IV at their proximal ends (Fig. 4.4). P2 of digits II and V are both effected with digit V showing the

Figure 4.3

Limb defects in (*hoxd-11/ hoxd-13*) *trans*-heterozygotes. Forelimbs of *trans*-heterozygotes (B) show a bony outgrowth of metacarpal III (white arrow) and the fusion of carpal bones d3 with a malformed (indented) d4 (black arrows) when compared to control heterozygotes (A). P2 of digit II in *trans*-animals is often eliminated (D) whereas P2 of digit V is greatly reduced in length (F).

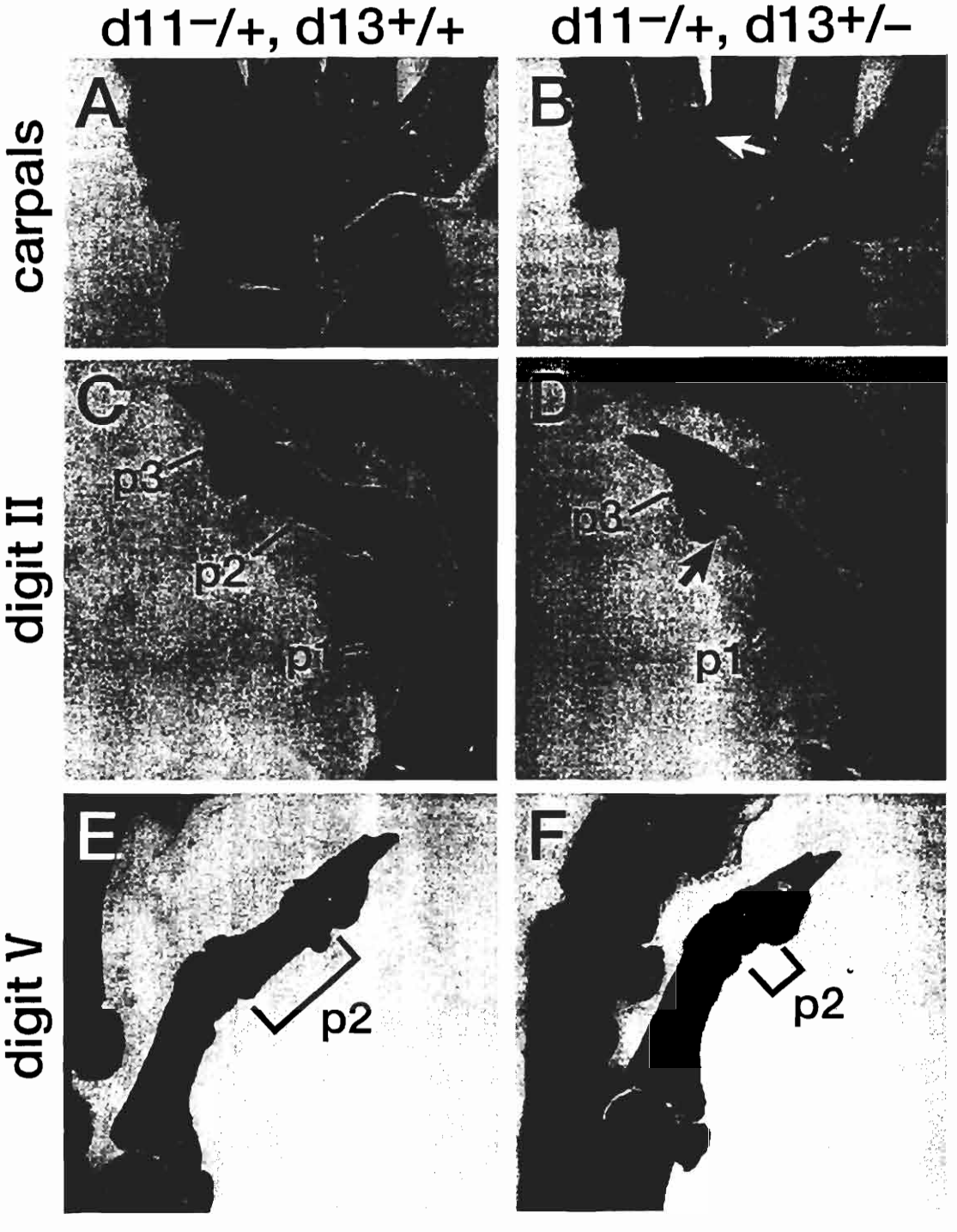
d11−/+, d13+/+
d11−/+, d13+/−
carpals
digit II
digit V
A
B
C
D
E
F
p3
p2
p
p1
p2
p2

Figure 4.4

Limb defects in (*hoxd-11/ hoxd-12*) and (*hoxd-12/ hoxd-13*) *trans*-heterozygotes. The control is a *hoxd-12* heterozygote littermate (A, E). In the carpal region, (*hoxd-11/ hoxd-12*) *trans*-animals often show a fusion between the navicular lunate and triangular carpal bones (B, arrow): a phenotype only seen in *hoxd-11* homozygous mutants but never in *hoxd-12* mice. In (*hoxd-12/ hoxd-13*) wrists, the same metacarpal and carpal defects as in (*hoxd-11/ hoxd-13*) *trans*-animals is detected: a bony outgrowth of metacarpal III (C, white arrow) with the fusion of d3 to a malformed (indented) d4 (C, black arrows); also note that in this animal, d4 is extended and covers the entire base of metacarpal V (C, black arrow). Another (*hoxd-12/ hoxd-13*) *trans*-littermate shows more severe defects with the fusion of metacarpals III and IV (D, star). P2 of digit V is reduced in both (*hoxd-11/ hoxd-12*) mice (F) and (*hoxd-12/ hoxd-13*) *trans*-animals (G). Most noticeably, (*hoxd-12/ hoxd-13*) mice are often characterized by the growth of an extra phalange-like postaxial digit (G, "VI").

d11−/+, d13+/+
d11−/+, d12+/−
d12−/+, d13+/−
carpals
digit V
A
B
C
D
E
F
G
p1
p2
p3
p2
p2
"VI"
*

most severe reduction in this bone (from 0% to 55% of normal P2 length; Table 4.1 and Fig. 4.4). These defects account for digits II and V being significantly shorter than in control limbs (Table 4.1).

Most noticeable, however, in (*hoxd-12/ hoxd-13*) *trans*-heterozygotes is the presence of a rudimentary phalange-like element seen as a postaxial digit VI (Fig. 4.4). To follow the development of this bone, we collected timed embryos and newborn pups for skeletal analysis. This digit VI is readily visible at embryonic day E14.5 as a cellular outgrowth on the postaxial side of the forelimb. Cartilaginous staining at this time reveals the initial condensation of the bone in the outgrowth (Fig. 4.5). An extra postaxial bone is sometimes seen in individual *hoxd-12* (-/+) and *hoxd-13* (-/+) heterozygotes. In these cases, however, the phenotype occurs with both low penetrance (6% for *hoxd-12* heterozygotes and 30% for *hoxd-13* heterozygotes) and weak expressivity, where the bone is extremely small and does not resemble the phalange-like element seen in the *trans*-heterozygote mice. In (*hoxd-12/ hoxd-13*) *trans*-animals, this extra digit VI occurs at 86% penetrance and with a stronger expressivity, producing a much larger and defined structure.

Subsequent developmental time points indicated that overall the (*hoxd-12/ hoxd-13*) *trans*-heterozygotes undergo a delay in the ossification events of the autopodal bones. In control littermates, the ossification center for metacarpal V has commenced by day 1 (D1) in newborns, yet in the *trans*-heterozygotes, this same bone does not begin ossifying until one full day later at D2 (Fig. 4.5). By D5 the final limb ossification event at P2 in digit V has been initiated but again lags behind in the *trans*-heterozygotes (Fig. 4.5). This may account for the severe reduction (and sometimes complete elimination) of P2 on digit V. Additionally, the indentation on the distal carpal bone d4 may be explained by a delay in the fusion of the two condensations that make up this bone. At D1 it can already be seen that this fusion has taken place in the control littermate, but in the *trans*-animal this growth appears to have been slowed down or delayed such that the two elements remain

Figure 4.5

Development of defects in (*hoxd-12/ hoxd-13*) *trans*-heterozygotes. Timed embryonic and newborn littermates were collected. By embryonic day E14.5, the *trans*-heterozygotes can be identified by a cellular outgrowth on the postaxial side of digit V. Cartilaginous staining at this time reveals the nucleus of a condensation event occurring in this outgrowth (B, arrow). At day 1 (D1) of birth, *trans*-animals differ from their littermates in ossification patterns. Control animals show ossification centers for all five digits (C, red staining). Especially note the centers for digits II and V (C, black arrows); additionally, in the wrist, the two prechondrogenic condensations have appropriately fused to form d4 which now appears as one large condensation (C, white arrow). *Trans*-animals show delays in all of these events. By D1, digit II has barely initiated its ossification center (compare the size of red staining of digit II in D with control littermate in C), and has no ossification at all in digit V (D, black arrows); as well, the prechondrogenic condensations still have not yet fused to form the d4 pattern, but remain separate as two individual units (D, white arrow). Note that this particular *trans*-heterozygote did not show the formation of the post-axial digit VI, a phenotype that shows incomplete penetrance; Table 4.2. One full day later, these two carpal condensations still have not completely fused (E, white arrow), yet an ossification center has finally commenced in digit V, and the postaxial digit VI is clearly visible. By D5, again the ossification pattern of P2 in digit V of the *trans*-animal lags behind the control littermates (compare black arrows in F,G). Still, d4 has not properly fused resulting in the indentation at its distal border (compare white arrows in F,G). Digit VI has begun ossifying in the *trans*-heterozygote (G).

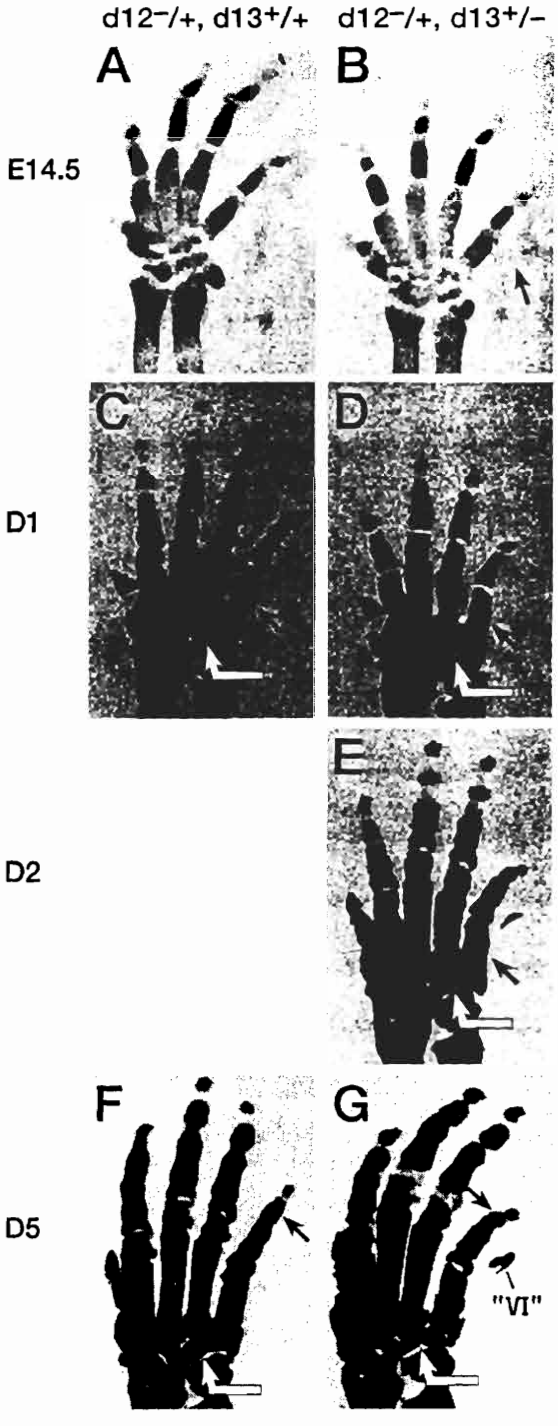
d12⁻/+, d13⁺/+
d12⁻/+, d13⁺/⁻
A
B
E14.5
C
D
D1
E
D2
F
G
D5
"VI"

separate (Fig. 4.5). By D5, these two condensations approach each other except at their most distal border which maintains a scalloped outline and leads to the indentation seen in the final ossified bone (Fig. 4.5).

Table 4.2 summarizes the limb defects for these *trans*-heterozygous strains.

Discussion

Mutant mice homozygous for *hoxd-12* are viable and fertile but show mild defects in the forelimb autopod. In these animals, the lengths of metacarpals in both digits II and V are significantly reduced. As well, P1 of digit II and P2 of digit V are smaller. Taken together, these phenotypes result in digits II and V being characteristically truncated. In addition, *hoxd-12* (-/-) mice have a subtle defect in the carpal bone d4 which is marked by a reproducible indentation at its distal edge.

Hoxd-13 mutant mice show more extensive phenotypes in the autopod. In these animals, the entire paw is smaller due to the strong reduction, complete absence, or improper segmentation of metacarpal and phalangeal bones on all of the digits, but especially for digits II and V. In the wrist, here too d4 is not properly formed and instead yields an extra carpal which often produces a rudimentary postaxial digit VI.

Interestingly, the hindlimbs of *hoxd-12* animals appear relatively normal, as was seen for *hoxd-11* mutant mice (Davis and Capecchi, 1994). *Hoxd-13* animals, however, display severe hindlimb defects (not shown here but identical to that reported by Dolle et al., 1993). This difference suggests that the various *Hox D* genes function independently in the different limbs. The apparent lack of function of *hoxd-11* and *hoxd-12* in the hindlimb probably reflects compensation by other genes, such as paralogues. This was demonstrated to be the case for *hoxd-11* (Davis et al., 1995) which has two additional paralogues in the Hox A and Hox C loci. There is no reported *Hox A* paralogue for *hoxd-12*, but a *Hox C* paralogue has been isolated (Peterson et al., 1994).

Table 4.2

Summary of limb defects in *trans*-heterozygotes

Genotype	Wild-Type	Mutant Phenotypes* II:P2	V:P2	C	M	VI	Frequency (%)#
d-11 (-/+)	X						100
d-12 (-/+)	X						94
						X	6
d-13 (-/+)	X						64
						X	18
				X			6
				X		X	6
			X	X		X	6
{*d-11* (-/+), *d-13* (+/-)}		X	X	X			60
		X	X	X	X		20
		X	X				10
			X	X	X		10
{*d-11* (-/+), *d-12* (+/-)}			X		X		68
			X	X	X		25
				X	X		7
{*d-12* (-/+), *d-13* (+/-)}		X	X	X		X	54
		X	X	X	X	X	32
		X	X	X	X		14

*Mutant Phenotypes: II:P2, V:P2 (a reduction in the length of P2 on digits II and V, respectively), C (carpal defects, excluding d4 indentation), M (metacarpal defects), VI (postaxial digit VI present).

#Between 16 to 22 limbs were observed for each genotype.

The relatively mild forelimb defects seen in *hoxd-12* mice suggested that compensation by other *Hox* genes may be masking this genetic lesion. The notion of spatial and temporal colinearity would have predicted a *hoxd-12* phenotype located between the sites of *hoxd-11* and *hoxd-13* (Davis and Capecchi, 1994; Dolle et al., 1993). However, since mutations in *hoxd-11* and *hoxd-13* independently show sites of overlapping defects (Fig. 4.1), it remains possible that either one or both of these genes products could provide sufficient compensation to allow the near normal development of the forelimb autopod in mice deficient for *hoxd-12*. Genetic redundancy and interaction within the *Hox Complex* has been demonstrated for paralogues in forming both the axial (Condie and Capecchi, 1994; Horan et al., 1995) and appendicular skeletons (Davis et al., 1995). As well, nonallelic noncomplementation occurs within the Hox B linkage group during formation of the vertebral column (Rancourt et al., 1995). We therefore speculated that similar genetic interactions within the same linkage group of the Hox D locus may be influencing appendicular patterning. To test for this possibility we analyzed strains of mice heterozygous for any two mutations at a given time in a *trans* state. Analysis of all three *trans*-heterozygotes showed autopodal defects not readily detectable in the individual heterozygotes.

We first produced (*hoxd-11/ hoxd-13*) *trans*-heterozygotes and demonstrated that these animals showed phenotypes not present in the individual control heterozygote littermates. Metacarpal III is deformed with a bony outgrowth, the carpal bones d3 and d4 fuse, and d4 has an indentation at its distal edge. P2 is often missing in digit II and greatly reduced on digit V resulting in these two fingers being shortened overall. For (*hoxd-11/ hoxd-12*) *trans*-heterozygotes, the phenotypes include the occasional fusion between the navicular lunate and triangular carpal bones. Additionally, reductions are seen in the lengths of metacarpals II , III, and V; in P1 of digit II; P2 of digit IV; and P2 of digit V. In (*hoxd-12/ hoxd-13*) *trans*-animals, the phenotypes are the most severe with the same metacarpal and carpal defects as seen in (*hoxd-11/ hoxd-13*) *trans*-heterozygotes

in addition to the production of an extra postaxial digit VI resembling a phalange-like element and the occasional massive fusion of the metacarpal bases. These *trans*-heterozygote phenotypes are not seen in the individual heterozygotes, except in some cases at very low penetrance and expressivity (Table 4.2).

The severity of phenotypes in these *trans*-animals increases from (*hoxd-11/ hoxd-12*) through (*hoxd-11/ hoxd-13*) to finally (*hoxd-12/ hoxd-13*) *trans*-heterozygotes. This pattern seems to reflect a dominant role for *hoxd-13* in the final structure of the autopod. This is not surprising considering that the *hoxd-13* individual homozygous mutant shows a stronger limb phenotype when compared to *hoxd-11* or *hoxd-12* individual mutants (Fig. 4.1B). From an evolutionary point, this hierarchy may have provided flexibility for modulating the autopod. A limb can be divided into three zones: the most proximal is the stylopod containing one large support bone; this is followed by the middle zeugopod with two similar bones the radius and ulna that usually functions as a hinge to allow limb flexibility; finally at the most distal end is the autopod with several carpal, metacarpal, and phalangeal bones. The most distal end of the limb holds the greatest potential for variation in form and function to be exploited by natural selection (e.g., the opposable thumb in primates, the wrist modification in pandas that allows for grasping bamboo, extensive phalangeal growth in bats to produce a large wing, the webbed feet of ducks, the frequent occurrence of polydactyly, etc.). Thus, it may be advantageous to let the last genes (the *Hox-13* cognates) involved in producing the last structures (the autopod) to have the greatest developmental "free play," extensively influencing and controlling the autopodal unit. This concept may underlie the phenomenon of "proximal stability/ distal variability" in limb structures (Hinchliffe, 1991).

It is important to note that in all three *trans*-animals created, the overall phenotype is the significant reduction in the total lengths of digits II and V. This is primarily caused by the shortening or elimination of the P2 bone in each finger. This phenotype is characteristically observed in numerous *Hox* mutant mice and is consistent with the idea of

these genes influencing cellular proliferation in limb patterning. Limb bones are formed from prechondrogenic condensations as the limb bud grows. Mesenchymal cells condense into these foci which subsequently bifurcate and segment to produce a primary pattern of the limb. Because of the ordered development of this primary pattern, a deficiency of limb bud cells will invariably cause truncations to be seen in the most terminal elements (Shubin and Alberch, 1986). These terminal elements are the P2 bones of digits II and V.

Various secondary modifications of this primary pattern can occur (Muller, 1991). For example, in mice two wrist condensations fuse together to form the one element that will eventually ossify into the d4 carpal bone. Also, the skeletal analysis of different developmental time points for (*hoxd-12/ hoxd-13*) *trans*-heterozygotes demonstrate a delayed timing in ossification events in the autopod, as was seen with *hoxd-13* homozygous mutants (Dolle et al., 1993). This altered timing of development ("heterochrony") also occurs in mice mutant for the two paralogues *hoxa-11* and *hoxd-11* (Davis et al., 1995). Thus, it appears that individual mutations in several different *Hox* genes result in a similar defect which could be explained by there not being enough cells left to finish the autopod (truncating digits II and V by the loss of P2) and delaying the ossification events.

Interestingly, the (*hoxd-12/ hoxd-13*) *trans*-animals also produce an extra rudimentary postaxial digit VI that has been observed in other mutant mice (Wurst et al., 1994; Lampron et al., 1995; Fawcett et al., 1995) and spontaneously occurring in a partially inbred strain (Cusic and Dagg, 1985). The production of this extra digit is preceded by a local outgrowth of mesenchymal cells on the postaxial side of the limb. The digit, therefore, may be the result of the increased amount of mesenchymal cells to condense by overcoming an "anti-chondrogenic factor" from the overlying ectoderm (Solursh, 1984; Hurle et al., 1991) or by initiating an intrinsic chondrogenic event (Hinchliffe and Horder, 1993). The frequent occurrence of this phenotype in a variety of

mice suggests this particular posterior region of the limb bud is very sensitive to cell concentration and/or interaction with the ectoderm.

As noted, in (*hoxd-11/ hoxd-12*) *trans*-heterozygotes, the phenotypes include the occasional fusion between the navicular lunate and triangular proximal carpal bones. This is an interesting defect because it was initially observed in animals homozygous mutant for *hoxd-11* (Davis and Capecchi, 1994). Neither *hoxd-11* (-/+) nor *hoxd-12* (-/-) animals ever show this phenotype, yet somehow the *trans*-combination of {*hoxd-11* (-/+), *hoxd-12* (+/-)} is able to reproduce the defect, as if half the amount of the *hoxd-12* gene product can phenocopy the amount of *hoxd-11* gene product from half to zero (i.e., creates a phenotype seen in *hoxd-11* null mice, but not in *hoxd-11* heterozygotes). Mice mutant for the paralogue *hoxa-11* also occasionally show this same fusion, and remarkably, compound heterozygotes between these two *Hox-11* cognate alleles {*hoxa-11* (-/+); *hoxd-11* (-/+)} also mimic the phenotype (Davis et al., 1995). From these results we concluded that *hoxa-11* and *hoxd-11* must be working together, since in order to produce this defect all that was required was for there to be any two mutant alleles of either *hoxa-11*, *hoxd-11*, or one from each locus. It would appear from this *trans*-heterozygote analysis that *hoxd-11* and *hoxd-12* might also genetically interact in the proper development of the wrist. It is important to note that not every genotype [*hoxa-11* (-/-) or *hoxd-11* (-/-) or {*hoxa-11* (-/+); *hoxd-11* (-/+)} or {*hoxd-11* (-/+), *hoxd-12* (+/-)}] always shows this phenotype with 100% penetrance. Instead, it is merely seen as an occasional subset of defects. This may suggest a degree of variability in the limb patterning program, where combinations of gene products can compensate, interact, or compete with each other.

Six genetic clues provide information as to the role of *Hox* genes in limb development. First, individual targeted disruptions of four of the 5' *Hox* genes (*hoxa-11*, *hoxd-11*, *hoxd-12*, and *hoxd-13*) have not resulted in digit homeosis. Instead, regional malformations in the shapes, lengths, and segmentations of bones are observed suggesting the *Hox* genes control the localized growth and/or recruitment of cells that

contribute to the formation of the appendicular skeleton. Second, these four mutant strains show sites of overlapping limb defects. Third, double mutants for the paralogues *hoxa-11* and *hoxd-11* revealed a major role for *Hox* genes in patterning the limb along the proximodistal axis. In these double mutants, only a vestige of the radius and ulna is formed (Davis et al., 1995). However, following this major discontinuity, limb development resumed. Based on this observation, we proposed that cognate genes of the posterior set of *Hox* genes work in union to specify limb bone formation in the proximal to distal direction. Fourth, the *trans*-genetic interactions reported here demonstrate that genes in the same linkage group also interact in patterning of the limb. Fifth, a characteristic phenotype seen in the majority of these mutant strains is the strong reduction or elimination of P2 in digits II and V, leading to the overall shortening of these two digits. These are the last elements formed in the last digits specified. Such a common endpoint for all of these mutations could be explained by these mutations resulting in a deficiency of cells for forming the final elements of the autopod. This observation again emphasizes a common role for these genes in controlling the proliferation of the precursor cells, positively or negatively, needed for forming the limb. Sixth, also common to all of these mutations is a delay in the growth of chondrogenic and ossification patterns. This heterochrony is certainly a major contributor to the final phenotypic consequences of these *Hox* mutations. The observed heterochrony may again result from a shortage of cells.

It is apparent from this genetic analysis that the formation of the vertebrate limb involves a complex set of interactions among multiple *Hox* genes. Due to the extensive overlap of function, the role of individual genes does not become apparent until they are combined with mutations in other members of the complex. A strong role in mediating the proper outgrowth of the limb along the proximodistal axis has been established. What needs to be resolved is how intimately these genes are involved in generating the final pattern of the tetrapod limb. Minimally, these genes appear to play a role in contributing the timed appearance of the precursor cells necessary for limb construction (Davis et al.,

1995). However, a more extensive role is likely. Through multiple combinatorial interactions among *Hox* genes, the needed complexity for controlling, positively and negatively, the detailed growth of the limb prechondrogenic condensations could be readily attained. Through such a mechanism the *Hox* genes could be directly responsible for the fine sculpting of the limb bones. In such models the growth and patterning of the limb are viewed as being inherently linked such that the branching and segmentation patterns of the prechondrogenic condensations are a direct consequence of the "developmental constraints" imposed by the changing limb bud geometry (Oster et al., 1988; Hurle et al., 1991; Hinchliffe and Horder, 1993). We can begin to address such potential roles for *Hox* genes by rearranging the sites and timing of *Hox* gene expression within the context of the native *Hox Complex*. Regardless of the extent of information that *Hox* genes mediate in patterning the limb, they clearly play an influential role in its formation. By varying the timing and expression domains of *Hox* genes in the limb, novel genetic combinations and interactions appear to have contributed profoundly to the amazing diversity of form and function visible in tetrapod limbs.

References

Capecchi, M. R. (1989). Altering the genome by homologous recombination. *Science* **244**, 1288-1292.

Cohn, M. J., Izpisúa-Belmonte, J.-C., Abud, H., Heath, J. K. and Tickle, C. (1995). Fibroblast growth factors induce additional limb development from the flank of chick embryos. *Cell* **80**, 739-746.

Condie, B. G. and Capecchi, M. R. (1994). Mice with targeted disruptions in the paralogous genes *hoxa-3* and *hoxd-3* reveal synergistic interactions. *Nature* **370**:304-307.

Cusic, A. M. and Dagg, C. P. (1985). Spontaneous and retinoic acid-induced postaxial polydactyly in mice. *Teratology* **31**, 49-59.

Davis, A. P. and Capecchi, M. R. (1994). Axial homeosis and appendicular skeleton defects in mice with a targeted disruption of *hoxd-11*. *Development* **120**, 2187-2198.

Davis, A. P., Witte, D. P., Hsieh-Li, H. M., Potter, S. S. and Capecchi, M. R. (1995). Absence of radius and ulna in mice lacking *hoxa-11* and *hoxd-11*. *Nature* **375**, 791-795.

Deng, C., Thomas, K. R. and Capecchi, M. R. (1993). Location of crossovers during gene targeting with insertion and replacement vectors. *Mol. Cell. Biol.* **13**, 2134-2140.

Dolle, P., Dierich, A., LeMeur, M., Schimmang, T., Schuhbaur, B., Chambon, P. and Duboule, D. (1993). Disruption of the *Hoxd-13* gene induces localized heterochrony leading to mice with neotenic limbs. *Cell* **75**, 431-441.

Dolle, P., Izpisua-Belmonte, J.-C., Brown, J. M., Tickle, C. and Duboule, D. (1991). *Hox-4* genes and the morphogenesis of mammalian genitalia. *Genes Dev.* **5**, 1767-1776.

Dolle, P., Izpisua-Belmonte, J.-C., Falkenstein, H., Renucci, A. and Duboule, D. (1989). Coordinate expression of the murine *Hox-5* complex homeobox-containing genes during limb pattern formation. *Nature* **342**, 767-772.

Dolle, P., Izpisua-Belmonte, J. C., Boncinelli, E. and Duboule, D. (1991). The *Hox-4.8* gene is localized at the 5' extremity of the *Hox-4* complex and is expressed in the most posterior parts of the body during development. *Mech. Dev.* **36**, 3-13.

Duboule, D. (1992). The vertebrate limb: a model system to study the Hox/HOM gene network during development and evolution. *BioEssays* **14**, 375-384.

Duboule, D. (1994a). *Guidebook to the Homeobox Genes*. New York: Oxford University Press, Inc.

Duboule, D. (1994b). Temporal colinearity and the phylotypic progression: a basis for the stability of a vertebrate Bauplan and the evolution of morphologies through heterochrony. *Development* (Suppl.), 135-142.

Duboule, D. (1995). Vertebrate *Hox* genes and proliferation: an alternative pathway to homeosis? *Curr. Opin. Genet. Dev.* **5**, 525-528.

Fallon, J. F., Lopez, A., Ros, M. A., Savage, M. P., Olwin, B. B. and Simandl, B. K. (1994). FGF-2: Apical ectodermal ridge growth signal for chick limb development. *Science* **264**, 104-107.

Favier, B., LeMeur, M., Chambon, P. and Dolle, P. (1995). Axial skeletal homeosis and forelimb malformations in *Hoxd-11* mutant mice. *Proc. Natl. Acad. Sci. USA* **92**, 310-314.

Fawcett, D., Pasceri, P., Fraser, R., Colbert, M., Rossant, J. and Giguere, V. (1995). Postaxial polydactyly in forelimbs of *CRABP-II* mutant mice. *Development* **121**, 671-679.

Hinchliffe, J. R. (1994). Evolutionary developmental biology of the tetrapod limb. *Development* (Suppl.), 163-168.

Hinchliffe, J. R. and Horder, T. J. (1993). Lessons from extra digits. In *Limb Development and Regeneration* (ed. J. F. Fallon, P. F. Goetinck, R. O. Kelley & D. L. Stocum) pp. 113-126. New York: John Wiley & Sons, Inc.

Hinchliffe, J. R. and Johnson, D. R. (1980). *The Development of the Vertebrate Limb*. New York: Oxford University Press, Inc.

Hinchliffe, R. (1991). Developmental approaches to the problem of transformation of limb structure in evolution. In *Developmental Patterning of the Vertebrate Limb* (ed. J. R. Hinchliffe, J. M. Hurle & D. Summerbell) pp. 313-323. New York: Plenum Publishing Corp.

Horan, G. S. B., Ramirez-Solis, R., Featherstone, M. S., Wolgemuth, D. J., Bradley, A. and Behringer, R. R. (1995). Compound mutants for the paralogous *hoxa-4*, *hoxb-4*, and *hoxd-4* genes show more complete homeotic transformations and a dose-dependent increase in the number of vertebrae transformed. *Genes Dev.* **9**, 1667-1677.

Hurle, J. M., Macias, D., Ganan, Y., Ros, M. A. and Fernandez-Teran, M. A. (1991). The interdigital spaces of the chick leg bud as a model for analysing limb morphogenesis and cell differentiation. In *Developmental Patterning of the Vertebrate Limb* (ed. J. R. Hinchliffe, H. M. Hurle & D. Summerbell) pp. 249-259. New York: Plenum Publishing Corp.

Izpisua-Belmonte, J.-C., Falkenstein, H., Dolle, P., Renucci, A. and Duboule, D. (1991). Murine genes related to the *Drosophila AbdB* homeotic gene are sequentially expressed during development of the posterior part of the body. *EMBO J.* **10**, 2279-2289.

Izpisua-Belmonte, J. C. and Duboule, D. (1992). Homeobox genes and pattern formation in the vertebrate limb. *Dev. Biol.* **152**, 26-36.

Lampron, C., Rochette-Egly, C., Gorry, P., Dollé, P., Mark, M., Lufkin, T., LeMeur, M. and Chambon, P. (1995). Mice deficient in cellular retinoic acid binding protein II (CRABPII) or in both CRABPI and CRABPII are essentially normal. *Development* **121**, 539-548.

Mansour, S. L., Thomas, K. R. and Capecchi, M. R. (1988). Disruption of the proto-oncogene *int-2* in mouse embryo-derived stem cells: a general strategy for targeting mutations to non-selectable genes. *Nature* **336**, 348-352.

Morgan, B. A., Izpisua-Belmonte, J., Duboule, D. and Tabin, C. J. (1992). Targeted misexpression of *Hox-4.6* in the avian limb bud causes apparent homeotic transformations. *Nature* **358**, 236-239.

Muller, G. B. (1991). Evolutionary transformation of limb pattern: heterochrony and secondary fusion. In *Developmental Patterning of the Vertebrate Limb* (ed. J. R. Hinchliffe, H. M. Hurle & D. Summerbell) pp. 395-405. New York: Plenum Publishing Corp.

Niswander, L., Tickle, C., Vogel, A., Booth, I. and Martin, G. R. (1993). FGF-4 replaces the apical ectodermal ridge and directs outgrowth and patterning of the limb. *Cell* **75**, 579-587.

Oster, G. F., Shubin, N., Murray, J. D. and Alberch, P. (1988). Evolution and morphogenetic rules: the shape of the vertebrate limb in ontogeny and phylogeny. *Evolution* **42**, 862-884.

Peterson, R. L., Papenbrock, T., Davda, M. M. and Awgulewitsch, A. (1994). The murine *Hoxc* cluster contains five neighboring *AbdB*-related Hox genes that show unique spatially coordinated expression in posterior embryonic subregions. *Mech. Dev.* **47**, 253-260.

Rancourt, D. E., Tsuzuki, T. and Capecchi, M. R. (1995). Genetic interaction between *hoxb-5* and *hoxb-6* is revealed by nonallelic noncomplementation. *Genes Dev.* **9**, 108-122.

Ruddle, F. H., Bartels, J. L., Bentley, K. L., Kappen, C., Murtha, M. T. and Pendleton, J. W. (1994). Evolution of *Hox* genes. *Annu. Rev. Genet.* **28**, 423-442.

Shubin, N. H. and Alberch, P. (1986). A morphogenetic approach to the origin and basic organization of the tetrapod limb. *Evol. Biol.* **20**, 319-387.

Small, K. M. and Potter, S. S. (1993). Homeotic transformations and limb defects in *Hoxa-11* mutant mice. *Genes Dev.* **7**, 2318-2328.

Solursh, M. (1984). Ectoderm as a determinant of early tissue pattern in the limb bud. *Cell Differ.* **15**, 17-24.

Tabin, C. (1995). The initiation of the limb bud: growth factors, *Hox* genes, and retinoids. *Cell* **80**, 671-674.

Thomas, K. R. and Capecchi, M. R. (1987). Site-directed mutagenesis by gene targeting in mouse embryo-derived stem cells. *Cell* **51**: 503-512.

Thomas, K. R., Deng, C. and Capecchi, M. R. (1992). High-fidelity gene targeting in embryonic stem cells by using sequence replacement vectors. *Mol. Cell. Biol.* **12**, 2919-2923.

Tickle, C. and Eichele, G. (1994). Vertebrate limb development. *Annu. Rev. Cell Biol.* **10**, 121-152.

Wurst, V., Auerbach, A. B. and Joyner, A. L. (1994). Multiple developmental defects in *Engrailed-1* mutant mice: an early mid-hindbrain deletion and patterning defects in forelimbs and sternum. *Development* **120**, 2065-2075.

CHAPTER 5

DISCUSSION

The genes *hoxd-11*, *hoxd-12*, and *hoxd-13* comprise the 5' end of the Hox D locus on chromosome 2 of the mouse. During development, these genes are expressed in three regions: the urogenital tract, the trunk paraxial mesoderm along the A-P axis, and the limb buds. Because of their unique overlapping expression domains, it has been suggested that the *Hox* gene products play a critical role by providing positional information during embryogenesis. This hypothesis can be addressed by creating mutations in these genes and observing the developmental consequences. Towards this end, this report examined three strains of mice individually mutant for *hoxd-11*, *hoxd-12*, and *hoxd-13*. Additionally, these strains were crossed to each other to generate all three *trans*-heterozygotes (Chapter 4), and *hoxd-11* was bred to a *hoxa-11* mutant mouse to look for paralogous gene interactions (Chapter 3). Phenotypes were detected in all three of the major expression sites.

Summary of Phenotypes

Urogenital defects

Male mice with mutations in *hoxd-11* or *hoxd-13* are sterile. The cause of infertility by *hoxd-11* has not been resolved but may involve defects in the structure of the vas deferens. *Hoxd-13* males have a deformed penile bone that is believed to interfere with mating. *Hoxd-12* mutant mice show no apparent defects in the urogenital tract as both sexes are fertile and healthy. Additional *Hox* genes may be compensating for some phenotypes. This was demonstrated by creating a mouse doubly mutant for both *hoxd-11* and its paralogue *hoxa-11*.

Neither *hoxa-11* nor *hoxd-11* individual mutants show any kidney defects. However, when both mutations are combined together, dramatic (and lethal) urogenital phenotypes, including kidney aplasia, result. Kidneys are formed by expansion of the primitive blastemal cells during organogenesis. Both *hoxa-11* and *hoxd-11* are expressed in these precursor cells during normal development. The severe renal phenotypes in the

double mutant may simply be the result of the failure of these cells to proliferate sufficiently to initiate kidney formation. Interestingly, however, the expressivity (but not the penetrance) of this defect is variable. Some double mutants are born without any kidneys and die immediately; others survive to adulthood and upon dissection show that they have either only one normal looking kidney (except for it being significantly larger than usual) or two grossly malformed kidneys (that are immediately recognizable as being defective due to their color, size, and fluid-filled sacs). This variability probably reflects additional functional redundancy from other *Hox* genes, including the third paralogue *hoxc-11*. This is a plausible explanation since the occurrence of the kidney defect mimics that of the hindlimb: these phenotypes are seen only in the homozygous double mutants (aa; dd) and not in any of the intermediate genotypes. Interestingly, however, when a single mutant allele for *hoxc-11* is added to the (*hoxa-11*; *hoxd-11*) strains, strong hindlimb defects are seen even without having to make the triple homozygous mutant mouse (aa; cc; dd). These preliminary data suggest that a quantitative effect of the *Hox-11* cognate genes in hindlimb development is now finally being seen, something that was absent in the (*hoxa-11*; *hoxd-11*) mice with regard to hindlimb and kidney development (Chapter 3). The prediction is that in the triple mutant (aa; cc; dd), kidneys will never be made and reflect the complete penetrance and expressivity that is now seen in the zeugopodal defect of (aa; dd) mice.

Axial skeleton

Hox genes are expressed in the paraxial mesoderm along the A-P axis in overlapping domains that differ in their most rostral expression boundaries reflecting the particular *Hox* gene's location on the chromosome (i.e., spatial colinearity). The mutational analysis of numerous *Hox* genes results in axial skeleton defects that are interpreted in terms of homeotic transformations of the vertebrae (LeMouellic et al., 1992; Ramirez-Solis et al., 1993; Condie and Capecchi, 1993; Dolle et al., 1993; Jeannotte et

al., 1993; Small and Potter, 1993; Condie and Capecchi, 1994; Davis and Capecchi, 1994 [Chapter 2]; Kostic and Capecchi, 1994; Davis et al., 1995 [Chapter 3]; Favier et al, 1995; Horan et al., 1995a,b; Rancourt et al., 1995; Rijli et al., 1995; Satokata et al., 1995; Suemori et al., 1995).

Mice with mutations in *hoxd-11* show an apparent homeotic transformation affecting the entire sacrum (S1-S4; Davis and Capecchi, 1994 [Chapter 2]; Favier et al., 1995), and the first paper describing a *hoxd-13* mutant allele suggested homeosis of S4 (Dolle et al., 1993). These positions reflect the colinearity models with *hoxd-11* affecting structures made earlier and more anteriorly that those affected by *hoxd-13*. A mutation in *hoxd-12* would therefore be predicted to cause a homeotic transformation at S2 or S3, the sites between the *hoxd-11* and *hoxd-13* phenotypes. Animals were examined for such transformations and failed to show any convincingly definitive homeosis. This came as a surprise, especially since S2 and S3 are distinguishable sacral vertebrae and a transformation should have been easily detectable. Scrutiny of this area initially suggested that perhaps a modest transformation of S3 --> S2 was occurring, but this analysis was complicated by the extreme subtly of the homeosis detected, the incomplete penetrance, and the fact that some wild-type controls showed a similar vertebral S3 morphology that was being interpreted as homeosis (unpublished data).

There are two potential explanations for the failure to detect any strong homeosis in the sacrum of *hoxd-12* mutant animals. The first may be partial compensation being provided by other *Hox* genes. For example, *hoxd-11* appears to influence the entire sacrum (S1-S2-S3-S4). As such, it is perhaps possible that a fairly normal looking sacrum can still be made even in the absence of *hoxd-12* with enough compensation being provided by *hoxd-11* to prevent detection. One test would be to examine the sacrum of *hoxd-12* mutant mice carrying additional mutations, such as in *hoxd-11*. To date, this type of genetic combination can only be made in the *trans*-heterozygous state (as was done to examine the effects of these genes on limb development, [Chapter 4]). A second

complication may be due to genetic background. The *hoxd-12* mouse was made on the 129/Sv strain. This particular mouse shows an inherent natural variation in the patterning of the lumbar-sacral region at a very high frequency (Green, 1954; Russell, 1979). Thus, potential homeotic transformations induced by a *hoxd-12* mutation may be obscured by strain-modifying factors in the genetic background making detection difficult. To circumvent this, the *hoxd-12* mutation is now being bred onto the stable C57BL/6 strain to then reexamine any sacral homeosis.

The *hoxd-13* mutation reported here may show similar problems with strain backgrounds and, as such, is also in the process of being bred onto a more stable genetic strain. The previous reported *hoxd-13* mutation, however, does suggest a homeotic transformation of S4 --> S3 (Dolle et al., 1993).

Thus, the *hoxd-11* and *hoxd-13* mutant alleles produce anterior homeotic transformations, as anticipated by both the "*Hox* code hypothesis" and the principle of colinearity. However, the degree of homeosis in *hoxd-11* mutant mice is inconsistent with the "*Hox* code hypothesis." Mutant mice would have been predicted to show the homeotic transformation of the sacral vertebrae into lumbar vertebrae (a block homeosis). Instead, the sacral vertebrae all transformed into the next most anterior vertebrae (a ratcheting homeosis). This implies some sort of a fine-tuning mechanism whereby transformations can occur over a large meristic series but where the vertebrae do not all transform into one structure but rather to the structure of the previous anterior vertebra. One possibility is that paralogous *Hox* genes with their overlaying expression domains are masking the full transformations. As such, when the *hoxd-11* mouse was crossed to the *hoxa-11* animal to produce the double homozygous mutant, the homeosis observed in the sacral region became more like a block transformation (with two sacral vertebrae transforming to lumbars and the apparent loss of one complete vertebrae). The production of additional mice mutant for paralogous *Hox* genes may elucidate this point.

The expression domains of *Hox* genes complicate any simple combinatorial model since the *Hox* genes vary in their rostral expression boundaries but all overlap in the posterior regions. Thus, whereas the anterior domains are molecularly defined by few *Hox* genes, the posterior domains contain greater and greater numbers of *Hox* genes' transcripts. Homeotic transformations in mice mutant for *Hox* genes, however, usually occur only at the most anterior expression domain. Strict interpretation of the "*Hox* code hypothesis," however, predicts that the entire A-P axis would be altered by the elimination of any one particular *Hox* gene. "Posterior prevalence" has been suggested to explain the lack of phenotypes in the more caudal regions of overlapping *Hox* expression domains (Duboule, 1991,1992). This represents another model based upon observations of the *Drosophila* homeotic genes (Gonzalez-Reyes and Morata, 1990). Posterior prevalence argues that the functional domain of a *Hox* gene will be restricted to the region to which the next colinear *Hox* gene shows its most anterior limit; in essence, posterior genes functionally prevail over anterior genes. Thus, mutations in a *Hox* gene will produce phenotypes restricted to the region defined by the anterior border of the next most posterior *Hox* gene. Therefore, the posterior region of the embryo is patterned by *Hox* genes and the anterior region is merely a default state acquired by the lack of these gene products.

It should be realized that at their simplest interpretations, the "*Hox* code hypothesis" and the "posterior prevalence" models inherently contradict themselves. Nonetheless, both of these ideas have been presented merely as working proposals to try to explain the accumulated data, with neither of them suggested as absolute truths. Even in *Drosophila* -- which only has eight *Hox* genes to deal with -- numerous exceptions have been found to these models. The ultimate patterning mechanism will undoubtedly prove to be a complicated scenario involving the complement of *Hox* gene products in a cell (versus a neighbor cell containing different *Hox* combinations), quantitative levels of gene products, interactions, competition (e.g., Lamka et al., 1992), compensation, and cross-

regulation. Any one or all of these possibilities could exist for the 38 mouse *Hox* genes, making simple model predictions a difficult task.

Interestingly, vertebral homeosis has also been induced in mice exposed to high levels of radiation during specific critical periods of development (E8.5-E12). This often produced anterior homeotic transformations of the axial column (Russell, 1956). These phenotypes are believed to be the result of cellular damage due to the irradiation, in effect causing a depletion of cells in the embryo (L. Russell, personal communication). This example of homeosis due to a deficiency of cells is reminiscent of the model whereby *Hox* genes influence proliferation (discussed below). The similarities are speculative yet nonetheless tempting.

Future directions in the role of *Hox* genes patterning the A-P axis will have to include detailed expression studies at the cell level using specific antibodies instead of relying on the lower resolution obtained with RNA *in situ* techniques. Second, the possibility of *Hox* gene cross-regulation will have to be more thoroughly addressed in the mouse. Additionally, isolation of downstream genes regulated by the *Hox* gene products may shed light on their patterning abilities. Finally, the functional information provided by *Hox* genes can be examined with novel gene targeting strategies (discussed below).

Appendicular skeleton

The initial expression domains of *Hox* genes in the developing limb bud suggested an ordered pattern of overlapping transcript regions reminiscent of that seen in the patterning along the A-P axis. From these results, an extension was made from the axial models to the limb, whereby the *Hox* genes were predicted to be establishing positional information by simple molecular combinatorial codes (Fig. 1.2). This report has directly tested these models by producing mice mutant for *hoxd-11*, *hoxd-12*, and *hoxd-13*.

No type of homeosis occurred in the limbs of mice mutant for any one of these genes or combinations of genes arguing against the molecular code models. Instead, what

was observed was the regional malformations in the shapes, lengths, and segmentations of bones. These defects all resulted in a common endpoint: the truncation of digits II and V by the significant reduction or elimination of the second phalangeal bone (P2) on each finger.

This study suggests that the *Hox* genes function in the limb by regulating cellular proliferation, as opposed to defining specific positional information by molecular codes. This regulation is influence by a multitude of genetic interactions, combinations, and compensation of paralogous and nonparalogous *Hox* gene products.

The Limb Pattern

Limb development occurs in a proximodistal direction as mesenchymal cells condense into foci that elongate as the limb grows out of the body of the embryo. A primary pattern of these prechondrogenic condensations is laid down and formed by a process of growth (recruitment of cells into the focus), bifurcations (where one focus divides into two new foci), and segmentations (where a focus buds off). These prechondrogenic condensations ossify into the final skeleton.

The vertebrate limb is one of the most beautiful examples of form and function arising from the selective forces of evolution. What is so remarkable about this unit is that throughout the extant animal kingdom and fossil record, the limb shows both an inherent similarity in design yet simultaneously a vast diversity in structure. This finding was interpreted by there being a fundamental "limb pattern" common to all vertebrates. The majority of limb varieties appear to be merely the result of altered growth rates (e.g., the humerus of a mouse and elephant is essentially the same except for the length and thickness of the bones). However, it is more difficult to explain the qualitative differences seen in some vertebrates. This is especially evident in the autopod where a direct one-to-one correspondence of bones cannot often be made between different species. This

homology problem still haunts any comprehensive theory of limb development and evolution (Muller, 1991).

Three general models have been proposed for creating the limb pattern: the archetypical model, the chemical model, and the reaction-diffusion model. These are briefly presented below with a description of what role the 5' *Hox D* genes may be contributing to the limb pattern in light of each individual model.

The archetypical model

The archetypical (or recapitulation) model was suggested by Holmgren (1933). It contains two parts, with the first proposing that all vertebrate limbs are laid down in the same primary pattern originally seen in a common ancestor (the "archetype"). This pattern is then subsequently modified in a species-specific manner to produce limb variations. The first part of this model has been disproved by tracing the detailed developmental profiles of numerous vertebrate limbs (reviewed in Shubin and Alberch, 1986). No single identical primary pattern is observed. However, the second part of this model is correct, as secondary modifications are used to vary the primary limb pattern (Muller, 1991).

Secondary modifications include the fusions of prechondrogenic condensations, the nonossification of some elements, and heterochrony (the altered rate and timing of developmental processes). Heterochrony has been suggested to be the major factor responsible for the evolutionary reduction in the number of carpal bones and digits. For example, the fossil record has produced vertebrates with up to eight digits per limb (Coates and Clack, 1990). In the extant animal kingdom, however, most vertebrates have five digits or less. Somehow three digits have been lost in the skeletogenic program.

By altering the timing of certain developmental events in constructing the autopod (i.e., heterochronic delay), the building of the most terminal elements (the digits) will lag behind and run the risk of never being formed (Hinchliffe, 1991). Five pieces of circumstantial evidence offer support to the model that heterochrony may induce digit

truncation. (1) The vertebrate limb produces five digits in the specific developmental sequence of IV-III-II-V-I. The pattern of digit I in mammals already demonstrates an inherent truncation. Whereas all other digits contain three phalanges, digit I has only two phalanges: an entire element has been permanently lost on the most terminal digit. (2) The analysis of digit structure in a related group of Australian sandswimming lizards (*Lerista*) shows that the digit patterns vary among species and are truncated by the specific formula of I-V-II-III-IV (Greer, 1987). That is, digit I is lost first followed by digit V, then II, III, and finally IV (to produce a limbless lizard). This truncation pattern is the exact opposite of digit formation, emphasizing that the most terminal structures formed are the most susceptible to reduction and loss. (3) In mouse limbs, the experimental arrest of cellular proliferation by injection of cytosine arabinoside (an inhibitor of DNA synthesis) results in autopodal malformation including digit truncation. In this case, digit IV (the first digit made) is always the most resistant to loss induced by the teratogen (Rooze, 1980). (4) A comparison of developmental incubation times and limb structures among various animals produces a speculative correlation. Crocodiles take an average of three weeks to finish autopod formation, whereas birds go through this in about five days. Birds also show a significant reduction in the number of digits and tarsal bones when compared to crocodiles, suggesting that perhaps speeding up limb development may influence reductions in some species (Muller, 1991). (5) This report and other studies demonstrate that *Hox* mutations in mice consistently show heterochronic delay in limb formation that culminates in a common phenotypic endpoint: the truncation of digits II and V by the specific reduction or elimination of the second phalange (Dolle et al., 1993; Davis and Capecchi, 1994 [Chapter 2]; Davis et al., 1995 [Chapter 3]; Favier et al., 1994; [Chapter 4]). In the mouse, second phalanges of digits II and V are the last elements made during limb development.

The chemical model

The chemical (or morphogen) model has received the most attention in the last two decades due to a number of transplantation experiments in the chick (reviewed in Hinchliffe and Johnson, 1990). The premise is that chemical gradients are established in the limb field, that the limb cells can both read and react appropriately to these gradients, and that different thresholds of the gradients change the developmental pathway of the cells. Thus, a coordinate grid of positional information could be achieved by relatively few chemicals ("morphogens"). The concentration of morphogens would determine the pattern of prechondrogenic condensations in the developing limb bud. Three sites in the limb have been tested for providing positional information: the zone of polarizing activity (ZPA), the progress zone (PZ), and the apical ectodermal ridge (AER).

Although the AER itself has been shown not to provide any type of positional information on its own (Rubin and Saunders, 1972), it appears to act in concert with the PZ to generate positional identity to cells. This was revealed in a set of elegant experiments where apical caps (a combination of the PZ + AER) were reciprocally transplanted between an older and younger chick wing bud (Summerbell and Lewis, 1975). When a cap was removed from an old limb bud and transplanted onto the end of a young limb (of which its own endogenous cap had been surgically removed), limb development continued but with a strange pattern being laid down. The limb consisted of a humerus bone immediately followed by a set of digits, completely bypassing the zeugopod (radius and ulna). In the reciprocal experiment (a young cap placed onto an older bud), the pattern was even more surprising: a humerus was followed by a radius and ulna, then by another set of the radius and ulna, and finally the digits. These results were explained by the apical cap knowing its own position in its original limb bud. For example, if the older cap had already produced a humerus and zeugopod, then when it was transplanted to the young limb bud it would not duplicate these structures but instead lay down its next limb set, the digits. Conversely, the young cap had not yet produced a

zeugopod and series of digits, so when transplanted to the older limb field, it continued with its normal limb patterning causing a reiteration of the radius and ulna.

These results led to the "progress zone hypothesis" where the rapidly dividing cells in the PZ are imparted with positional information (Summerbell and Lewis, 1975). The cells that leave the PZ first are programmed to form the humerus, those that leave midway will form the zeugopod, and the final cells to vacate the PZ will ultimately form the digits. Years later when the limb *Hox* genes were discovered, it was thought that the *Hox D* genes may be providing the molecular positional information to the PZ cells. In this revised interpretation, as the PZ cells rapidly divide they activate the set of 5' *Hox D* genes in order of the spatial and temporal colinearity principles (i.e., *hoxd-9*, *-10*, *-11*, *-12*, and then *-13*). The vacating PZ cells would then be molecularly distinguished by different subsets of *Hox D* gene products, which may translate into distinct positional information in the limb field (Izpisua-Belmonte and Duboule, 1992). This idea was later discarded (perhaps prematurely) in favor of the RNA *in situ* expression data of the *Hox D* genes generating A-P polarity (instead of P-D polarity as suggested in the progress zone hypothesis).

The ZPA is defined as the posterior-distal region of the limb that when transplanted to the anterior side of another limb causes the mirror-image duplication of the digit pattern (Tickle et al., 1975). These results have been interpreted as the ZPA producing a morphogen that diffuses across the A-P axis of the limb bud establishing positional information by threshold gradients. Cells closest to the source of the morphogen are programmed to build the most posterior digit while the cells furthest away (receiving the lowest amount of morphogen) are instead directed to produce the most anterior digit. The intervening digits are specified by intervening threshold gradients of the morphogen. This model received substantial support from an experiment that blocked the secreted morphogen by insertion of a nonpermeable membrane in the limb field: the posterior digits, but not the anterior ones, were made (Summerbell, 1979).

For a long time, retinoic acid (RA) was believed to be the morphogen since RA-soaked beads could replace the ZPA in transplantation experiments (Tickle et al., 1982; Eichele, 1989). This view, however, has been modified as a result of a series of experiments that demonstrate RA can induce formation of a ZPA but is not the actual morphogen secreted by the ZPA (Noji et al., 1991; Wanek et al., 1991). Since then, a new candidate has emerged: Sonic hedgehog (Shh). *Sonic hedgehog* is one of the vertebrate homologs of the *Drosophila* segment polarity gene *hedgehog* (Echelard et al., 1993; Riddle et al., 1993). Several lines of evidence implicate Shh intimately involved in the ZPA: (1) endogenous expression patterns of *Shh* in the limb localize it to the physical region of the native ZPA, (2) RA induces *Shh* expression, and (3) the ectopic expression of *Shh* in the anterior region of a limb bud results in mirror-image digit duplications. Additionally, ectopic expression of *Shh* induces the ectopic expression of some of the 5' *Hox D* genes prior to digit duplications.

The *Hox D* genes have been repeatedly associated with establishing A-P digit polarity in the vertebrate limb (Dolle et al., 1989; Izpisua-Belmonte et al., 1991; Morgan et al., 1992; Tabin, 1992; Morgan and Tabin, 1993). Initially, expression patterns of the 5' *Hox D* genes were interpreted as defining five molecular zones along the A-P axis corresponding to the five distinct vertebrate digits (Fig. 1.2). This model has been so well received that it can still be found in comprehensive reviews of limb formation and developmental text books (Tickle and Eichele, 1994; Gilbert, 1994). Support of this model has come from two sources. First, anteriorly placed RA-soaked beads ectopically induce a nested set of the 5' *Hox D* genes prior to mirror-image digit duplication (Izpisua-Belmonte et al., 1991; Nohno et al., 1991). Second, the ectopic expression of mouse *hoxd-11* in developing chick hindlimbs produces an apparent posterior homeotic transformation of digit I --> II. This homeosis, however, was a rare event. The majority of the limb phenotypes were merely dysmorphologies, primarily resulting in digit fusions (Morgan et al., 1992). However, since the reports of mice mutant for *Hox D* genes, this

result has been reinterpreted. Instead, the ectopic *hoxd-11* gene is believed to now cause extra proliferation of limb cells, which results in an additional phalangeal bone on digit I "transforming" it to look like digit II (Morgan and Tabin, 1994). This reinterpretation has, in essence, retracted the *Hox D* molecular code model for digit identity.

The reaction-diffusion model

The reaction-diffusion model is another example of chemicals patterning the limb but was hypothesized entirely from a mathematical perspective (Turing, 1952). The premise is that in a defined space, an initially homogenous distribution of two chemicals (*A* and *B*) will ultimately produce a specific and definable pattern given a limited set of parameters. The parameters include the following: (1) *A* inhibits the production of *B*, (2) *B* stimulates the production of *A* and *B*, and (3) *A* diffuses faster than *B*. When these requirements are met, a series of periodic standing waves is established relative to the defined space. This pattern is suggested to then impart positional information in the same way of the above chemical model, whereby cells can read and respond to threshold levels. Specifically in the limb, it is believed that the pattern of prechondrogenic condensations is responding to this information.

Critical to this model is the concept of the defined space. As the shape of the space is altered, the amount of standing waves that can be generated fluctuates. The limb undergoes dramatic changes in its geometry during embryogenesis. The number of waves that can be generated in the limb bud at various stages of development has been considered (Newman and Frisch, 1979; Oster et al., 1988). Initially, only one wave can be produced (interpreted to correspond to the one condensation that will give rise to the humerus); then with further development, the geometry expands to allow two waves to fit (the radius and ulna); and finally, the limb grows to resemble a paddle, and at this point numerous waves can be patterned (the many carpal and digit condensations).

The formation of condensation foci is believed to involve both a recruitment of cells into a focus and a lateral inhibition preventing additional foci from arising. For a progressive increase in condensations to occur in the P-D direction, the shape of the limb must increase to accommodate these foci (or else the lateral inhibition must decrease). The net result of this theory is that subtle changes in the limb geometry can have radical effects upon the condensation patterns, especially in the autopod where slight increases in cell concentrations would produce polydactyly and decreases result in digit loss, a common feature in evolutionary history (Hinchliffe, 1991)

This model (more than the other two) stresses the concept of growth and patterning as being inherently linked during development. Thus, the pattern of the limb can be altered by changing the growth of the limb. As a consequence, if the 5' *Hox D* genes are regulating cellular proliferation, then the mutant analysis of these genes would invariably alter the geometry of the limb bud which in turn would modify the prechondrogenic condensation patterns. The phenotypes produced by mutating these genes would not necessarily be easily predicted, except with respect to their spatiotemporal colinearity. For example, the earlier expressed genes should influence limb structure in a more proximal domain than the later expressed genes. The analysis of mice mutant for *hoxd-11*, *hoxd-12*, and *hoxd-13* reflects this pattern: *hoxd-11* (in conjunction with *hoxa-11*) influences the zeugopod, *hoxd-12* is restricted to the proximal autopod, and *hoxd-13* has its major effect on the distal autopod (Dolle et al., 1993; Davis and Capecchi, 1994 [Chapter 2]; Davis et al., 1995 [Chapter 3]; [Chapter 4]).

It should be emphasized that these three general models for the limb pattern are not mutually exclusive of one another. The limb pattern will undoubtedly prove to be an intricate developmental program probably incorporating many features of all three of these models.

The Role of the 5' *Hox D* Genes?

Where does all of this leave the 5' *Hox D* genes with regard to limb patterning? This report examines the phenotypic consequences in mice mutant for *hoxd-11*, *hoxd-12*, *hoxd-13*, and various combinations of these alleles. As such, it directly tests specific molecular combinatorial models for these genes in establishing defined positional information along the A-P axis with regard to digit formation (a chemical model; Tabin, 1992). The results reported here cannot confirm this model. (This is not to say that a chemical model for limb patterning does not exist, but merely that the *Hox D* genes are not involved in generating a pattern by this method.) Instead, this work suggests that the *Hox D* genes are involved in regulating cellular proliferation in the limb and, as such, may influence limb patterning by heterochrony and/or altering limb geometry.

The evidence connecting *Hox* genes with cell proliferation is still circumstantial yet can be rationalized as the common denominator to all of the major phenotypes in *Hox* mutant mice. For example, in (*hoxa-11*; *hoxd-11*) double mutant animals, there are three primary defects: renal aplasia, severe limb deformities, and axial homeosis (Chapter 3). Normal kidney development requires proliferation of the primitive blastemal cells. Both *hoxa-11* and *hoxd-11* are expressed in these cells during the initiation of organogenesis. In the double mutant, the failure of these *Hox* gene products to be present may cause the failure of these blastemal cells to proliferate, thereby resulting in the lack of kidneys. In the forelimbs, the defect in the double mutant is primarily restricted to the zeugopod which is almost completely eliminated. Intermediate genotypes such as (Aa; dd) and (aa; Dd) show intermediate phenotypes with a reduced zeugopod. The progressive shortening of the radius and ulna with the progressive increase in mutant *Hox* alleles favors the argument that the *Hox* genes are contributing to the building materials of the limb. Axial homeosis can also be thought of in terms of a deficiency in cellular proliferation. Vertebrae are formed from a meristic series of somites patterning the A-P axis of the mouse embryo. These somites are laid down in an A-P direction. Two requirements are

necessary for patterning a vertebra: (1) a collection of cells to build the bone and (2) a pattern to dictate how those cells will ultimately shape themselves into the structure of the vertebra (e.g., a lumbar versus a sacral). As somites are generated along the A-P axis, a pattern may be imparted onto them. If proliferation is slowed down, then cells which normally would have passed onto the next most posterior region (and received a more posterior pattern signal) may instead become stalled in a more anterior domain and have imparted onto them a more anterior pattern. The result in the final axial skeleton would be the apparent anterior homeotic transformation of a vertebra. (This scenario may additionally explain why the *hoxd-11* mutant animal shows a ratcheting homeosis instead of a block homeosis of the sacrum: instead of all the somites receiving one pattern, they subsequently receive the next most anterior pattern phase-shifted by one vertebra.)

That *Hox* mutations can induce homeosis in the axial column but not in the limb is an intriguing fact. Again, there is the (*hoxa-11*; *hoxd-11*) double mutant mouse in which the zeugopod is almost entirely eliminated. It is critical to realize that no other structure develops to take its place, as happens in homeosis. Why should this be? One potential answer is that although growth and patterning may be inherently linked in limb development, these two processes may actually be unlinked in forming the vertebral column. The primary axis of the vertebrate embryo is a truly segmented structure with the reiteration of a single morphological unit (the somite). In the limb, no strict segmentation is present. This fundamental distinction in morphological structure may underlie patterning mechanisms. How this might be achieved for vertebral patterning is unknown yet may be reminiscent of somitic musculature patterning where signals are sent from the neural tube, notochord, and lateral plate to specify development (Pouriquie et al., 1995).

Direct tests connecting *Hox* genes with cellular proliferation will eventually have to be done. This might be resolved by examining the rate and pattern of mitosis (and/or apoptosis) of cells in *Hox* mutants by markers for cell proliferation or cell death. The isolation of immediate downstream genes will also shed light on the function of the *Hox*

genes. Additionally, a fundamental question as to the role of *Hox* genes is to resolve exactly what type of developmental information they contain. Does each individual *Hox* gene merely function by nonspecifically regulating cell proliferation (i.e., are the 5' *Hox D* genes functionally equivalent)? Or does each gene additionally impart some aspect of positional information to the proliferating cells? Ectopic expression of the 5' *Hox D* genes in transgenic mice may be difficult to interpret for a number of reasons, not which of least will be the fact that in such constructs the *Hox* gene will have been removed from the context of the native *Hox Complex* genetic matrix and probably disengage the colinearity principles. A better test will be to alter the positions of *Hox* genes within the confines of the *Hox D* locus. Several types of experiments can be performed by gene targeting to rearrange the order of *Hox* genes (Table 5.1). The limb pattern in such mice should be informative as to the type of information *Hox* genes provide to the limb (and axial column) during development.

A Common Genetic Philosophy

Genetic pathways controlling developmental programs are subjected to natural selection and invariably become modified during evolution. A consequence to the theory of evolution is the notion that life can be traced back through a common ancestor. Thus, the patterning of ancestral characteristics may still lurk in the modern genome. The emergence of atavistic features during embryogenesis and their reappearance in adult humans and other species support this idea (Hall, 1995). It may not be surprising, therefore, that mutations in some of these genetic programs may occasionally produce atavistic phenotypes of a more primitive developmental structure. This indeed seems to be the case. The targeted disruption of two *Hox* genes both produced phenotypes that can be viewed as atavistic. Mice mutant for *hoxd-13* have autopods that, among other things, have an increased number of carpal bones and digits (Dolle et al., 1993; [Chapter 4]) reminiscent of ancient vertebrate tetrapod limbs (Shubin, 1991).

Table 5.1

Gene targeting experiments that rearrange the 5' end of the Hox D locus

Structure of the Locus	Comments
d-11 --- d-12 --- d-13	Wild-type
d-11 --- d-12 --- d-11 *d-13 --- d-12 --- d-13* *d-11 --- d-11 --- d-13*	Gene swapping: how functionally equivalent are the 5' *Hox D* genes?
d-13 --- d-12 --- d-11	Reversal of colinearity?: reversal of limb pattern?
[*a-11* - (*a-11*) ---------- *a-13*] *d-11* - (*d-11*) - *d-12 --- d-13*	Insertion of an extra set of *Hox-11* cognate genes: is an extra zeugopod now duplicated?

Similarly, the jaws of animals mutant for *hoxa-2* produce a reptilian pterygoquadrate bone (Gendron-Maguire et al., 1993; Rijli et al., 1993), suggesting that the *Hox Complex* may be modifying the developmental programs of an ancestral architecture.

How far back, however, can common genetic pathways be detected? When the homeobox gene was originally discovered in *Drosophila* and then found also to exist in mice, researchers became intrigued. When it was demonstrated that the mouse *Hox* genes mimic their invertebrate homologues with respect to expression pattern domains reflecting their chromosomal order (Lewis, 1978; Duboule and Dolle, 1989: Graham et al., 1989), people were astounded. Finally, the mouse *Hox* genes were shown to control developmental planning similar to that observed in the fly, as mutational analysis of these genes produced region-specific defects and homeotic transformations.

Since then, several *trans*-species experiments have been performed testing the equivalency of developmental genes. For example, when mouse *hoxd-11* is ectopically expressed in *Drosophila*, the gene functions like its invertebrate counterpart *Abdominal-B* (*Abd-B*): it activates the endogenous *Abd-B* and regulates the downstream gene *empty spiracles* (Bachiller et al., 1994). These activation patterns ultimately produce ectopic filzkorpers, a phenotype associated with the overexpression of *Abd-B* in *Drosophila* (Lamka et al., 1992). When *hoxd-11* is added to a fly strain deficient for *Abd-B*, it can still activate *empty spiracles* and induce the formation of filzkorpers, demonstrating a degree of functional equivalency (Bachiller et al., 1994).

However, an even more surprising example of functional equivalency in developmental genes was recently discovered with the mouse *Pax-6* gene and its fly homologue *eyeless*. Both of these genes are involved in eye development in their respective hosts. This alone was a startling discovery since the mammalian eye is structurally quite different from the insect compound eye and not believed to share any type of evolutionary history or developmental similarity (Hill and Davidson, 1994). When *eyeless* is ectopically expressed in *Drosophila*, it induces the formation of complete,

functioning eyes in various parts of the fly body, indicating *eyeless* to be a master developmental switch. Even more astounding, when the mouse *Pax-6* gene was ectopically expressed in *Drosophila*, it induced similar ectopic compound eyes (Halder et al., 1995). This may be only the first example of detailed common genetic programs between flies and mice, whereby functionally similar structures that are developmentally quite distinct are grounded to a similar genetic circuitry. Additional situations may be occurring in both the heart and brain -- two structures very different in the mouse and fly yet the respective development of these organs employs homologous genes in the two species (Hill and Davidson, 1994; Scott, 1994). On an even grander scale, there is the emergence of a developmental concept called the "zootype," a conserved spatial pattern of *Hox* genes that may define the entire animal kingdom (Slack et al., 1993).

So then exactly how different are mammals from invertebrates? Perhaps by not as much as we may have thought 10 years ago just before the homeobox gene was discovered in *Drosophila*. The intervening decade has generated an enormous amount of information concerning this gene, and not only in the fruit fly but now also in a multitude of other creatures. The next 10 years are undoubtedly going to be even more exciting.

References

Bachiller, D., Macias, A., Duboule, D. and Morata, G. (1994). Conservation of a functional hierarchy between mammalian and insect Hox/HOM genes. *EMBO J.* **13**, 1930-1941.

Coates, M.I. and Clack, J.A. (1990). Polydactyly in the earliest tetrapod limbs. *Nature* **347**, 66-69.

Condie, B.G. and Capecchi, M.R. (1993). Mice homozygous for a targeted disruption of *hoxd-3* (*hox-4.1*) exhibit anterior transformations of the first and second cervical vertebrae, the atlas and the axis. *Development* **119**, 579-595.

Condie, B. G. and Capecchi, M. R. (1994). Mice with targeted disruptions in the paralogous genes *hoxa-3* and *hoxd-3* reveal synergistic interactions. *Nature* **370**,304-307.

Davis, A. P. and Capecchi, M. R. (1994). Axial homeosis and appendicular skeleton defects in mice with a targeted disruption of *hoxd-11*. *Development* **120**, 2187-2198.

Davis, A. P., Witte, D. P., Hsieh-Li, H. M., Potter, S. S. and Capecchi, M. R. (1995). Absence of radius and ulna in mice lacking *hoxa-11* and *hoxd-11*. *Nature* **375**, 791-795.

Dolle, P., Dierich, A., LeMeur, M., Schimmang, T., Schuhbaur, B., Chambon, P. and Duboule, D. (1993). Disruption of the *Hoxd-13* gene induces localized heterochrony leading to mice with neotenic limbs. *Cell* **75**, 431-441.

Dolle, P., Izpisua-Belmonte, J.C., Falkenstein, H., Renucci, A. and Duboule, D. (1989). Coordinate expression of the murine *Hox-5* complex homeobox-containing genes during limb pattern formation. *Nature* **342**, 767-772.

Duboule, D. (1991) Patterning in the vertebral limb. *Curr. Opin. Genet. Dev.* **1**, 211-216.

Duboule, D. (1992). The vertebrate limb: a model system to study the Hox/HOM gene network during development and evolution. *BioEssays* **14**, 375-384.

Duboule, D. and Dolle, P. (1989). The structural and functional organization of the murine *Hox* gene family resembles that of *Drosophila* homeotic genes. *EMBO J.* **8**, 1497-1505.

Echelard, Y., Epstein, D.J., St-Jacques, B., Shen, L., Mohler, J., McMahon, J.A. and McMahon, A.P.C. (1993). *Sonic hedgehog*, a member of a family of putative signaling molecules, is implicated in the regulation of CNS polarity. *Cell* **75**, 1417-1430.

Eichele, G. (1989). Retinoic acid induces a pattern of digits in anterior half wing buds that lack the zone of polarizing activity. *Development* **107**, 863-867.

Favier, B., Le Meur, M., Chambon, P. and Dolle, P. (1995). Axial skeleton homeosis and forelimb malformations in *Hoxd-11* mutant mice. *Proc. Natl. Acad. Sci. USA* **92**, 310-314.

Gilbert, S. (1994). *Developmental Biology*, 4th edition. Sunderland, Massachusetts: Sinauer Associates, Inc.

Gonzalez-Reyes, A. and Morata, G. (1990). The developmental effect of overexpressing a *Ubx* product in *Drosophila* embryos is dependent on its interactions with other homeotic products. *Cell* **61**, 515-522.

Graham, A., Papalopulu, N. and Krumlauf, R. (1989). The murine and *Drosophila* homeobox gene complexes have common features of organization and expression. *Cell* **57**, 367-378.

Green, E.L. (1954). Quantitative genetics of skeletal variations in the mouse. I. Crosses between three short-ear strains (P, NB, SEC/2). *J. Natl. Cancer Inst.* **15**, 609-627.

Greer, A.E. (1987). Limb reduction in the lizard genus *Lerista*. 1. Variation in the number of phalanges and presacral vertebrae. *J. Herpet.* **21**, 267-276.

Halder, G. Callaerts, P., and Gehring, W.J. (1995). Induction of ectopic eyes by targeted expression of the *eyeless* gene in *Drosophila*. *Science* **267**, 1788-1792.

Hall, B.K. (1995). Atavisms and atavistic mutations. *Nature Genet.* **10**, 126-127.

Hill, R.E. and Davidson, D.R. (1994). Seeing eye to eye. *Curr. Biology* **4**, 1155-1157.

Hinchliffe, J. R. and Johnson, D. R. (1980). *The Development of the Vertebrate Limb.* New York: Oxford University Press, Inc.

Hinchliffe, R. (1991). Developmental approaches to the problem of transformation of limb structure in evolution. In *Developmental Patterning of the Vertebrate Limb* (ed. J. R. Hinchliffe, J. M. Hurle & D. Summerbell) pp. 313-323. New York: Plenum Publishing Corp.

Holmgren, N. (1933). On the origin of the tetrapod limb. *Acta Zoologica* **14**, 184-295.

Horan, G.S.B., Kovacs, E.N., Behringer, R.R. and Featherstone, M.S. (1995). Mutations in paralogous *Hox* genes result in overlapping homeotic transformations of the axial skeleton: evidence for unique and redundant function. *Dev. Biol.* **169**, 359-372.

Horan, G. S. B., Ramírez-Solis, R., Featherstone, M. S., Wolgemuth, D. J., Bradley, A. and Behringer, R. R. (1995). Compound mutants for the paralogous *hoxa-4, hoxb-4,* and *hoxd-4* genes show more complete homeotic transformations and a dose-dependent increase in the number of vertebrae transformed. *Genes Dev.* **9**, 1667-1677.

Izpisua-Belmonte, J.C., Tickle, C., Dolle, P., Wolpert, L. and Duboule, D. (1991). Expression of the homeobox *Hox-4* genes and the specification of position in chick wing development. *Nature* **350**, 585-589.

Izpisua-Belmonte, J.C. and Duboule, D. (1992). Homeobox genes and pattern formation in the vertebrate limb. *Dev. Biol.* **152**, 26-36.

Jeannotte, L., Lemieux, M., Charron, J., Poirier, F. and Robertson, E.J. (1993). Specification of axial identity in the mouse: role of the *hoxa-5* (*hox1.3*) gene. *Genes Dev.* **7**, 2085-2096.

Kostic, D. and Capecchi, M.R. (1994). Targeted disruptions of the murine *hoxa-4* and *hoxa-6* genes result in homeotic transformations of components of the vertebral column. *Mech. Dev.* **46**, 231-247.

Lamka, M.L., Boulet, A. and Sakonju, S. (1992). Ectopic expression of UBX and ABD-B proteins during *Drosophila* embryogenesis: competition, not a functional hierarchy, explains phenotypic suppression. *Development* **116**, 841-854.

LeMouellic, H., Lallemand, Y. and Brulet, P. (1992). Homeosis in the mouse induced by a null mutation in the *Hox-3.1* gene. *Cell* **69**, 251-264.

Lewis, E.B. (1978). A gene complex controlling segmentation in *Drosophila. Nature* **276**, 565-570.

McGinnis, N., Kuziora, M.A. and McGinnis, W. (1990). Human *Hox-4.2* and *Drosophila Deformed* encode similar regulatory specificities in *Drosophila* embryos and larvae. *Cell* **63**, 969-976.

Morgan, B.A., Izpisua-Belmonte, J.C., Duboule, D. and Tabin, C.J. (1992). Targeted misexpression of *Hox-4.6* in the avian limb bud causes apparent homeotic transformations. *Nature* **358**, 236-239.

Morgan, B.A. and Tabin, C.J. (1993). The role of homeobox genes in limb development. *Curr. Opin. Genet. Dev.* **3**, 668-674.

Morgan, B.A. and Tabin, C.J. (1994). Hox genes and growth: early and late roles in limb bud morphogenesis. *Development* (Suppl.) 181-186.

Muller, G.B. (1991). Evolutionary transformation of limb pattern: heterochrony and secondary fusion. In *Developmental Patterning of the Vertebrate Limb* (J.R. Hinchliffe, J.M. Hurle, and D. Summerbell, eds.), pp. 395-406. New York: Plenum Press.

Nohno, T., Noji, S., Koyama, E., Ohyama, K., Myokai, F., Kuroiwa, A., Saito, T. and Taniguchi, S. (1991). Involvement of the *Chox-4* chicken homeobox genes in determination of anteroposterior axial polarity during limb development. *Cell* **64**, 1197-1205.

Noji, S. Nohno, T., Koyama, E., Muto, K., Ohyama, K., Aoki, Y., Tamure, J. Ohsugi, K., Ide, J., Taniguchi, S. and Saito, T. Retinoic acid induces polarizing activity but is unlikely to be a morphogen in the chick limb bud. *Nature* **350**, 83-86.

Newman, S.A. and Frisch, H.L. (1979). Dynamics of skeletal pattern formation in developing chick limb. *Science* **205**, 662-668.

Oster, G. F., Shubin, N., Murray, J. D. and Alberch, P. (1988). Evolution and morphogenetic rules: the shape of the vertebrate limb in ontogeny and phylogeny. *Evolution* **42**, 862-884.

Pourquie, O., Coltey, M. Breant, C. and Le Douarin, N.M. (1995). Control of somite patterning by signals from the lateral plate. *Proc. Natl. Acad. Sci. USA* **92**, 3219-3223.

Ramirez-Solis, R., Zheng, H., Whiting, J., Krumlauf, R. and Bradley, A. (1993). *Hoxb-4* (*Hox-2.6*) mutant mice show homeotic transformation of a cervical vertebra and defects in the closure of the sternal rudiments. *Cell* **73**, 279-294.

Rancourt, D. E., Tsuzuki, T. and Capecchi, M. R. (1995). Genetic interaction between *hoxb-5* and *hoxb-6* is revealed by nonallelic noncomplementation. *Genes Dev.* **9**, 108-122.

Rijli, F.M., Mark, M., Lakkaraju, S., Dierich, A., Dolle, P. and Chambon, P. (1993). A homeotic transformation is generated in the rostral branchial region of the head by disruption of *Hoxa-2*, which acts as a selector gene. *Cell* **75**, 1333-1349.

Rijli, F.M., Matyas, R., Pellegrini, M., Dierich, A., Gruss, P., Dolle, P. and Chambon, P. (1995). Cryptorchidism and homeotic transformations of spinal nerves and vertebrae in *Hoxa-10* mutant mice. *Proc. Natl. Acad. Sci. USA* **92**, 8185-8189.

Riddle, R. Johnson, R.L., Laufer, E. and Tabin, C.J. (1993). *Sonic hedgehog* mediates the polarizing activity of the ZPA. *Cell* **75**, 1401-1416.

Rooze, M.A. (1980). The effect of cytosine-arabinoside on limb morphogenesis in the mouse. In *Teratology of the Limbs* (ed. H.J. Merker, H. Nau, and D. Neubert), pp. 355-362. New York: Walter de Gruyter, & Co.

Rubin, L. and Saunders, J.W. (1972). Ectodermal-mesodermal interactions in the growth of limbs in the chick embryo: constancy and temporal limits of the ectodermal induction. *Dev. Biol.* **28**, 94-112.

Russell, L.B. (1956). X-ray-induced developmental abnormalities in the mouse and their use in the analysis of embryological patterns. II. Abnormalities of the vertebral column and thorax. *J. Exp. Zool.* **131**, 329-395.

Russell, L.B. (1979). Sensitivity patterns for the induction of homeotic shifts in a favorable strain of mice. *Teratology* **20**, 115-126.

Satokata, I. Benson, G. and Maas, R. (1995). Sexually dimorphic sterility phenotypes in *Hoxa-10*-deficient mice. *Nature* **374**, 460-463.

Scott, M. (1994). Intimations of a creature. *Cell* **79**, 1121-1124.

Shubin, N.H. (1991). The implications of "The Bauplan" for development and evolution of the tetrapod limb. In *Developmental Patterning of the Vertebrate Limb* (J.R. Hinchliffe, J.M. Hurle, and D. Summerbell, eds.), pp. 411-421. New York: Plenum Press.

Shubin, N.H. and Alberch, P. (1986). A morphogenetic approach to the origin and basic organization of the tetrapod limb. *Evol. Biol.* **20**, 319-387.

Slack, J.M.W., Holland, P.W.H. and Graham, C.F. (1993). The zootype and the phylotypic stage. *Nature* **361**, 490-492.

Small, K. M. and Potter, S. S. (1993). Homeotic transformations and limb defects in *Hoxa-11* mutant mice. *Genes Dev.* **7**, 2318-2328.

Suemori, H., Takahashi, N. and Noguchi, S. (1995). *Hoxc-9* mutant mice show anterior transformation of the vertebrae and malformation of the sternum and ribs. *Mech. Dev.* **51**, 265-273.

Summerbell, D. (1979). The zone of polarizing activity: evidence for a role in normal chick limb morphogenesis. *J. Embryol. Exp. Morph.* **50**, 217-233.

Summerbell, D. and Lewis, J.W. (1975). Time, place, and positional value in the chick limb bud. *J. Embryol. Exp. Morph.* **33**, 621-643.

Tabin, C.J. (1992). Why we have (only) five fingers per hand: *Hox* genes and the evolution of paired limbs. *Development* **116**, 289-296.

Tickle, C., Alberts, B., Wolpert, L. and Lee, J. (1982). Local application of retinoic acid to the limb bud mimics the action of the polarizing region. *Nature* **296**, 564-566.

Tickle, C., Summerbell, D. and Wolpert, L. (1975). Positional signalling and specification of digits in chick limb morphogenesis. *Nature* **254**, 199-202.

Tickle, C. and Eichele, G. (1994). Vertebrate limb development. *Annu. Rev. Genet.* **10**, 121-152.

Turing, A. (1952). The chemical basis for morphogenesis. *Phil. Trans. Roy. Soc. Lond. B.* **237**, 37-72.

Wanek, N., Gardiner, D.M., Muneoka, K. and Bryant, S.V. (1991). Conversion by retinoic acid of anterior cells into ZPA cells in the chick wing bud. *Nature* **350**, 81-83.